Ally, adversary or something else: do co-occurring *Phytophthora* pathogens influence each other in culture?

A thesis presented in partial fulfilment of the requirements for the degree of Master of Science (MSc)

in Biological Science

at Massey University, Manawatu,

New Zealand

Taylah Josie Dagg

2023

Abstract

Kauri (*Agathis australis*), a New Zealand native and taonga tree species, is currently under threat from the devasting disease, kauri dieback, caused by the oomycete *Phytophthora agathidicida*. Recent research highlighted that, along with *P. agathidicida*, two other *Phytophthora* species, *Phytophthora cinnamomi* and *Phytophthora multivora*, can co-occur in the soil surrounding kauri trees, and that both *P. cinnamomi* and *P. multivora* cause lesions on kauri seedlings in glasshouse trials. Whether all three *Phytophthora* species interact, whether cooperatively or antagonistically, remains unknown. Such information is needed because it may mean that kauri dieback disease control strategies need to target all three species. In an attempt to gain such information, macroscopic inter- and intra-species colony interaction assays were first carried out on solid growth media; however all colonies formed a zone of growth inhibition around themselves irrespective of the media type or species tested. However, it was anticipated that interactions between the three species could occur at the molecular level through secreted proteins, a proteomic analysis was then carried out to determine how the repertoire of secreted proteins changed when multiple species were grown together in liquid culture, relative to grown alone. In total, 20 putatively secreted proteins, termed effector candidates (most of which had predicted enzymatic functions), were identified that were only produced, or that significantly increased in abundance, during co-culturing. All but one of these were from *P. agathidicida* and most were encoded by genes that were upregulated during infection of kauri leaves and/or roots, suggesting that they may play an important role during host colonisation. As a starting point for future experiments aiming to investigate *Phytophthora*–*Phytophthora* as well as *Phytophthora*–candidate effector interactions *in planta*, each *Phytophthora* species was tested for its ability to infect the model host plant, *Nicotiana benthamiana*. This test revealed large differences in the consistency and rate of infection between the *Phytophthora* species, meaning that interaction assays in this host would likely be difficult. But interestingly, *P. agathidicida* and *P. multivora* more readily infected plants lacking SOBIR1, a major component of extracellular immunity-related signalling, suggesting that extracellular immunity plays a significant role in slowing infection of *N. benthamiana* by these species. Taken together, the results of this study have considerably advanced our understanding of how *Phytophthora* species interact at the molecular level and provide a solid foundation for determining whether *Phytophthora* species work together to cause kauri dieback disease.

Acknowledgements

To my supervisor Carl, I am very grateful for the opportunity to join your lab and to be your first master's student. I can't thank you enough for all the time and effort you have put into this project, you go above and beyond for all your students. To my co-supervisor, Rosie, thank you for your guidance throughout the project. Thank you both for believing in me and for your constant motivation and problem-solving skills throughout it all.

A huge thank you to my lab mates for the laughs we had during our lunchtime conversations. A special thank you to Ellie for your patience and help throughout the proteomics aspect of my research, I would've been lost without you! Thank you to Dr Trevor Loo for all of your help on the LC–MS component of my research and for processing the many samples.

This project could not have been completed without the support and funding from Bioprotection Aotearoa. I was also awarded a Department of Conservation scholarship which was in collaboration with Tiakina Kauri as well as a LA Alexander Trust scholarship; I am very grateful for both.

To my family, especially my Mum and Dad, thank you for always believing in me and encouraging me to pursue this. I am very grateful for your love and support; I wouldn't be where I am today without you both.

And to Jarrod, I can't thank you enough for your continuous love, support, and words of motivation throughout this journey. Thank you for always picking me up when I was down and making sure I was always fuelled with coffee to get me through the day.

Table of Contents

List of Figures

List of Tables

Abbreviations

˚C	Degrees Celsius
µL	Microliter(s)
aa	Amino acid
AA	Auxiliary Activity
ATP	Adenosine triphosphate
ATTA	*Agrobacterium tumefaciens*-mediated transient transformation assay
BAK1	BRI1-associated kinase 1
BLASTp	Protein database search using a protein query
bp	Base pair(s)
CAZyme	Carbohydrate-active enzyme
cm	Centimetre(s)
Da	Daltons
DAMP	Damage-associated molecular pattern
dpi	Days post-inoculation
ETI	Effector-triggered immunity
FDR	False discovery rate
FPKM	Fragments per Kilobase of transcript per million mapped reads
g	Gram
GH	Glycoside hydrolase
h	Hour(s)
hpi	Hours post-inoculation
kb	Kilobase pair
KO	Knockout
L	Litre
LC–MS	Liquid chromatography–mass spectrometry
LPMO	Lytic polysaccharide monooxygenases
m	Metre
M	Molar
m/z	Mass-to-charge ratio
MAMP	Microbe-associated molecular pattern

mg	Milligrams
min	Minute(s)
mL	Millilitre
mm	Millimetre
mM	Millimolar
NAD+	Nicotinamide adenine dinucleotide
NCBI	National Centre for Biotechnology Information
nr	Non-redundant
nt	Nucleotide(s)
p	Probability
P. a	*Phytophthora agathidicida*
P. c	*Phytophthora cinnamomi*
P. m	*Phytophthora multivora*
PAMP	Pathogen-associated molecular pattern
PARP	Pimaricin, Ampicillin, Rifampicin, Pentachloronitrobenzene
PCD	Programmed cell death
PTI	Pattern-triggered immunity
qPCR	Quantitative polymerase chain reaction
qRT-PCR	Quantitative reverse transcriptase polymerase chain reaction
RLK	Receptor like kinase
RLP	Receptor like protein
ROS	Reactive oxygen species
rpm	Revolutions per minute
RPMK	Reads per million per Kilobase
RXEG1	Receptor of XEG1
SDS	Sodium dodecyl sulphate
SDS-PAGE	Sodium dodecyl sulphate–polyacrylamide gel electrophoresis
sec	Second(s)
SOBIR1	Suppression of BIR1
V	Volt(s)
VOC	Volatile organic compound
w/v	Weight/volume ratio
WT	Wildtype

Chapter One: Introduction

Microbial organisms, including fungi, oomycetes, bacteria and viruses, are responsible for some of the most devastating diseases of plants worldwide (Anderson et al., 2004; Dobson & Foufopoulos, 2001). In many cases, these diseases affect economically significant crop species, decreasing yield and/or killing the host, which in turn limits the sale, export and consumption of the commodities produced. As a consequence, many of these diseases threaten the security of food globally (Strange & Scott, 2005). In addition to economically important crop species, many diseases threaten environmentally and culturally important plant species, including those that form part of native forests. Some of the disease-causing pathogens also pose a serious threat to the biosecurity of countries that do not yet possess them, a factor that is exacerbated by extensive travel capabilities and global trade, which facilitate movement of microbes to locations outside their natural origin (Andronis et al., 2022). The diseases caused by these pathogens have the ability to damage forest ecosystems and disturb the habitats that wildlife and other plant flora depend on and in some cases, destroy aspects of the natural environment relied on by the tourism sector.

1.1: Plant pathogens

Many plant-pathogenic microbes are eukaryotes belonging to the fungal kingdom (Andersson, 2006; Heitman, 2011; Latijnhouwers et al., 2003) and, until the late 1980s, oomycetes were classified as fungi (Baldauf et al., 2000; Gunderson et al., 1987; Sogin & Silberman, 1998). This classification was based on the fact that, like fungi, oomycetes have a filamentous vegetative growth phase made up of hyphae. They are heterotrophic in terms of nutrient acquisition thorough absorption, and they reproduce and spread through the use of spores (Fawke et al., 2015; Latijnhouwers et al., 2003). However, based on biochemistry and genetics, including differences in cell wall composition (i.e. cellulose rather than chitin (Hardham, 2006)), and a diploid lifestyle alongside major differences in *COX2* mitochondrial gene and large ribosomal subunit DNA sequences (Fawke et al., 2015), oomycetes are now classified in the kingdom Stramenopiles (Dick, 2001). Stramenopiles are a part of a major subclass SAR, which also includes Alveolata and Rhizaria (Fang et al., 2020). This kingdom also contains brown and red algae which unlike oomycetes, possess chloroplasts that enable them to undergo photosynthesis (Sogin & Silberman, 1998). Notably, fungi are more closely related to humans than they are to oomycetes (Baldauf et al., 2000). Within this new classification, oomycetes are phylogenetically assembled into clades (Cooke et al., 2000) (Figure 1.1) and phenotypic and behavioural similarities are often observed between species found within the same clade (Brasier et al., 2022).

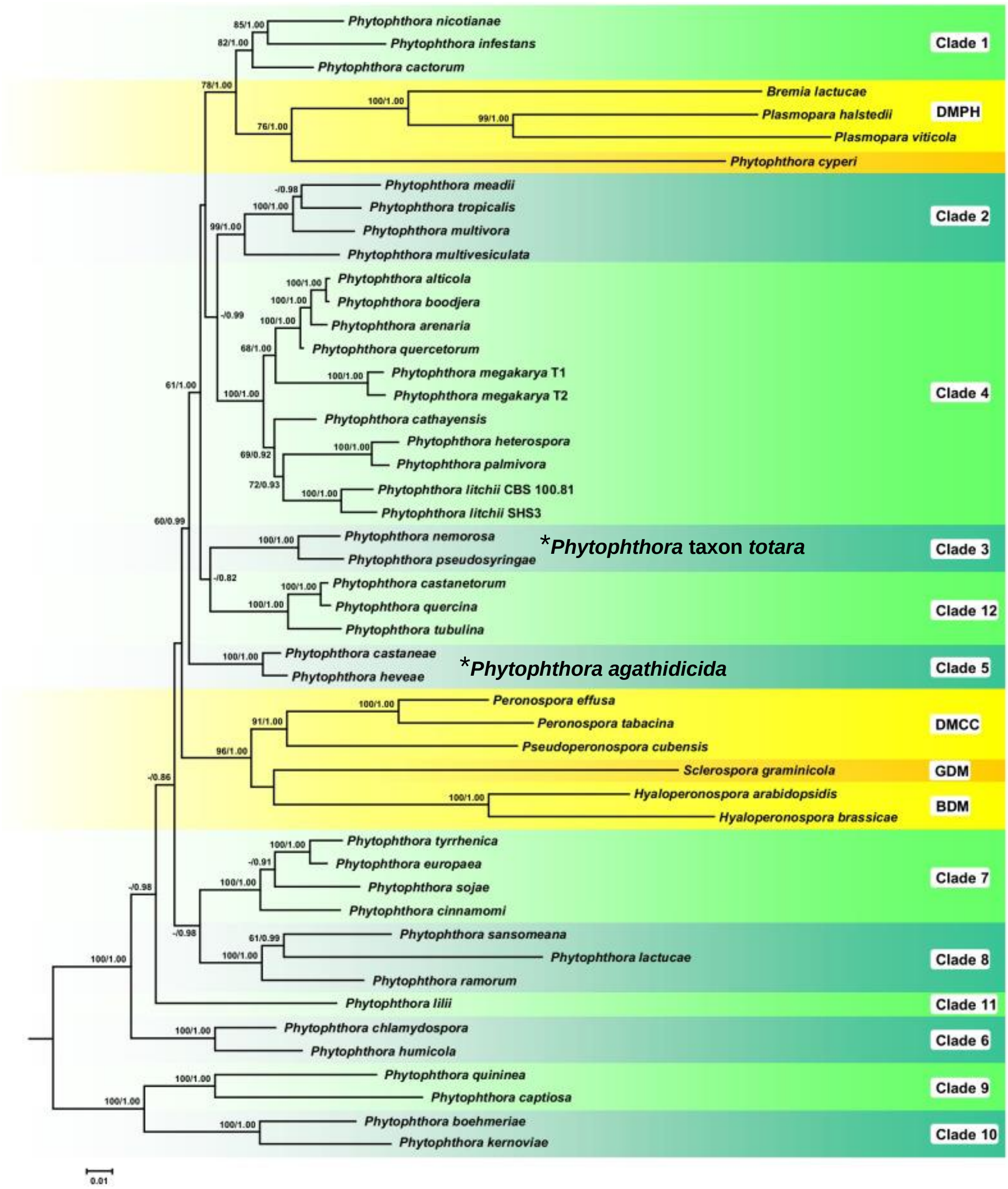

***Figure 1. 1*. Phylogenetic tree of selected *Phytophthora* and downy mildew species clades.** The phylogenetic tree was sourced from (Brasier et al., 2022) and based on four concatenated genes (ITS, *Btub*, *cox*1, *nadh*1). The figure was modified to show that *Phytophthora agathidicida* belongs to clade 5 and *Phytophthora* taxon *totara* belongs to clade 3. Alternating shades of green represent *Phytophthora* clades and alternating yellow shades represent downy mildew clades. The phylogenetic tree shows how closely related each species is to each other indicated by maximum bootstrap and Bayesian posterior probability values at each node. Scale bar = 0.01, which indicates expected changes per site per branch. DMPH = downy mildews with paraphyletic haustoria, DMCC = downy mildews with coloured conidia, GDM = graminicolous downy mildews, BDM = brassicolous downy mildews.

1.2: *Phytophthora* pathogens affect crop plants

Like fungi, oomycetes can colonise plants readily and therefore, can be detrimental pathogens (Doehlemann et al., 2017; Judelson & Blanco, 2005). Amongst these are members of the *Phytophthora* genus, which occupy six places in the top ten oomycete plant pathogens based on scientific and economic importance as voted by scientists (Kamoun et al., 2015). At number one on this list is *Phytophthora infestans*, which causes late blight disease of potato and tomato plants (Ivanov et al., 2021), and was the pathogen responsible for the Irish potato famine in the mid-1800s (Kamoun et al., 2015). Ireland only had one variety of potato at the time, which *P. infestans* infected readily (Powderly, 2019). Strikingly, through crop losses, late blight disease of potato led to the death of one million people and caused malnutrition for many others. In addition, approximately two million people emigrated from Ireland as a result of the famine (Powderly, 2019). *P. infestans* causes rapid necrosis on aerial plant tissue (Whisson et al., 2016), which leads to the death of the entire plant, causing almost complete yield loss (Nowicki et al., 2012). Nowadays, the effects of late blight disease in tomato and potato are still severe, causing upwards of 3.5 billion and 66 million US dollars per annum in losses, respectively (Judelson & Blanco, 2005; Nowicki et al., 2012).

1.3: *Phytophthora* pathogens affect trees in forest settings

Although *P. infestans* infects crop plants, many other *Phytophthora* species are major pathogens of trees, including those in forest settings (Table 1). An example is *P. cinnamomi*, which was initially discovered as the causal agent of stripe canker disease in cinnamon trees of Sumatra during the early 1920’s (Rands, 1922). While this species is predicted to have originated in the islands of South-East Asia, it has since spread worldwide to infect upwards of 4,000 different plant species (Dell & Malajczuk, 1989; Hardham & Blackman, 2018). Of its host species, many are used for the production of foods that have high economic importance, such as cinnamon, avocado and pineapple (Andronis et al., 2022; Hardham, 2005). However, the pathogen also affects forests, and has resulted in the death of millions of forest trees in Australia, South Africa and parts of Europe (Cahill et al., 2008; de Sampaio e Paiva Camilo-Alves et al., 2013; Sena et al., 2018). Common symptoms of disease caused by *P. cinnamomi* include rotting of roots and cankers in the stem of the tree, with infection also preventing the formation and maintenance of new shoots due to damaged roots being unable to take up water efficiently (Hardham, 2005). Since symptoms in the plant are expressed at a late stage of infection, routine screening is often necessary to determine how widespread *P. cinnamomi* infection is, as has been performed for eucalyptus trees in Western Australia (Scott et al., 2009)

Table 1. 1. **Examples of important tree diseases caused by *Phytophthora* species.**

***Phytophthora* Species**	**Common Host(s)**	**Disease Caused**	**Clade**	**Reference**
P. agathidicida	*Agathis australis* (Kauri)	Dieback disease	5	(Bradshaw et al., 2020)
P. cinnamomi	*Cinnamomum zeylanicum* (Cinnamon tree), *Eucalyptus marginata* (Jarrah)	Root rot, dieback	7	(Hardham, 2005; Hardham & Blackman, 2018)
Phytophthora taxon *totara*	*Podocarpus totara* (Tōtara)	Needle blight	3	(Bourret et al., 2018; Dobbie et al., 2022)
P. multivora	*Eucalyptus* species, *Agonis* (Willow peppermint)	Dieback disease	2	(Scott et al., 2009)
P. pluvialis	*Pinus radiata* (Radiata Pine)	Red needle cast	3	(Reeser et al., 2013)
P. ramorum	*Quercus* species (Oak)	Sudden oak death	8	(Rizzo et al., 2002)
P. kernoviae	*P. radiata* (Radiata pine), *Fagus sylvatica* (Beech)	Red needle cast Bleeding stem	10	(Brasier et al., 2022; Dick et al., 2014)

Interestingly, *P. cinnamomi* was often co-isolated with another *Phytophthora* species from the soil surrounding infected eucalyptus trees, *Phytophthora multivora* and, as such, it was thought that this co-isolated species may also have a role in dieback disease progression (Scott et al., 2009). Although infection and ecosystem collapse was due to *P. cinnamomi* infection, it is thought that in many cases, *P. multivora* is the causative agent of tree mortality (Scott et al., 2009). *P. multivora* was initially identified as *Phytophthora citricola* (Scott et al., 2009), but was later re-classified to be a new species. *P. multivora* primarily infects woody plants in nurseries and urban plantations, and was first isolated in and thought to be native to Western Australia, but has since been found on five continents (Europe, North America, Oceania, Africa and Asia) (Tsykun et al., 2022).

Another *Phytophthora* species that has been found to cause terminal disease of forest trees is *Phytophthora agathidicida,* which is responsible for causing a root and collar dieback of New Zealand's most iconic and oldest tree species, *Agathis australis* (kauri) (Black et al., 2018). Symptoms of this disease, commonly referred to as kauri dieback, develop relatively late in the infection cycle after a dormancy period which can range in time up to ten years (Bradshaw et al., 2020). Common symptoms of infection are eventually visible above ground, which include thinning and yellowing of leaves in the canopy, as well as excessive resin production, known as gummosis, which leaks out of lesions in the trunk of the tree (Waipara et al., 2013) (Figure 1.2).

Figure 1. 2. **Symptoms of kauri dieback disease.** (A) Visible canopy thinning of a mature kauri tree on the left. (B) Excess resin leakage from a trunk lesion (gummosis). (C) The outer layers of the vascular tissue has become discoloured (white arrow) leading to dysfunction. (D) Kauri supports an abundant range of species to form an epiphyte community. (E) A lesion at the base of an untreated, diseased kauri tree. (F) A lesion in the trunk of a phosphite-treated tree. Figured sourced from Bradshaw et al. (2020).

1.4: Identification of kauri dieback disease

Kauri dieback was first identified in 1972 on Great Barrier Island, when a few dead trees were noticed in a stand, while others were visibly symptomatic, having discoloured foliage and cankers with resin leakage (Gadgil, 1974). The species responsible was initially identified as *Phytophthora heveae*, but then re-classified as *Phytophthora* taxon *agathis* (Beever et al., 2009) and, more recently, *P. agathidicida* (Weir et al., 2015). The disease was identified on the mainland 34 years later in 2006 in the Waitakere Ranges, located on the west coast of the Auckland region, and was likely brought over through movement of contaminated soil and soil water (Beever et al., 2009). However, there are two suggested theories about the origin of *P. agathidicida* and how it came about in New Zealand. One theory is that *P. agathidicida* was introduced to New Zealand around the 1940s–1950s, and is based on the observation that this species demonstrates a high level of genomic diversity to other *Phytophthora* species, indicative of recent divergence (The introduction of *Phytophthora agathidicida* to Aotearoa, 2021; Weir et al., 2015). This theory would suggest that the movement of *P. agathidicida* to New Zealand occurred relatively recently. In contrast, there is evidence to indicate this pathogen has been here for a long time. In a study by Winkworth et al. (2021), research suggested divergence from an ancestor that was already prominent in New Zealand. The mitochondrial genomes of *P. agathidicida* showed similarities in size and gene arrangement with other *Phytophthora* species, allowing a timeline to be constructed which suggests divergence around 300 years ago, differing from the theory of a recent introduction to New Zealand.

1.5: Lifecycle of soil-borne *Phytophthora* species

The lifecycle of plant-pathogenic soil-borne *Phytophthora* species consists of both a sexual and asexual phase (Figure 1.3). Zoospores are motile, unicellular, biflagellate structures that can move through water in the soil to initiate contact with a susceptible host root and are often guided by chemotaxis in the form of root exudate (Tyler, 2002). Upon contact, the zoospores initiate cyst formation, which triggers hyphal growth and subsequent penetration of the root and colonisation of vascular tissue (Bradshaw et al., 2020; Bronkhorst et al., 2021). *Phytophthora* has evolved a slicing mechanism to generate damage to allow access to the apoplast of the roots and continue the infection cycle (Bronkhorst et al., 2021). Here, hyphae grow along the cell before pressing into the cell to create an indentation, the pressure of which results in enough tension to fracture the cell surface. Inside the root, sexual reproduction occurs to produce oospores which germinate to give sporangia containing the motile zoospores. The zoospores are then released, and the infection cycle continues.

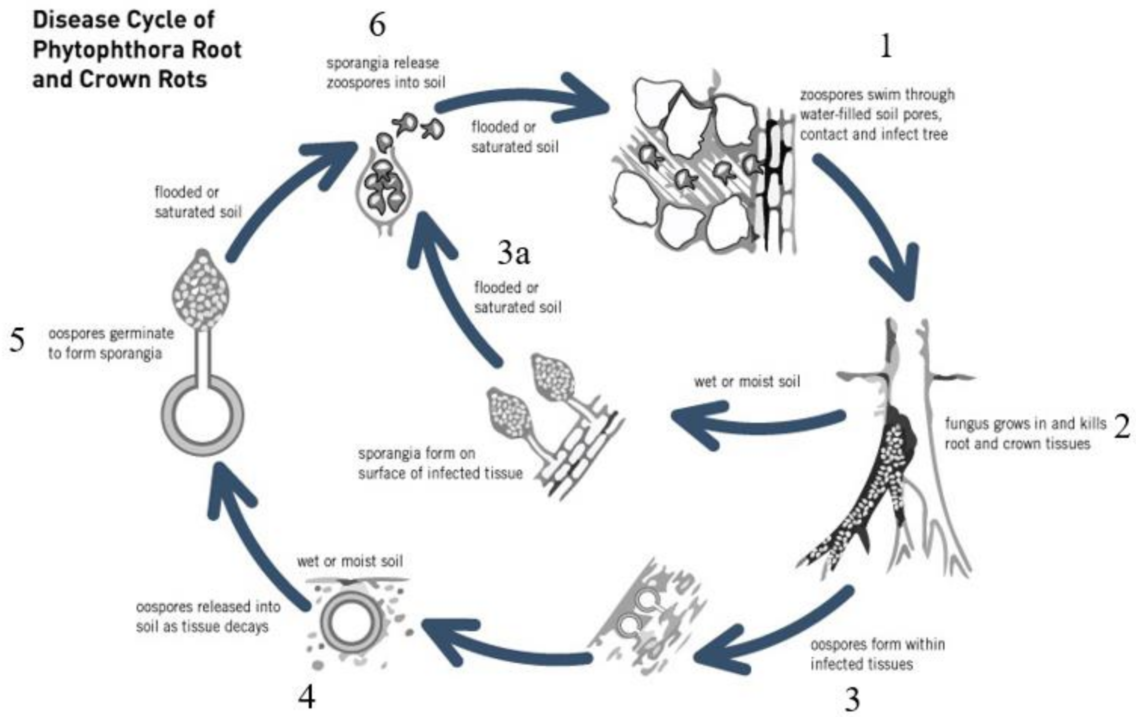

Figure 1. 3. **Disease and infection cycle of *Phytophthora* pathogens.** 1. Motile zoospores initiate infection on host root through cyst formation. 2. Hyphae grow from cysts and colonise the root. 3. Reproduction occurs to form oospores. 4. The oospores formed are released into the surrounding soil. 5. Oospores germinate to produce sporangia and release zoospores. 3a. Sporangia can be produced directly from colonised roots. Figure sourced from New York State Integrated Pest Management Program (Wilcox, 1992).

1.6: Kauri and kauri dieback distribution

Kauri trees are culturally significant as they are considered living ancestors to Māori and their health directly correlates to the health of the people and of the forest. Thus, finding ways to protect kauri is of the upmost importance. Kauri was widely distributed throughout New Zealand prior to European colonisation. The original forests were over one million hectares in size, but now only 7,500 hectares of the original forest remain (Steward & Beveridge, 2010) (Figure 1.4). An additional 60,000 hectares have naturally regenerated; however, this is approximately a 90% reduction compared to pre-European colonization (Halkett, 1983; Winkworth et al., 2021). The reduction was due to unregulated logging and burning of the forests which were to clear land for other uses as well as to meet demands for export and building supply due to the high durability of the timber (Powderly, 2019). The remaining original forests are restricted to the upper North Island and Great Barrier Island; however, smaller plantations exist further south in protected reserves (Silvester & Orchard, 1999).

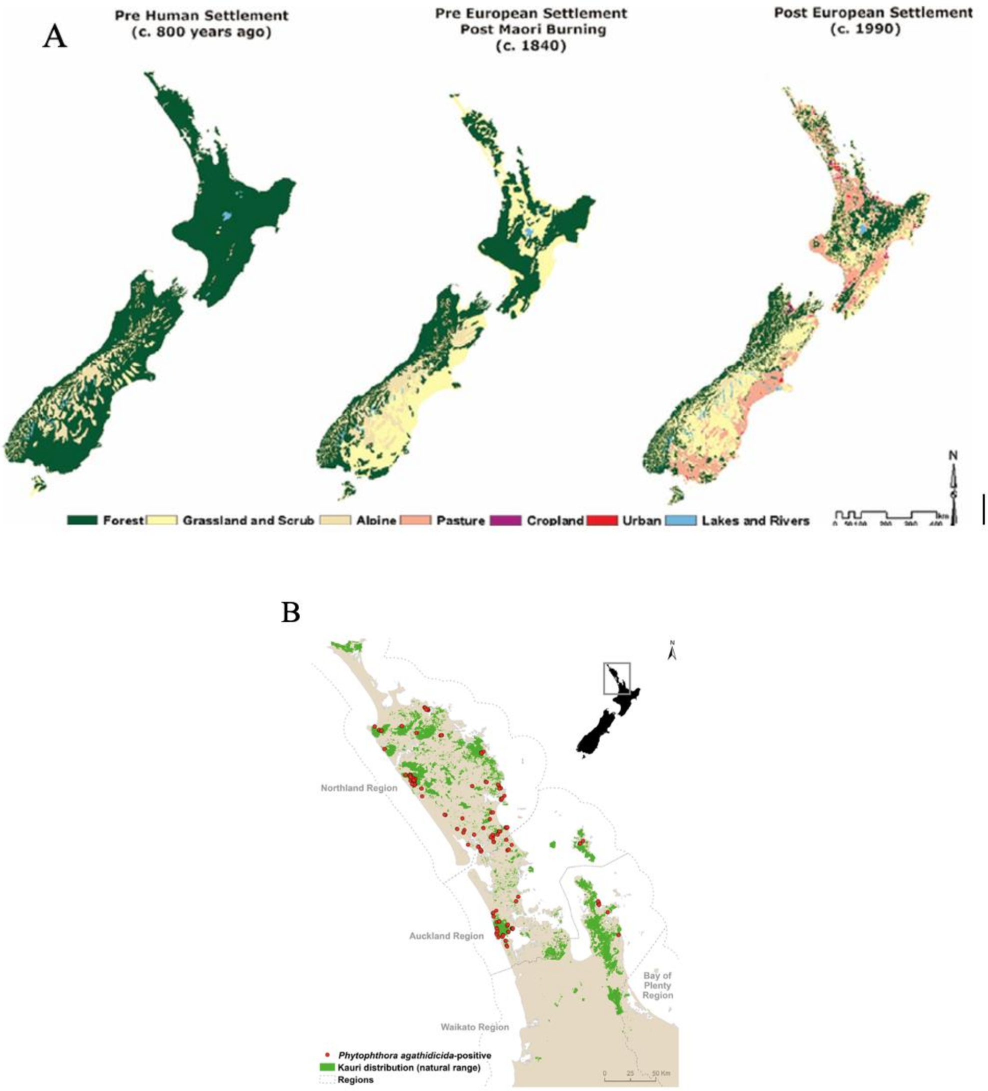

Figure 1. 4. **Reduction in native forests in New Zealand.** (A) A map of New Zealand showing the reduction in native forests pre-, during and post-European settlement. Colour-coded key below stating the types of terrain. Map sourced from Weeks et al. (2012). (B) Current distribution map of natural kauri forests in the upper North Island of New Zealand. Kauri forests are indicated by green areas and red dots show where *Phytophthora agathidicida* has been identified. The distribution map was sourced from Biosecurity New Zealand, Ministry of Primary Industries (Crown copyright), is based on data from various sources as of 14 August 2019 and published in Bradshaw et al (2020).

1.7: Kauri dieback spread in New Zealand forests

Of the remaining original kauri forests, many have trees that are infected with kauri dieback disease. There are minimal data showing total kauri infections by *P. agathidicida* nationally; however, in the Waitakere Ranges, there is a good amount of data for the largest kauri forest (16,000 hectares) in New Zealand (Hill et al., 2017). In this forest, 18.95% of kauri trees had confirmed infection in 2016, with another 5% probable infection (Hill et al., 2017). It is likely that this number was an underestimation due to this study primarily looking at visible symptoms above ground, especially because *P. agathidicida* infects via roots and can therefore go undetected due to a dormancy phase prior to causing visible disease symptoms which varies depending on tree age. Sampling in 2021 revealed that the prevalence of *P. agathidicida* has remained localised in the areas identified from previous sampling runs and has not become more distributed (Froud et al., 2022). In 2022, a national plan to protect kauri was established which provides funding to support the regular testing undertaken in the Waitakere Ranges by local councils. This testing involves aerial surveillance to identify disease progression and to identify areas of high risk, which is followed by routine soil sampling to detect the presence of *P. agathidicida* (Froud et al., 2022).

1.8: The importance of kauri

Minimising the spread of kauri dieback disease is important because kauri trees also play a critical role in the forest ecosystem (Ryder, 2016). Kauri is considered a foundation species, which is defined as a species that has a significant role in changing the surrounding environment characteristics but, in doing so, supports a stable environment that can support other species (Wyse et al., 2013). The soil has a low pH and is nutrient-poor, which affects other species and communities surrounding the trees. Kauri also provide protection through shelter to smaller species and some plants, such as tropical pacific species, which can only survive in these environments due to the podzol soil kauri create (Silvester & Orchard, 1999; Verkaik et al., 2006). Additionally, kauri itself provides an environment for epiphyte species: 48 species which live on the trunk bark were reported by Wyse and Burns (2011).

1.9: Prevention and treatments used for kauri dieback

Although the ability to identify how many kauri trees are infected with *P. agathidicida*, as well as to find trees at an early stage of infection, which may provide good information for further studies, there is currently no cure for kauri dieback disease. The current treatment for this disease involves multiple injections of phosphite into the base of the tree, which is extremely time consuming due to the manual work involved for each tree (Andronis et al., 2022; Hardy et al., 2001). Phosphite has a complex mode of action but is thought to promote an intense immune response within a plant while inhibiting the growth of the oomycete; however it is only capable of reducing disease severity (Guest & Grant, 1990; Horner & Hough, 2011). While phosphite injections have not been shown to cure the disease, healing of active lesions or a reduction of symptoms has been observed at an appropriate concentration for each specific tree (Horner et al., 2015). However, phytotoxicity has also been noticed in a small proportion of trees alongside rapid decline in severely diseased trees following injection (Horner et al., 2015).

Following the phosphite treatment study by Horner et al (2015), cleaning stations to remove soil and disinfect walking equipment and shoes with Sterigene were set up by the Department of Conservation (DOC) in April 2018. However, public compliance was poor (Aley et al., 2023). Following this, in October 2018, 21 kauri tracks were closed to the public as a part of a rāhui to prevent further spread of the disease. Alternative methods of control are now being investigated as phosphite injections, closure of tracks and washing stations are not a viable long-term solution for effective control of kauri dieback disease.

Recently, a study by Lacey et al. (2021) investigated the effectiveness of the commonly used anti-oomycete treatment oxathiapiprolin. It is an oomycide compound that targets oxysterol-binding proteins and inhibits multiple lifecycle stages of *Phytophthora* (Miao et al., 2016). This compound was tested on both *P. agathidicida* and *P. cinnamomi* for inhibitory effects on mycelial growth, zoospore motility and oospore and zoospore germination. It was found that at very low concentrations (0.01 ng/ml), inhibition of mycelial growth was observed, with *P. agathidicida* determined to be around five to ten times more sensitive than other *Phytophthora* species tested (Lacey et al., 2021). However, these effects were not shown on zoospore motility as motility was still observed at high concentrations (1 µg/mL). Oospores in culture were unable to germinate in the presence of oxathiapiprolin but were still viable even at high concentrations. In zoospores, inhibition of germination was achieved at varying concentrations dependent on which isolate of *P. agathidicida* was tested.

Interestingly, another study investigated the effect of root and leaf exudates from native plant species on both *P. agathidicida* and *P. cinnamomi* and showed complete inhibition of zoospore motility (Lawrence et al., 2019). Four native plant species; kānuka (*Kunzea ericoides*), kawakawa (*Piper excelsum*), karamū (*Coprosma robusta*) and nīkau (*Rhopalostylis sapida*), were identified for testing due to these species having a role in the early stages of kauri forest establishment, along with their natural medicinal properties, which were highlighted from working with local Māori communities. Of interest, three compounds from kānuka were identified as flavanones and were able to completely inhibit zoospore motility at very low concentrations. The ability to prevent zoospore motility means that the infection cycle does not begin and may be beneficial in a kauri forest setting.

1.11: The plant immune system and effector proteins

Plants have preformed defences that consist of physical barriers such as the plant cell wall and cuticle (Newman et al., 2013), as well as chemical defences such as antimicrobial secondary metabolites and proteins (Neilson et al., 2013), which provide a first line of defence against potential microbial pathogens. A subset of microbial pathogens, however, will be able to breach or overcome these preformed physical and chemical defences and, in these situations, plants must rely on their second line of defence, their innate immune system, to deliver induced defence responses that will ultimately provide resistance.

The plant immune system is made up of two branches: extracellular immunity, which occurs in the plant apoplast and is commonly referred to as pattern-triggered immunity (PTI), and intracellular immunity, which occurs inside plant cells and is commonly referred to as effector-triggered immunity (ETI) (Jones & Dangl, 2006). Despite these spatial differences in immunity, there is extensive crosstalk between the branches, with PTI and ETI mutually potentiating each other to provide robust defence responses during infection by microbial pathogens (Pruitt et al., 2021).

In the first branch of the immune system, PTI, plants use cell surface-localized immune receptors called pattern recognition receptors (PRRs) to recognize extracellular invasion patterns. PRRs can be divided into receptor-like proteins (RLPs) and receptor-like kinases (RLKs); however, unlike RLKs, RLPs lack an intracellular kinase domain which enables signal transduction following invasion pattern recognition. To enable signal transduction, RLPs usually must constitutively interact with an RLK co-receptor called SOBIR1 (Liebrand et al., 2013; Liebrand et al., 2014). Following invasion pattern recognition, this RLP–SOBIR1 complex typically then recruits another RLK co-receptor, BAK1 (Li & Tax, 2013), which can transphosphorylate the complex, initiating an intracellular signal cascade that triggers immune responses (Albert et al., 2015; van der Burgh & Joosten, 2019). In terms of the invasion patterns recognised by PRRs, these can be pathogen-associated molecular patterns (PAMPs), which are conserved structures such as flagellin or β-glucan (Newman et al., 2013), or damage-associated molecular patterns (DAMPs), which are plant-derived molecules that are released during infection or damage (Boller & Felix, 2009).

To circumvent, suppress or prevent PTI, as well as to overcome constitutive chemical defences in the apoplast, microbial pathogens must deliver a collection of virulence factors, termed effector proteins, into the apoplast and the cytoplasm of their host cells. These are called apoplastic and cytoplasmic effectors, respectively, and are typically proteins or secondary metabolites (Fabro, 2022; Rocafort et al., 2020). Of note, in addition to modulating the plant immune system, a subset of these effectors will promote host colonization through other means such as through the acquisition of nutrients or the modulation of host physiology (Doehlemann et al., 2017; Franceschetti et al., 2017). In the case of *Phytophthora* pathogens, the delivery of effector proteins into the cytoplasm of plant cells is achieved through specialized infection structures called haustoria (Panstruga & Dodds, 2009).

An example of an apoplastic *Phytophthora* effector protein is aldose-1-epimerase (AEP1), which functions in sugar uptake (Xu et al., 2021), while an example of a cytoplasmic *Phytophthora* effector is PsCRN70, a crinkler (CRN) protein that suppress plant defences (Rajput et al., 2014). Notably, in some cases, apoplastic effector proteins can also be recognized as invasion patterns, leading to PTI. One example is XEG1 of the soybean pathogen, *Phytophthora sojae*, which is a carbohydrate-active enzyme (CAZyme) effector of glycoside hydrolase family 12 (GH12) that functions to degrade the cell wall and is recognised by the RLP XEG1 in *Nicotiana benthamiana* (Ma et al., 2015).

To reinstate resistance, in the second branch of the plant immune system (ETI), intracellular immune receptors called resistance (R) proteins recognize specific intracellular effectors. These proteins are typically nucleotide-binding leucine-rich repeat receptors (NLRs) (Zipfel, 2014). In any case, recognition by PRRs in PTI or NLRs in ETI triggers several immune responses such as localized cell death that function to restrict or halt the pathogen (Tsuda & Katagiri, 2010). Successful microbial pathogens may, however, also possess effectors that are capable or circumventing, suppressing or preventing ETI (Jones & Dangl, 2006).

1.12: Effectors with roles in microbiota modulation

As mentioned above, effectors do not only function in overcoming preformed chemical defences or defences associated with PTI and ETI. Indeed, emerging evidence suggests that a subset of effectors function in manipulating the microbiota of host plants (phyllosphere) or the microbiota of their surrounding environments (rhizosphere) to promote host colonization (Rovenich et al., 2014; Snelders et al., 2020). Such manipulation is important, as it may allow the pathogens to antagonise or ward off microbial enemies, or to outcompete microbial competitors for essential nutrients.

Most of the research surrounding host microbiome manipulation has been undertaken in fungi and largely involves secondary metabolites. As oomycetes do not have a large capacity to produce secondary metabolites (Soanes et al., 2007), it is likely that antagonistic interactions between oomycetes and other microbes involve proteinaceous effectors. A well-known example of an effector protein that functions in microbiota manipulation is Ave1 from the fungal wilt pathogen *Verticillium dahliae* (Snelders et al., 2020). Ave1 was shown to have antimicrobial activity associated with the microbiota of soil. More specifically, the study showed that Ave1 could selectively inhibit gram-positive bacteria and was shown to have bactericidal properties. This allows suppression of antagonistic bacteria that colonise the host enabling *V. dahliae* to outcompete and to promote disease progression. Ave1 was also tested against fungal species, however no antifungal activity was detected. In another example, Eitzen et al. (2021) found that MbA-GH25 is a glycoside hydrolase family 25 effector protein secreted by the yeast *Moesziomyces bullatus ex Albugo* (MbA) that can manipulate the growth of the oomycete *Albugo laibachii* during colonization of *Arabidopsis* (Eitzen et al., 2021). This enables MbA to efficiently colonise the host cell surface, shielding the host from pathogenic competition, in turn reducing symptoms and disease. Finally, *Zymoseptoria tritici*, a fungal pathogen of wheat, secretes a ribonuclease effector (Zt6) that functions by cleaving rRNA, resulting in toxicity to those it encounters, but is ineffective against itself (Kettles et al., 2018). Being able to effectively eliminate competition through use of Zt6 is anticipated to promote host colonisation by the pathogen and therefore enhance disease.

Currently, there are few oomycete effectors that have been characterised with antimicrobial activity. However, it is known that *Albugo candida*, an oomycete, can change the growth of surrounding bacterial species through the secretion of yet-unidentified apoplastic effectors (Gómez-Pérez et al., 2023). Furthermore, crinkler effectors from *P. sojae* (PsCRN63) and

Phytophthora capsici have been shown to impair the growth of *Escherichia coli* in culture through some sort of yet-uncharacterized toxic activity (Wang et al., 2020). In the same study, other effectors were also shown to interfere with bacterial motility (specifically, the *P. capsisci* CRN effector PcCRN173 and RXLR effector PcAvh540).

1.13: *Phytophthora agathidicida–Phytophthora* interactions

Interestingly, *P. agathidicida* is commonly co-isolated with other *Phytophthora* species. More specifically, *P. cinnamomi* and *P. multivora* were co-isolated from the rhizosphere surrounding infected kauri trees (Waipara et al., 2013). Furthermore, in glasshouse trials both *P. multivora* and *P. cinnamomi* were found to cause disease lesions on kauri seedlings (Horner & Hough, 2014). This infers that these two species may have a role in causing disease within forests and it has been suggested that these species could act synergistically to enhance disease if conditions were right (Waipara et al., 2013). However, this is the extent of our knowledge surrounding their interactions. It could be possible that effectors produced by these species promote the growth of each other during infection or that one species is able to hijack or piggyback off the effectors produced by another (e.g. *P. multivora* could benefit from effectors produced by *P. agathidicida*). Alternatively, these effectors could have a role in antagonism (e.g. specific *P. agathidicida* effectors could ward off or be used to outcompete *P. cinnamomi* and/or *P. multivora*). Understanding whether *P. agathidicida*, *P. cinnamomi* and *P. multivora* interact with each other to cause disease is vital to the successful control of kauri dieback. Indeed, this information will not only help identify the need to target a broader range of species in a treatment but may also provide further information about the infection of kauri, and whether all species being isolated together is an indicator of the potential for more severe infection. It may be that successful control measures need to not only target *P. agathidicida*, but also other co-occurring *Phytophthora* pathogens. Experiments are now needed to investigate these questions.

1.14: Hypothesis, Aims and Objectives

The **hypothesis** of this study is that *P. agathidicida*, *P. multivora* and *P. cinnamomi* antagonise each other in culture at both a visual macroscopic level and the molecular protein level. To test this hypothesis, the **aims** of this study are to: 1) determine whether colonies of *P. agathidicida*, *P. cinnamomi* and *P. multivora* interact with or repel each other during growth on solid growth media (**Objective 1**); 2) determine whether the secreted protein profiles of *P. agathidicida*, *P. cinnamomi* and *P. multivora* change upon co-culturing in liquid growth media (**Objective 2**); and 3) investigate whether the angiosperm plant *Nicotiana benthamiana* can be used as a model host for studying antagonistic or disease-promoting interactions between *P. agathidicida, P. cinnamomi* and *P. multivora* (**Objective 3**).

Objective 1: To determine if colonies of *P. agathidicida*, *P. cinnamomi* and *P. multivora* interact with or repel each other at the macroscopic level in culture, an interspecies colony interaction test will be carried out on different solid media types: two nutrient-rich (clarified V8 and carrot) and two nutrient-poor (plich and cornmeal + PARP antibiotics). Here, *P. agathidicida*, *P. cinnamomi* and *P. multivora* will be co-cultured on solid media plates to determine whether a barrage zone (line of growth inhibition) is formed between colonies of the three different species. At the same time, an intraspecies interaction assay will be carried out between colonies of the same species to ensure that any observed barrage zones are specific to a given interspecies interaction.

Objective 2: To determine if *P. agathidicida*, *P. cinnamomi* and *P. multivora* interact at the molecular level in culture, a proteomic analysis of culture filtrate following growth in clarified V8 liquid broth will be completed using liquid chromatography–mass spectrometry (LC–MS). Here, a specific focus will be on determining whether qualitative (presence/absence) and quantitative differences occur between the secreted protein profiles of the three species when cultured in the presence of one or both of the other species, relative to when cultured alone.

Objective 3: To investigate whether *N. benthamiana* can be used as a model plant host for studying antagonistic or disease-promoting interactions between *P. agathidicida*, *P. cinnamomi* and *P. multivora* in future studies, each will be assessed for their ability to cause disease lesions on detached leaves over time.

Chapter Two: Materials and Methods

2.1: Biological materials

The microorganism and plant species used in this study are listed in Table 2.1.

***Table 2. 1*. Microorganism and plant species used in this study.**

Species	Isolate/accession and characteristics	Notes	Reference
Microorganisms	**Isolate**		
Phytophthora agathidicida	NZFS 3770. Wild-type.	Isolated from *Agathis australis* in Great Barrier Island, New Zealand	(Studholme et al., 2016)
Phytophthora cinnamomi	NZFS 3750. Wild-type.	Isolated from *Pinus radiata* in Nelson, New Zealand	(Studholme et al., 2016)
Phytophthora multivora	NZFS 3378. Wild-type.	Isolated from *Idesia polycarpa* in Auckland, New Zealand	(Studholme et al., 2016)
Plants	**Accession**		
Nicotiana benthamiana	No accession number known (Goodin et al. 2008). Wild-type		Dr. K. Sohn (formerly Massey University)
N. benthamiana	No accession number known (Goodin et al. 2008). Wild-type		(Huang et al., 2020)
N. benthamiana	No accession number known (Goodin et al. 2008). Δ*sobir1* mutant[1]		(Huang et al., 2020)

[1]The *SOBIR1* gene encodes a co-receptor of extracellular plant immune receptors called receptor-like proteins (RLPs) and is involved in transducing defence response signals following extracellular (apoplastic) pathogen recognition by RLPs (Liebrand et al., 2013).

2.1.1: *Phytophthora* species

Phytophthora agathidicida strain NZFS 3370, *Phytophthora multivora* strain NZFS 3778 and *Phytophthora cinnamomi* strain NZFS 3750 were used throughout the study for all culturing and *in planta* work (Table 2.1). These strains were selected because they have sequenced genomes that are well-annotated (Cox et al., 2022; Studholme et al., 2016). The three species were chosen as they had previously been co-isolated together from soil samples taken from the surroundings of infected kauri trees (Waipara et al., 2013). It is important to note, however, that the specific isolates used in this study were not co-isolated from soil samples taken from the surroundings of infected kauri trees, as no co-isolated isolates were stored by Waipara et al. (2013).

2.1.2: *Nicotiana benthamiana*

Wild-type *Nicotiana benthamiana* (model) plants were used for *in planta* infection assays (lesion assessments) involving the three *Phytophthora* species (Table 2.1). A Δ*sobir1* knockout mutant of *N. benthamiana* (Huang et al., 2021) was also used to determine whether receptor-like protein (RLP) plant immune receptors play an active role in determining the size of lesions formed by the three *Phytophthora* species (Table 2.1).

2.2: Culturing of *Phytophthora* species

2.2.1: Growth on solid media

All solid media types (clarified V8, carrot, plich, cornmeal + PARP antibiotics) used for the culturing of *Phytophthora* species were prepared following the recipes provided in Appendix 1.1. Prior to solidification, agar media were poured into nine cm Petri dishes (plates; LabServ), left to solidify, and then stored at 4°C until required. *Phytophthora* species were initially cultured from pre-existing stocks that had been stored at 4°C on either clarified V8 agar plugs in sterile water or clarified V8 agar plates. Here, individual plugs, or plugs generated through use of a sterile cork borer, were placed onto fresh agar plates and incubated at 22°C in the dark for ten days to promote active growth. Next, a sterile cork borer was used to extract uniform agar plugs from the outer margin (i.e. up to one cm from the advancing front) of actively growing cultures, and transferred to a specific agar media type for use in the various experiments (see below for more information). All agar plug transfers were undertaken in a Class II biohazard cabinet (BH2000 Series, model BHA120). Once the agar plugs had been transferred, all *Phytophthora* species were cultured as above for different time periods depending on the experiment being performed.

2.2.2: Growth in liquid media

All liquid media types (clarified V8 vegetable juice, carrot, plich and cornmeal + antibiotics) used for the culturing of *Phytophthora* species were prepared following the recipes provided in Appendix 1.1. A total of 10 mL liquid medium was pipetted into nine cm plates and then up to three five mm agar plugs carrying the *Phytophthora* species of interest were transferred to the medium according to Section 2.2.1, with the plates subsequently sealed with Parafilm M (Bemis). Once sealed, the plates were transferred to a plastic box which was wrapped in tinfoil and cultured as described in Section 2.2.1, without shaking, for three or seven days.

2.2.3: Passaging of *Phytophthora* species through pear

To ensure *Phytophthora* remained healthy after regular subculturing, each species was passaged through a green pear purchased from the local supermarket (PAK'nSave). First, the pear was left to ripen until it was soft to the touch. Then, the outside of the pear was surface-sterilised with 70% ethanol before a sterile scalpel was used to cut a "door" (3 sides of a box, 1 cm x 1 cm) into different faces of the pear. Once these "doors" had been created, an agar plug carrying the *Phytophthora* species to be passaged, prepared as described in Section 2.2.1, was placed inside. Each "door" with an agar plug inside was then closed and the pear wrapped in Parafilm M and tinfoil before being maintained at 22°C in the dark for at least one week inside sealed plastic boxes. After visible lesions were observed on the outside of the pear, a sterile scalpel was used to cut the pear in half vertically. A small 1 cm x 1 cm square was subsequently taken from the outside edge of each lesion, placed onto a cornmeal agar plate containing PARP antibiotics (Appendix 1.1), and then incubated for one week under the conditions described in Section 2.2.1. Finally, the outside edge of the resulting colony was transferred onto clarified V8 agar and cultured as per Section 2.1.1 for storage or use in subsequent experiments.

2.2.4: Intraspecific and interspecific colony interactions assays (for Objective 1)

Intraspecific (single-species) and interspecific (multi-species) *Phytophthora* colony interaction assays were set up according to specific combinations shown in Table 2.2, each with four biological replicates. Briefly, agar plugs were taken from actively growing regions of *Phytophthora* culture plates as described in Section 2.2.1 and placed onto a new set of agar plates (clarified V8, carrot, plich, and cornmeal + antibiotics) in a triangular formation (Figure 2.1A). Plates were then sealed with Parafilm M, covered in tinfoil, and cultured as described in Section 2.2.1 for four to seven days. Plates were checked daily to determine whether a zone of growth inhibition had formed between the colonies, and to determine when the radial growth of each colony had stopped. As part of this experiment, a single plug from each species was also placed onto a fresh agar plate of each media type (at the corresponding location of one of the three agar plugs in Figure 2.1A) to ensure that differences in the observed growth profile were specifically due to the presence of other colonies or species (Figure 2.1B).

***Table 2. 2. Phytophthora* species combinations used for the intraspecific and interspecific colony interactions assays in Objective 1.**

***Phytophthora* species combination**
***P. agathidicida* + *P. agathidicida* + *P. agathidicida*[1]**
***P. cinnamomi* + *P. cinnamomi* + *P. cinnamomi*[1]**
***P. multivora* + *P. multivora* + *P. multivora*[1]**
P. agathidicida* + *P. agathidicida* + *P. cinnamomi
P. agathidicida* + *P. agathidicida* + *P. multivora
P. cinnamomi* + *P. cinnamomi* + *P. multivora
P. cinnamomi* + *P. cinnamomi* + *P. agathidicida
P. multivora* + *P. multivora* + *P. cinnamomi
P. multivora* + *P. multivora* + *P. agathidicida
P. agathidicida* + *P. cinnamomi* + *P. multivora
***P. agathidicida*[2]**
***P. cinnamomi*[2]**
***P. multivora*[2]**

[1]Control for barrage zone formation and colony growth.

[2]Control for growth of single colonies.

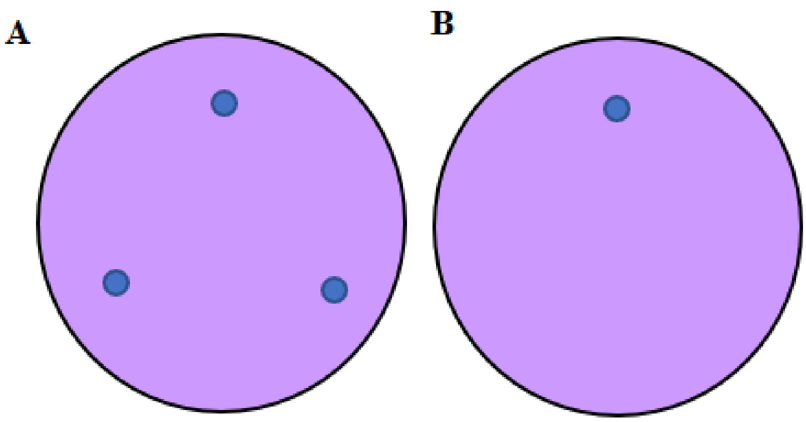

Figure 2. 1. **Schematic showing the positioning of *Phytophthora* agar plugs on nine cm solid growth medium plates for intraspecific and interspecific colony interactions assays.** A = positioning of agar plugs for a three-way colony interaction assay. B = positioning of an agar plug for a single-colony growth assay.

2.3: Proteomic analysis of *Phytophthora* culture filtrates (for Objective 2)

Single- and multi-species liquid cultures were set up as per Section 2.2.2 according to the combinations shown in Table 2.3, each with four biological replicates.

A flowchart summary of the proteomic and subsequent bioinformatic work in provided in Appendix 1: Figure A7.

Table 2. 3. Phytophthora **species combinations used for Objective 2.**

***Phytophthora* species combination**
P. agathidicida[1]
P. cinnamomi[1]
P. multivora[1]
P. agathidicida* + *P. cinnamomi
P. agathidicida* + *P. multivora
P. cinnamomi* + *P. multivora
P. agathidicida* + *P. cinnamomi* + *P. agathidicida

[1]Proteomics baseline to which multi-species samples containing the species in question were compared.

2.3.1: Harvesting, freeze-drying and storage of culture filtrate samples

At three or seven days post-inoculation, culture filtrates from Section 2.3 were harvested by filtration through a single layer of Miracloth (EMD Millipore) into a 50 mL Falcon tube (FisherScientific), frozen at –20°C, and then freeze-dried. Freeze-drying was carried out as follows: the lids of the tubes were pierced with a flame-sterilized needle, arranged into a 10 L freeze-drying container, and maintained at –20°C for a further 10 min to ensure samples were completely frozen. The culture filtrate samples were then freeze-dried for three days at –91°C, with the tubes subsequently removed from the freeze-drier and returned to –20°C until required. Of note, the *Phytophthora* biomass captured by the Miracloth (EMD Millipore) was retained, dried with paper towels and wrapped in tinfoil, then snap-frozen in liquid nitrogen before being stored at –80°C (in case they were required for evaluation of gene expression or total protein levels in future studies).

2.3.2: Gel electrophoresis, staining and de-staining

The freeze-dried culture filtrate samples from Section 2.3.1 were resuspended in 100 μL of sterile milliQ water, and 20 μL of the resuspended samples were each transferred to an independent 1.5 mL microcentrifuge tube (Axygen) containing 10 μL of loading dye (2.1% (v/v) Tris-HCl (Invitrogen) from a 15% (w/v) pH 6.8 stock solution, 52% (v/v) glycerol (Sigma-Aldrich), 4.2% (v/v) SDS (Invitrogen) from a 20% stock solution and 0.02% (v/v) bromophenol blue (Bio-Rad Laboratories) from a 1% stock solution). At the same time, 20 μL of BSA (bovine serum albumin) was added to 10 μL loading dye as a positive control. Next, the samples were resolved by sodium dodecyl sulphate–polyacrylamide gel electrophoresis (SDS-PAGE) to separate the proteins based on molecular weight using a 4–20% precast Mini-PROTEAN TGX gel (BioRad), which was set up with 1 x SDS running buffer (Appendix 1.2). Here, the samples were loaded onto the precast gel according to Figure 2.2, with the gel subsequently run at 100 V for 10 min followed by a further 20 min at 200 V.

Gel lane	1	2	3	4	5	6	7	8	9	10
Content	Ladder		Rep 1		Rep 2		Rep 3		Rep 4	BSA

Figure 2. 2. **Map of precast gel specifying the sample present in each lane.** Rep = Biological replicate 1–4, BSA = Bovine Serum Albumin.

Following SDS-PAGE, the gel cassette was opened and rinsed with milliQ water before being transferred to a plastic container for staining overnight on a gentle orbital shaker with 25 mL Colloidal Coomassie stain (0.1% (w/v) brilliant blue G250 Coomassie (Sigma), 10% (w/v) ammonium sulphate $(NH_4)_2SO_4$ (Sigma), 1% (v/v) phosphoric acid (Ajax FineChem)) and methanol (Fisher Scientific), mixed in a 4:1 ratio.

Upon completion of staining, the gel was rinsed with milliQ water to draw out excess stain, before being cut into lanes with a sterile scalpel blade. Each lane was then cut into six sections, labelled A–F, with A being the higher molecular weight portion of the gel and F the lower molecular weight portion. From here, each section was diced and placed into an independent 1.5 mL Lo-Bind centrifuge tube (Eppendorf) containing 500 µL of 1 x ABC/methanol (0.4% (v/v) ammonium bicarbonate (Fisher Scientific), 50% (v/v) methanol, 25% (v/v) mass spectrometry (MS)-grade water (Fisher Scientific)). Finally, the tubes were incubated at 45°C for 20 min before the supernatant was pipetted out and the process repeated with 300 µL of 1 x ABC/methanol until gel pieces were completely transparent and colourless.

2.3.3: Protein reduction and alkylation

To the de-stained gel pieces of Section 2.3.2, 500 µL of 80% acetonitrile (MeCN (Fisher Scientific)) was added and vortexed briefly until the gel pieces were dry and white in colour. The supernatant was discarded and tubes were placed in a SpeedVac (Savant SPD131DDA SpeedVac Concentrator, Thermo Scientific) for 10 min and 0.01 torr and 45°C to remove residual liquid. To the gel pieces, 150 µL of reducing solution (10 mM dithiothreitol ((DTT), Sigma) from a 1 M stock solution (15.4% (w/v) in 1 x ABC) was then added and left to incubate at 45°C for 1 h. Following this step, the supernatant was discarded, and gel the pieces rinsed with 200 µL 1 x ABC. The previous steps were repeated, substituting the reduction solution with 200 µL alkylation solution (20 mM iodoacetamide (Sigma-Aldrich) in 1 x ABC). The tubes containing the gel pieces were then left in the dark at room temperature for 30 min. The supernatant was subsequently removed and discarded, and the following steps were repeated twice, removing the supernatant in between: 150 µL 1x ABC followed by 500 µL 80% (v/v) $MeCN/H_2O$. Finally, the samples were added to the SpeedVac for 10 min as above to remove residual liquid before 130 uL of trypsin digestion solution (0.1% (v/v) 20 mM $CaCl_2$ in 75 µL of trypsin (Sigma Aldrich), held on ice for 2 min before being added to 3.75 mL 1 x ABC to give a 2% (v/v) trypsin solution) was added and incubated overnight at 37°C.

2.3.4: Protein extraction

Tubes containing the trypsin-treated samples from Section 2.3.3 were vortexed briefly and sonicated (Elmasonic, ELS030H) for two min in room-temperature water. The supernatant from each sample was then transferred to a fresh Protein LoBind (Eppendorf). Following this step, 110 µL of 5% (v/v) formic acid (Ajax Finechem) in 40% (v/v) MeCN was added to each sample and sonicated for 2 min before the supernatant was again transferred to the new Lo-Bind tube. Next, 110 µL of 0.1% (v/v) formic acid in 80% (v/v) MeCN was added to each sample and sonicated as above. This was repeated until the gel pieces were white in colour, with the supernatant subsequently transferred to their corresponding Lo-Bind tube. Finally, the samples were concentrated using a SpeedVac as per Section 2.3.3 until the final volumes were reduced to approximately 30 µL and then transferred to glass vials (ThermoFisher Scientific). The glass vials were stored at –80°C in preparation for liquid chromatography–mass spectrometry (LC–MS) analysis.

2.3.5: Liquid Chromatography–Mass Spectrometry

LC–MS analysis of peptides present in samples from Section 2.3.4 was carried out by Trevor Loo (T.L.) at Massey University in Palmerston North, New Zealand.

The peptides generated through trypsin digestion in Section 2.3.4 were differentiated based on their affinity for water on a reverse-phase C18 column and analysed via MS according to the Top10 method (Michalski et al., 2011). Table 2.4 and Table 2.5 detail the chromatography and spectrometry instrument settings used, respectively. As a first step, a given sample was ionized, accelerated and analysed by MS (MS1). Here, MS1 scans were acquired over a mass-to-charge ratio range of 375–1,600 *m/z*, with detection using an Orbitrap mass analyser set to a resolution of 70,000. Next, the ten most intense ions from the MS1 spectra in each scan cycle were selected for fragmentation via higher energy collisional dissociation (HCD) and analysed by MS to generate spectra for the ion fragments (MS2) using the Orbitrap mass analyser set to a resolution of 17,500. Here, exclusion conditions were optimized to the target properties according to the observed chromatographic peak width (12 sec).

Table 2. 4. **Liquid chromatography–mass spectrometry (LC–MS) instrument configuration.**

nanoLC system	Dionex UltiMate™ 3000 RSLCnano System (ThermoFisher Scientific, Waltham, MA, USA)
Mass spectrometer	Q Exactive™ Plus (ThermoFisher Scientific)
Ionisation source	Nano Flex™ (ThermoFisher Scientific)
Trapping column	Acclaim™ PepMap™ 100 C18, 3µm particle size, 75 µm inner diameter, 2 cm length (ThermoFisher Scientific)
Analytical column	Acclaim™ PepMap™ 100 C18, 2 µm particle size, 75 µm inner diameter, 50 cm length (ThermoFisher Scientific)
Flow rates	Trap: 15 µL/min Analytical: 300 nL/min
Column oven temperature	50°C
Gradient	3–30% acetonitrile in 0.1% formic acid/water over 60 min
Mobile phase	Trap loading: 0.1% TFA/2% MeCN/water Analytical A: 0.1% formic acid/2% MeCN/water Analytical B: 0.1% formic acid/98% MeCN/water

Table 2. 5. **Liquid chromatography–mass spectrometry (LC–MS) mass spectrometer settings.**

Capillary temperature	250°C
S-Lens RF level	50%
Polarity	Positive
Source voltage	1.6 kV
AGC target	Full MS: 3e6, MS2: 1e5
Max. injection times	Full MS: 150 ms, MS2: 110 ms
Full MS scan range	375–1600 *m/z*
Resolution settings	Full MS: 70,000, MS2: 17,500
Number of microscans	1
Isolation width	1.4 m/z
Loop count (TopN)	10
MSX count	1
Normalised collision energy	28
Charge exclusion	Unassigned 1, >6
Peptide match	Preferred
Exclude isotopes	On
Dynamic exclusion	12 sec
Spectrum data type	Full MS: Profile, MS2: Centroid

2.3.6: Analysis of raw LC–MS data

The database search was carried out by T.S.L. and Taylah Dagg (T.D.).

The raw data generated in Section 2.3.5 were searched against proteome databases for each of the *Phytophthora* species on the Proteome Discoverer™ search engine (version 2.4.1.15, ThermoFisher Scientific). These proteome databases were generated by Cox et al. (2022) for *P. agathidicida* and Nick Cauldron (Oregon State University, USA; unpublished results) for *P. cinnamomi* and *P. multivora* (Studholme et al., 2016). The outputs for each gel section (A–F) were then grouped according to the respective gel lane they originated from (one complete lane corresponds to one complete biological replicate of a given sample type).

The search engine outputs using the groups from above were generated according to the parameters and possible modifications (resulting from chemical treatment and suspected natural modifications) listed in Table 2.6. The search parameters also matched the settings of the Q Exactive Plus instrument, meaning that the detected ion mass and the theoretical parental and fragmented ion mass were within a certain range of each other (parental ions are ± 10 ppm and fragment ions are ± 0.02 Da).

Finally, the search engine output was filtered to ensure all peptides had a false discovery rate (FDR) of ≤1%, with at least two unique peptides across a minimum of two biological replicates of a given sample type. A high FDR confidence was required in at least 50% of samples.

Table 2. 6. **Proteome Discoverer search parameters.**

Search engine	Proteome Discoverer™ v2.4.1.15
Databases	*Phytophthora agathidicida* NZFS 3770 predicted proteins, *Phytophthora cinnamomi* NZFS 3750 predicted proteins, *Phytophthora multivora* NZFS 3378 predicted proteins
Taxonomy	*P. agathidicida, P. cinnamomi, P. multivora*
Enzyme	Trypsin
Max number of missed cleavages	2
Minimum peptide length	6
Precursor mass tolerance	10 ppm
Fragment mass tolerance	0.02 Da
Decoy database search	Enabled (default)
Static modifications	Carbamidomethyl (C)
Variable modifications	Oxidation (M), Protein N-terminal acetylation, Met-loss, Met-loss+ Protein N-terminal acetylation
False discovery rate (FDR)	1%
Display Filter	Number of unique peptides ≥ 2

2.3.7: Analysis of proteins identified by LC–MS

All data were sorted and analysed on Microsoft Excel, following file merging using RStudio v4.2.1. The presence of an amino (N)-terminal signal peptide in proteins identified by LC–MS in Section 2.3.6 was determined using SignalP v3.0 (Bendtsen et al., 2004). This version was used as it is the preferred version for predicting oomycete signal peptides (Sperschneider et al., 2015). Here, proteins were determined to have a predicted signal peptide based on the D score generated (>0.43). TMHMM v2.0 (Krogh et al., 2001; Sonnhammer et al., 1998) was used to predict whether the protein possessed a transmembrane domain. The proteins predicted to have a signal peptide and no transmembrane domain (excluding those with a transmembrane helix within the putative signal peptide) were analysed. The remaining proteins were analysed using InterProScan (Paysan-Lafosse et al., 2023) to predict protein function using the Protein family (Pfam) database. dbCAN2 was used to predict carbohydrate-active enzyme (CAZyme) classes using HMMER, DIAMOND and eCAM1 databases (Yin et al., 2012; Zhang et al., 2018); however, at least two of these tools were required to give a CAZyme prediction in order for a given protein to be classified as a CAZyme in this study.

2.3.8: Qualitative analysis (protein presence/absence)

The main objective in this section was to determine which specific proteins were present in all multi-species samples but were not present in a single-species sample. Initially, a presence/absence analysis was performed to compare proteins present in a multi-species sample relative to proteins produced in a single-species sample (i.e. a proteomics baseline). This was achieved by aligning the proteins manually based on their protein ID to identify what proteins were present in each sample type. These data were used to generate a heat map and Venn diagram in R Studio. Those proteins that were present in every sample type that was grown in the presence of one or more other species, but not present when a species was cultured on its own, were selected as candidate effector proteins for further analysis.

2.3.9: Quantitative analysis (protein abundance)

The main objective in this section was to determine which specific proteins were more abundant in a multi-species sample when compared to a single-species sample. To achieve this, each species was analysed separately to enable subsequent normalisation of data. One multi-species sample was compared to a respective single-species species baseline (e.g. the *P. agathidicida* proteins from the multi-species sample *P. agathidicida* + *P. cinnamomi* were compared to the single-species *P. agathidicida* sample).

Normalisation

The aim of normalisation was to make all independent samples comparable to each other.

1. All raw abundance data from the proteins which had, for example, a *P. agathidicida* protein ID, irrespective of whether it was derived from a single-species or multi-species sample type, were arranged in a Microsoft Excel spreadsheet. Each protein identified from each sample type had a unique row with the corresponding data. This was repeated for each species in separate Microsoft Excel spreadsheets as they were analysed independently.
2. For each protein, the abundance value (i.e. the sum of integrated peak areas of each precursor ion) was divided by the abundance count (the number of identified and validated peptides used to calculate abundances for each protein) for each biological replicate to give an abundance/ abundance count value (adjusted abundance value).
3. The adjusted abundance values from the previous step were summed for all of the proteins in each biological replicate.

4. These sums were then used to normalise across the four replicates to take into account any overall differences between the biological replicates within each sample. This was done by scaling up all the values using a multiplier calculated from the highest total out of the four biological replicates, divided by the total for each individual replicate. For example, if the highest total of the adjusted abundance values was in biological replicate one and was 1.2-fold higher than the total in biological replicate three, all of the adjusted abundance values were scaled up by 1.2-fold in replicate three to give the final normalised abundance values.

Quantitative comparison

The aim of this section was to compare the normalised abundance values from each multi-species sample type to the corresponding single-species sample type (baseline) to determine which specific proteins were more abundant when in the presence of other species.

1. The single-species data set (baseline) and one set of multi-species data samples were selected to be compared (e.g. proteins from *P. agathidicida* cultured alone were compared with *P. agathidicida* proteins from *P. agathidicida* + *P. cinnamomi* samples). The data were aligned so one protein ID was displayed per row; within this row all abundance data from both sample types, each with four biological replicates, were displayed in columns.
2. The final normalised values from one sample type for each protein were averaged. This was repeated for the other sample type.
3. The averages from both data sets were used to determine an overall fold change between the two datasets (combination/baseline).
4. The overall fold change between the two datasets were converted to $\log_2$ values.
5. Log_{10} values were calculated for the normalised abundance values from each biological replicate for each protein. The four $\log_{10}$ values were grouped for a T-test. The $\log_{10}$ values of the combination sample were compared to those of the baseline protein values (e.g. TTEST(*P. agathidicida* + *P. cinnamomi* : *P. agathidicida*)).
6. The T-test results in a probability (P) score which was transformed to -$\log_{10}$ value.
7. The negative $\log_{10}$ probability value (y-axis) and the $\log_2$ normalised abundance value (x-axis) for each protein were used to generate a volcano plot.

The proteins that had a -$\log_{10}$ probability value above 1.3 (-log10(0.05)=1.3) and a positive $\log_2$ normalised abundance value (representing an increase in abundance in multi-species samples compared to single-species baseline samples) were considered significantly different. Those proteins that had a significant increase in abundance across both pairwise and the all-species sample were selected as candidate effector proteins for further analysis.

2.3.10: Analysis of candidate effector proteins

Characterization of hypothetical proteins

All candidate effector proteins from the qualitative and quantitative analyses that lacked a functional domain or annotation were analysed with AlphaFold2 (Jumper et al., 2021), in conjunction with ColabFold (Mirdita et al., 2022), to predict their tertiary structure. This predicted structure was run through both the DALI (Holm et al., 2023) and FoldSeek (van Kempen et al., 2023) webservers to identify structural homologs. The structures of the top hit and the hypothetical protein were then aligned with the CEalign tool and visualised in PyMol v2.5 (Schrödinger & DeLano, 2020). An RMSD score was provided by the program which described how well the two structures aligned (the smaller the score, the better the two structures align/match). PONDR VLXT (Romero et al., 2001) was used to predict disordered regions within the protein sequences.

BLASTp search

The candidate effector proteins identified from the qualitative and quantitative analysis were screened for sequence homologs in the National Center for Biotechnology Information (NCBI) non-redundant (nr) protein database using the Basic Local Alignment Search Tool for proteins (BLASTp) (Altschul et al., 1997).

2.4: *In planta* growth assessments (for Objective 3)

Wildtype and Δ*sobir1* mutant seeds of *Nicotiana benthamiana* (Goodin et al., 2008) were propagated in Daltons premium seed mix soil (Fruitfed) which had been heat-treated at 60°C for three days. At two weeks post-sowing, seedlings were transferred into larger nine cm x nine cm individual pots for four to six weeks. The plants were grown at 22°C under a 12-hour light:12-hour dark photoperiod with 80–85 µmol/m^2/s light intensity. Once plants were six weeks old (prior to flowering), the leaves were detached, leaving a portion of the stem attached. The leaves were surface-sterilised with 70% ethanol, with each stem wrapped in a paper towel soaked in milliQ water, and then placed abaxial-side-up in a shallow container lined with a moist paper towel. A 20-gauge sterile needle (Becton Dickinson Medical Products) was used to make six small incisions on the abaxial side on each half of the leaf. An agar plug of the *Phytophthora* species of interest was placed mycelium-side-down directly on top of the induced damage (Figure 2.3), following the same protocol as mentioned in Section 2.2.1. The containers were wrapped in tinfoil and incubated at 22°C, and then monitored and digitally photographed daily for lesion progression for up to seven days or when the leaf was no longer viable. Infrared images (Zahid et al., 2021) were also generated using ChemiDoc™ MP Imaging system (Bio-Rad Laboratories) on a Blot/UV tray using a Cy7 setting.

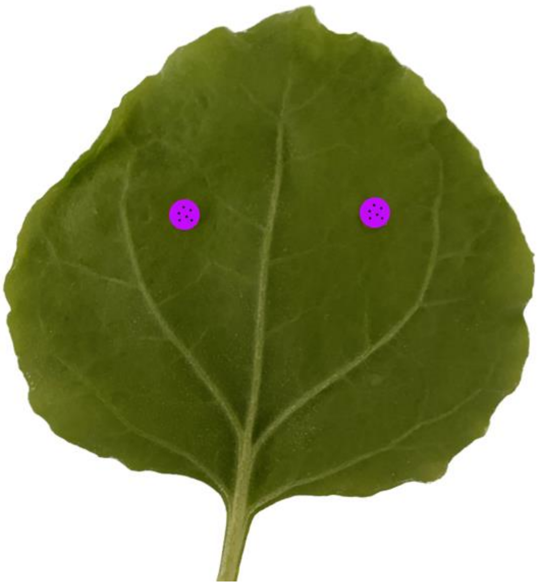

Figure 2. 3. **Schematic showing the positioning of *Phytophthora* agar plugs on detached leaves of *Nicotiana benthamiana* for lesion area quantification assays.** The purple circles represent five mm agar plugs containing the *Phytophthora* species of interest that were placed mycelium-face-down on the abaxial leaf surface. The black dots within the purple circle represent the six points of needle-induced damage on the abaxial leaf surface under the agar plugs.

The lesion area was calculated manually on Image J JS (Schneider et al., 2012) using a global scale based on the ruler placed in the ChemiDoc™ MP Imaging system. Only the biological replicates of *P. multivora* and *P. agathidicida* wildtype and Δ*sobir1* mutants were calculated. The outside edge of each lesion was traced and the in-built measure tool was used to calculate the area. In excel, the total lesion area per leaf was calculated by summing each lesion from each biological replicate. The average lesion size across the four biological replicates was graphed and error bars were calculated based on the standard deviation calculated across the four biological replicates. A T-test was performed for each pathogen species individually to determine the statistical significance between lesion sizes on wildtype and Δ*sobir1* mutants, using the lesion area values for each biological replicate.

Chapter Three: Results

1: Macroscopic *Phytophthora* interaction assays on solid growth media

To determine whether colonies of the same or different species of *Phytophthora* interact with or repel each other at the macroscopic level, a colony interaction assay was carried out on culture plates containing one of two nutrient-rich media (clarified V8 agar or carrot agar), as well as one of two nutrient-poor media (cornmeal agar inclusive of PARP antibiotics or plich agar). For this purpose, the various media plates were each co-inoculated with three agar plugs containing a specific *Phytophthora* species to determine whether a zone of growth inhibition (gap of no growth) was formed between the colonies.

1.1: Intraspecies colony interaction assays and single-colony control plates

As a starting point, a macroscopic colony interaction assay involving three colonies of the same *Phytophthora* species (i.e. an intraspecies assay) was carried out, each with four biological replicates. Initial observations indicated that each of the three species had a different growth pattern on solid agar. More specifically, *P. agathidicida* produced thin, transparent mycelium and had a wispy colony morphology that had no obvious differences in colouring or patterning from the centre to the advancing edge. Meanwhile, the mycelium of *P. multivora* was more opaque and fluffy in appearance, exhibiting a darker star-like pattern that radiated out from the centre of the colony. As the mycelium of *P. multivora* aged, it became fluffier, with more vertical growth compared to newer hyphae formed at the outer edge of the colony. Finally, like *P. multivora*, the mycelium of *P. cinnamomi* became fluffier with age (Figure 3.1).

In all cases, irrespective of which species or media type was being tested, a zone of growth inhibition was observed between all three colonies (Figures 3.1 and 3.2, Appendix 1: Figures A1 and A2). However, the appearance of this zone, including how distinct it was across its entire length, differed depending on which species was inoculated. On all media types, colonies of *P. agathidicida* and *P. multivora* showed complete separation right to the edge of the agar plates, with the largest zone of separation observed in the centre between the edges of the three colonies (Figures 3.1and 3.2, Appendix 1: Figures A1 and A2). However, *P. cinnamomi* showed variability in terms of whether the zone of growth inhibition reached the outer edge of the plate. On cornmeal and carrot agar, a visible inhibition zone was observed to the outside edge of the plate, but on both clarified V8 and plich agar this was not always the case (Figures 3.1 and 3.2). Upon further observation, there appeared to be diffuse hyphae present where the zone of growth inhibition would have been expected if *P. cinnamomi* followed the same pattern of growth as *P. agathidicida*. This indicated an incomplete zone of growth inhibition can sometimes be formed between colonies of the same species. In general, on the nutrient-poor plich and cornmeal agars, a wider zone of growth inhibition was generally observed between the colonies, irrespective of the species being tested (Figure 3.2, Appendix 1: Figure A2), while a much thinner zone was generally observed between colonies on nutrient-rich agar (Figure 3.1 and Appendix 1: Figure A1).

The four different media types used in this experiment caused each of the three *Phytophthora* species to grow at different rates, likely due to the presence or absence of specific nutrients. As such, it took more time for a zone of growth inhibition to form on different media types than others (i.e. where no further radial growth was observed and the colony reached the outside edge of the plate). For carrot agar, a zone of growth inhibition was formed by four days post-inoculation (dpi), for clarified V8 agar six dpi, and for both cornmeal agar and plich agar seven dpi. Notably, once a zone of growth inhibition was formed, no further growth into this zone of inhibition was observed, even if the *Phytophthora* species were cultured under optimal growth conditions for a further week. From ten dpi onwards, there was an increase in aerial hyphae formation toward the outer edges of the colony by all three species, but primarily by *P. cinnamomi* and *P. multivora*, causing the colony to become opaque and fluffy in texture (results not shown).

To ensure that the observed zones of growth inhibition were not simply the result of natural limitations on colony size, each *Phytophthora* species was inoculated singly, as above, onto each of the media types in one of the three set locations on the agar plate, each with four biological replicates, and the radial growth of each colony observed over the same time period. Radial growth was observed with the same morphology and growth pattern to that seen in the intraspecies interaction assays (Figures 3.1 and 3.2, Appendix 1: Figures A1 and A2). However, in the absence of other colonies, *P. cinnamomi* had a less symmetrical (more lobed) outer edge than *P. agathidicida* or *P. multivora* (Figures 3.1 and 3.2, Appendix 1: Figures A1 and A2). Importantly, at the equivalent time points, the colony sizes of each species had exceeded the sizes of the colonies observed in the intraspecies interaction assays. This result confirms that zones of growth inhibition were indeed observed in the intraspecies interaction assays and indicates that colony growth can be halted by the presence of another colony from the same species.

In summary, a zone of growth inhibition was always formed between colonies of the same species, however the distance that this line extended toward the outer edge of the plate, as well as the width of this zone, varied. When colonies were grown singly, radial growth was far greater than that observed when grown next to colonies of the same species.

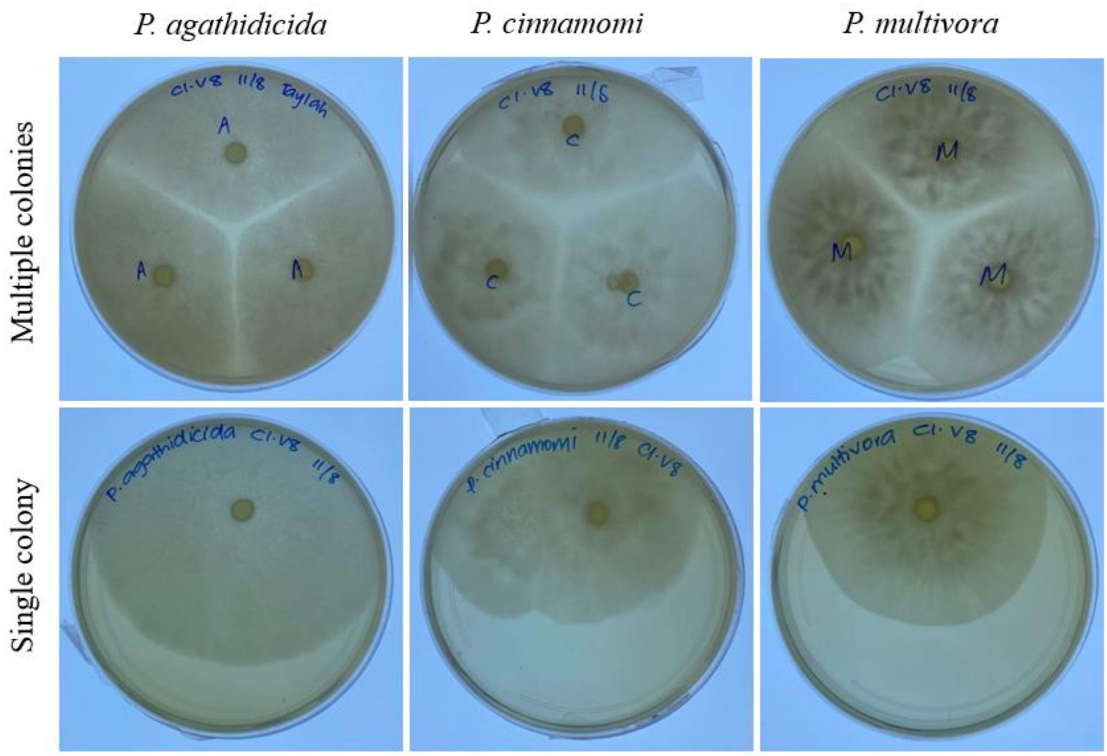

Figure 3. 1. **Intraspecific colony interaction assays of *Phytophthora* species on nutrient-rich clarified V8 agar plates.** The top three images show three colonies each of *P. agathidicida*, *P. cinnamomi* and *P. multivora* initiated from agar plugs five mm in diameter (small darker circles), that have grown towards each other until zones of growth inhibition (gaps) between them have been formed. The bottom three images show single-colony-only plates to illustrate that growth of a single colony from each of *P. agathidicida*, *P. multivora* and *P. cinnamomi* is not restricted in the absence of other colonies from the same species, and that they grow out past the point where a zone of inhibition is typically formed. Colonies were cultured on nine cm plates at 22°C for six days and are representative of what was observed across four independent biological replicates. In blue marker pen: A = *P. agathidicida*; C = *P. cinnamomi*; M = *P. multivora*.

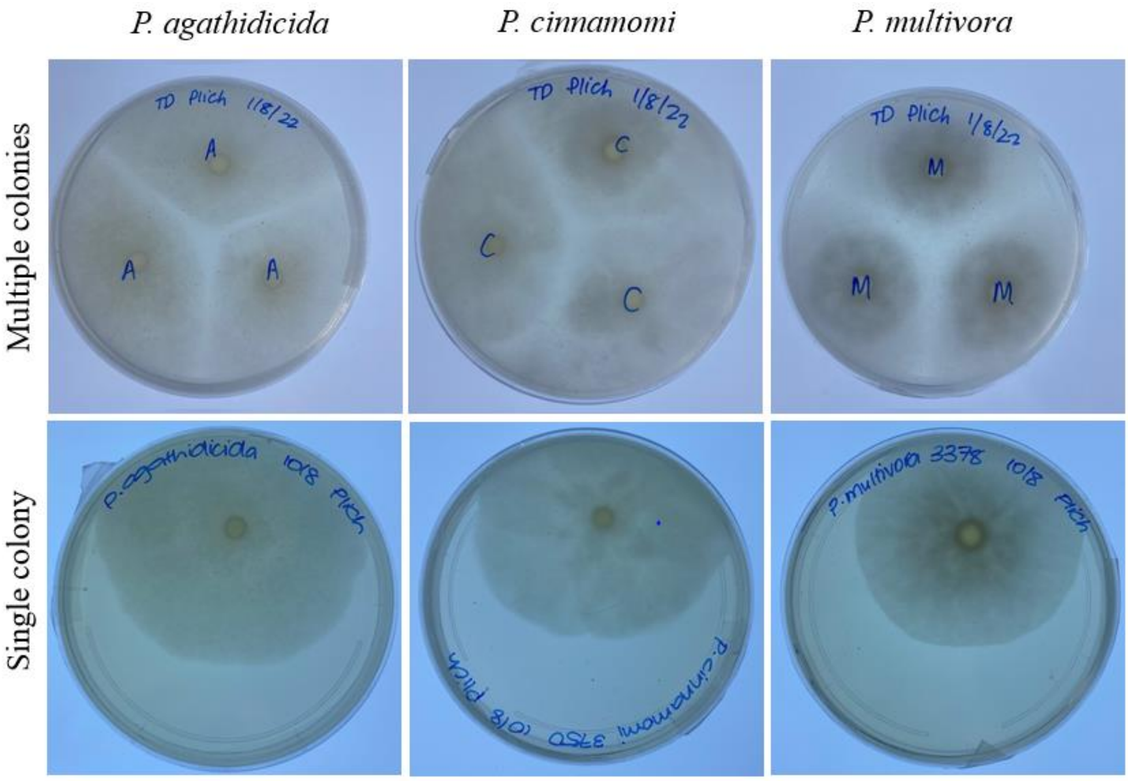

Figure 3. 2. **Intraspecific colony interaction assays of *Phytophthora* species on nutrient-poor plich agar plates**. The top three images show three colonies each of *P. agathidicida, P. cinnamomi* and *P. multivora* initiated from agar plugs of five mm in diameter (small darker circles), that have grown towards each other until zones of growth inhibition (gaps) between them have been formed. The bottom three images show single-colony-only plates to illustrate that growth of a single colony from each of *P. agathidicida, P. multivora* and *P. cinnamomi* is not restricted in the absence of other colonies from the same species, and that they grow out past the point where a zone of inhibition is typically formed. Colonies were cultured on nine cm plates at 22°C for seven days and are representative of what was observed across four independent biological replicates. In blue marker pen: A = *P. agathidicida*; C = *P. cinnamomi*; M = *P. multivora*.

1.2: Interspecies colony interaction assays

Next, an interspecies colony interaction assay was carried out in which different *Phytophthora* species were co-cultured on the four different media types, each with four biological replicates. The combinations of species used in the interspecies colony interaction assays are shown in Table 2.2 of Chapter Two (Materials and Methods). The interaction assays were photographed once no further colony expansion was observed, which was four dpi for carrot agar, six dpi for clarified V8 agar, and seven dpi for both plich agar and cornmeal agar.

As observed for the intraspecies colony interaction assays (Section 1.1), all three *Phytophthora* species formed a zone of growth inhibition between colonies, irrespective of what media type was used or which species was next to it (Figures 3.3 and 3.4, Appendix 1: Figures A3 and A4). Similarly, as mentioned for the intraspecies colony interaction assays, the width of the zone of growth inhibition was dependent on the media type used and the length likely dependent on the species present.

On clarified V8 agar particularly, some plates appeared to show a minimal zone of growth inhibition between colonies (Figure 3.3). For example, very little separation was observed between the *P. cinnamomi* and *P. multivora* colonies in Figure 3.3F. However, upon closer inspection, the mycelia from each colony were found to be distinct and did not merge. Additionally, colonies on the carrot agar plates had defined zones of growth inhibition, however the separation between the colonies was narrower visually. On all media types, the zones of growth inhibition were always at their widest at the centre of the plate where the three colonies would grow towards each other, however this was most evident for zones of growth inhibition on cornmeal agar (compare Figures 3.3 and 3.4 and Appendix 1: Figure A3 and A4). Additionally, the majority of colonies grown on plich and cornmeal agar plates had a zone of growth inhibition that clearly reached the outside edge of the plate and were much more defined and thicker than that shown on clarified V8 or carrot agar.

In summary, like the intraspecies interaction assays, a zone of growth inhibition was formed irrespective of what species or media type was present. The zones of growth inhibition were widest at the centre of the three colonies but differed in width depending on the media type used and species present.

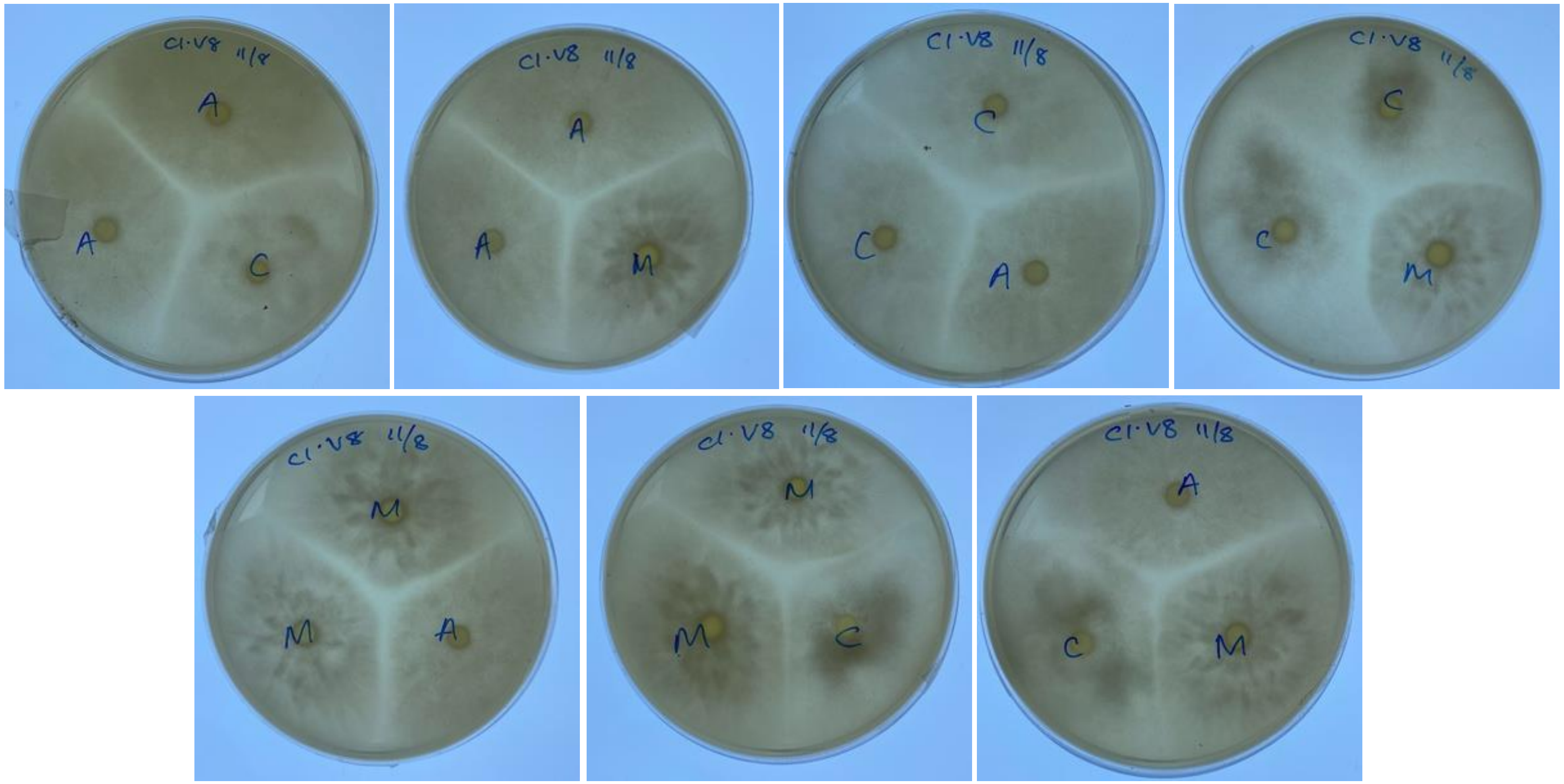

Figure 3. 3. **Interspecific colony interaction assays of *Phytophthora* species on nutrient-rich clarified V8 agar plates.** All plates show three colonies of *Phytophthora* (*P. agathidicida*, *P. cinnamomi* and *P. multivora*) in differing species combinations, initiated from an agar plug five mm in diameter (small darker circles), that have grown towards each other until zones of growth inhibition (gaps) between them have been formed. Colonies were cultured on nine cm plates at 22°C for six days and are representative of what was observed across four independent biological replicates. Combinations of each agar plate are indicated by letters in blue marker pen: A = *P. agathidicida*; C = *P. cinnamomi*; M = *P. multivora*.

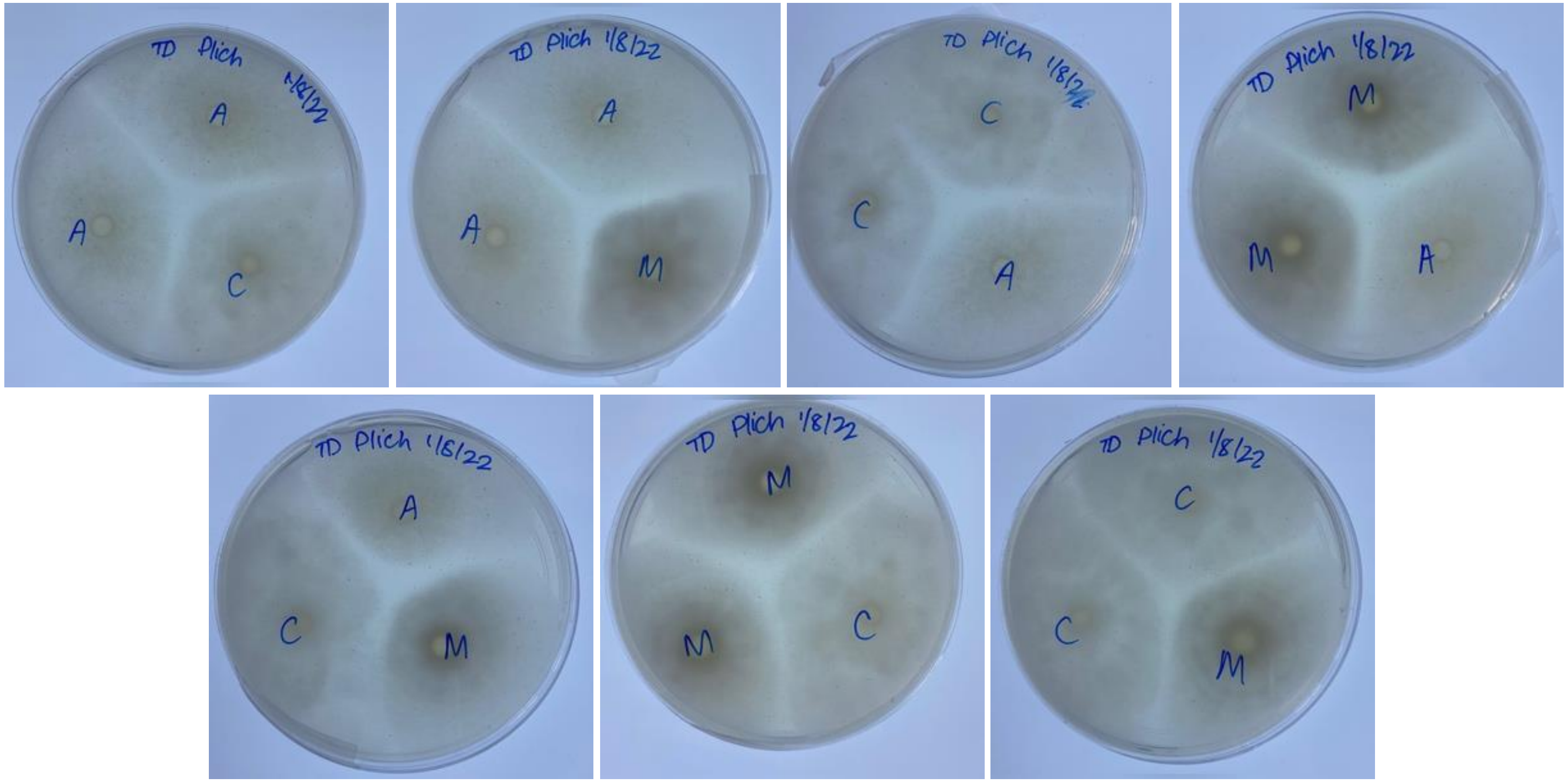

Figure 3. 4. **Interspecific colony interaction assays of *Phytophthora* species on nutrient-poor plich agar plates**. All plates show three colonies of *Phytophthora* (*P. agathidicida*, *P. cinnamomi* and *P. multivora*) in differing species combinations, initiated from an agar plug five mm in diameter (small darker circles), that have grown towards each other until zones of growth inhibition (gaps) between them have been formed. Colonies were cultured on nine cm plates at 22°C for six days and are representative of what was observed across four independent biological replicates. Combinations of each agar plate are indicated by letters in blue marker pen: A = *P. agathidicida*; C = *P. cinnamomi*; M = *P. multivora*.

2: Proteomic *Phytophthora* interaction assays in liquid growth media

2.1: Growth in liquid culture

From the results observed on solid growth media in Section 1, there was no clear indication whether colonies of the three different *Phytophthora* species repelled or interacted with each other beyond what was observed for colonies of the same species. Thus, to better understand whether the three *Phytophthora* species interact with each other at the molecular level, a proteomic analysis of secreted proteins produced during co-culture in liquid growth media was performed using liquid chromatography–mass spectrometry (LC–MS).

Clarified V8 broth (nutrient-rich) and plich broth (nutrient-poor) were selected as the liquid media types for this analysis, as both media types had recently been shown to support a high level of secreted protein production by *P. agathidicida* when compared to other liquid media types (Bradley, 2022). Here, cultures were set up in Petri dishes to contain one, two, or three *Phytophthora* species, with each combination ('sample type') having four biological replicates (species combinations are shown in Table 2.3 of Chapter 2) and were grown statically (without shaking) for three or seven days.

Photographs were taken of each sample type prior to harvesting the culture filtrate for LC–MS analysis. The individual species showed substantial variation in colony growth between the two liquid media types (Figure 3.5, Appendix 1: Figure A5). Considerably more growth was observed for each species when cultured in clarified V8 broth compared to in plich broth, especially for *P. cinnamomi* and *P. multivora*. This trend was also seen when each species was grown in combination with other species (Figure 3.5, Appendix 1: Figure A6). In some cases, smaller satellite colonies were produced from the larger original colony which likely occurred during transportation of the plates to the warm room and were not a sign of contamination. Notably, the samples that contained a combination of species did not produce colonies as large as those shown for the samples containing single species. However, an increase from two to three species did not cause an obvious observable difference in colony size (Figure 3.5, Appendix 1: Figure A6). Finally, differences in colony morphology between the three *Phytophthora* species were observed when grown in liquid media, but these differences were similar to those observed during growth on solid media. In the samples containing a combination of species, each species was identifiable by their distinct morphological differences (Figure 3.6, Appendix 1: Figure A6). Growth of *P. agathidicida* was consistent with what was observed on the agar plates, producing a thin, transparent colony, while *P. cinnamomi* and *P. multivora* produced opaque colonies. *P. multivora* tended to produce much denser mycelia compared to *P. cinnamomi*.

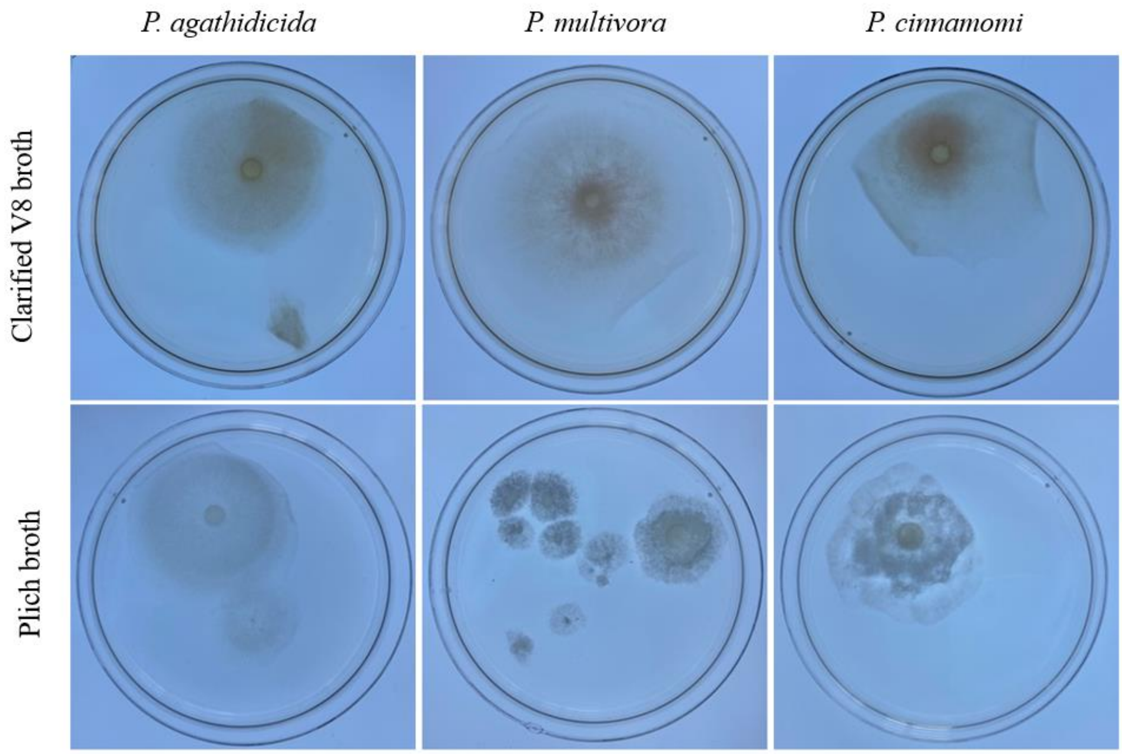

Figure 3. 5. **Growth of single *Phytophthora* species in clarified V8 broth and plich broth media.** *P. agathidicida*, *P. multivora* and *P. cinnamomi* were each grown from a single five mm agar plug (extracted from the outer edge of an actively growing colony on clarified V8 agar) in 10 mL of clarified V8 broth in nine cm Petri dishes for seven days in the dark at 22°C without shaking (i.e. as static cultures). The Petri dishes are representative of four independent biological replicates.

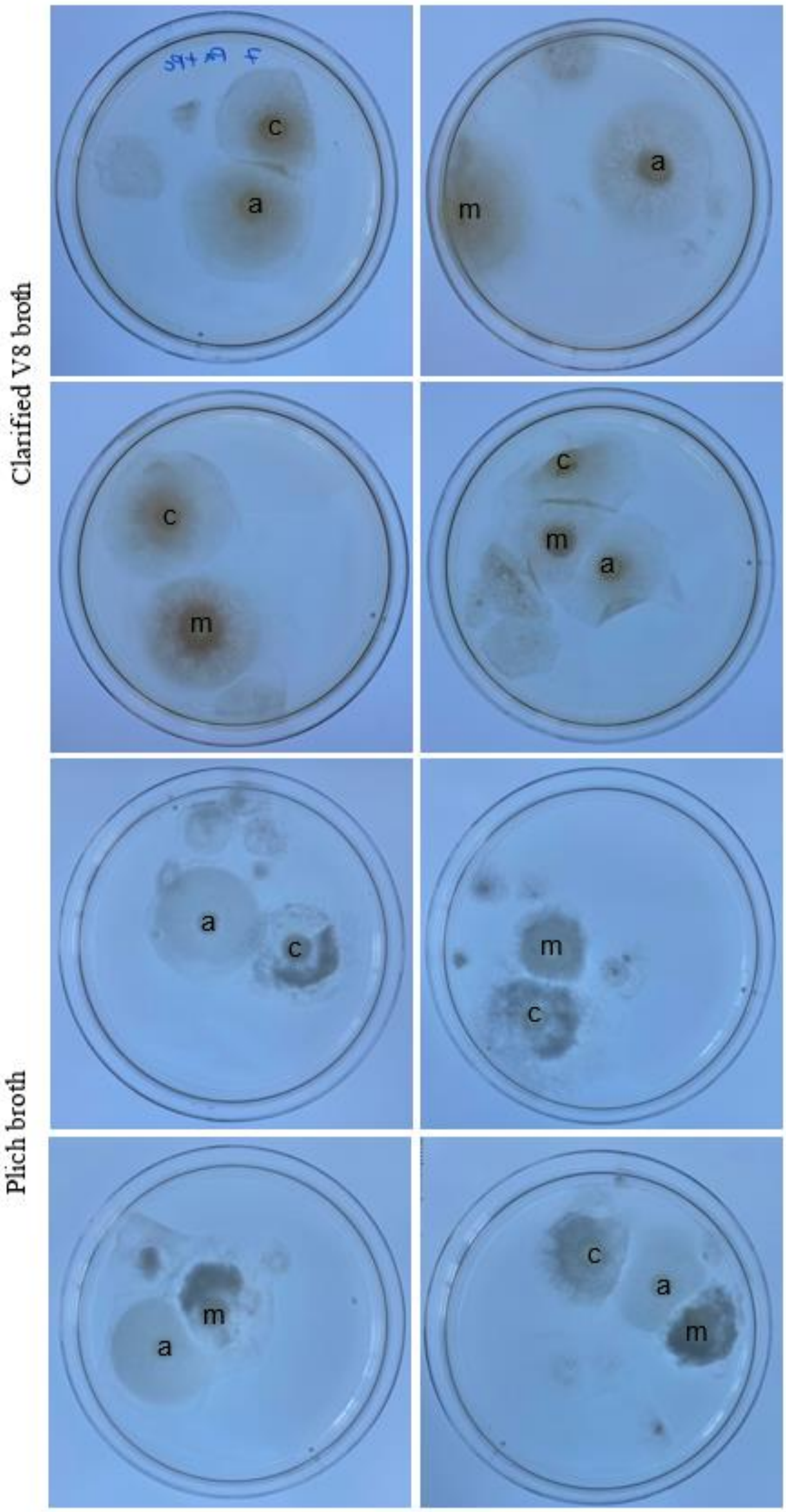

Figure 3. 6. **Growth of multiple *Phytophthora* species in clarified V8 broth and plich broth media.** *P. agathidicida* (a), *P. cinnamomi* (c) and *P. multivora* (m) were each grown from a single five mm agar plug (extracted from the outer edge of an actively growing colony on clarified V8 agar) in 10 mL of clarified V8 broth in nine cm Petri dishes for seven days in the dark at 22°C without shaking (i.e. as static cultures). The Petri dishes are representative of four independent biological replicates.

2.2: Culture filtrate protein profiles

Due to time and financial constraints, only one liquid media type and one time point across sample types from Section 2.1 could be characterized by proteomics using LC–MS. Given that the three *Phytophthora* species each visually produced more biomass in the static liquid cultures of clarified V8 broth than plich broth, and that more secreted protein was anticipated to be produced at seven dpi than three dpi (i.e. from a culture with higher biomass), clarified V8 broth and seven dpi were selected as the best liquid medium and time point, respectively, to use for the proteomics analysis. In any case, the culture filtrates of samples not selected for LC–MS were stored at –20°C for future analysis if deemed necessary.

In preparation for LC–MS analysis, the culture filtrates of all sample types from clarified V8 broth at seven dpi were resolved by sodium dodecyl sulfate–polyacrylamide gel electrophoresis (SDS-PAGE) (Figures 3.7 and 3.8). The protein gels which contained culture filtrate from each individual species (Figure 3.7) showed differences in their banding profiles. More specifically, when compared to both *P. agathidicida* and *P. multivora*, the culture filtrate of *P. cinnamomi* appeared to have more well-defined bands (i.e. of approximately 130 kDa and 45 kDa in size). Likewise, the culture filtrates of *P. multivora* and *P. cinnamomi* appeared to have a more prominent band at 70 kDa, when compared to *P. agathidicida*.

The protein banding profiles observed for the culture filtrates of the various *Phytophthora* species combinations were fairly similar with that observed for the individual *P. cinnamomi* sample (compare Figures 3.7 and 3.8). Indeed, like the individual *P. cinnamomi* sample, the 70 kDa and 130 kDa bands were the most prominent across all multi-species samples. Although the *P. agathidicida* + *P. cinnamomi* + *P. multivora* combination had bands present at both these molecular weights, they were less well-defined compared to all pairwise combinations and appeared to be smeared particularly between 100 kDa to 70 kDa, perhaps indicative of a greater concentration of total protein (Figure 3.8). All species combinations showed a light banding profile at 45 kDa and 35 kDa (Figure 3.8).

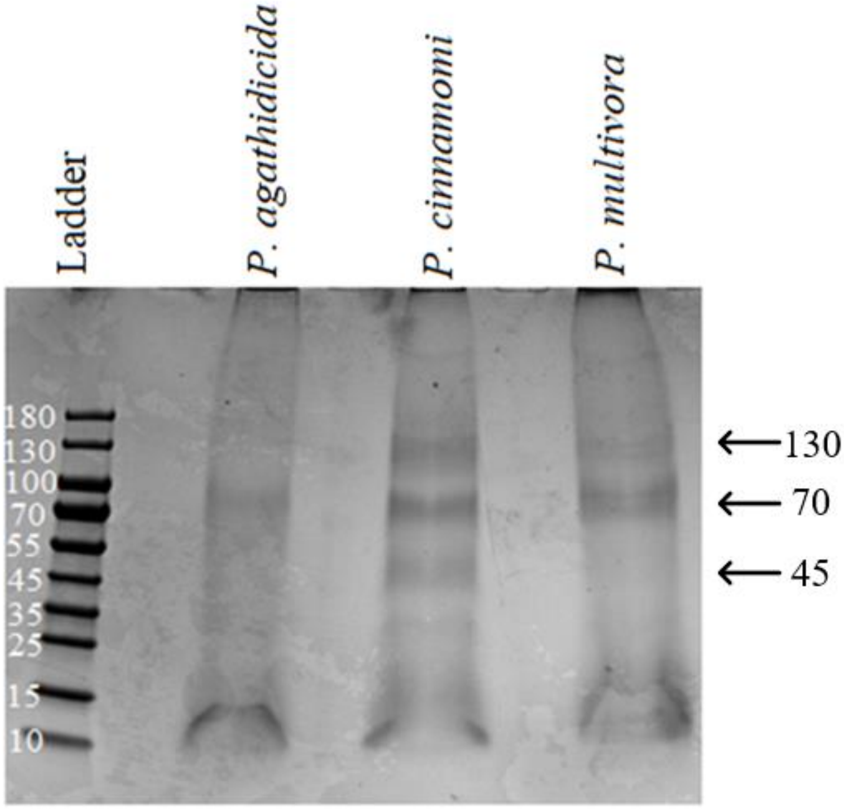

Figure 3. 7. **Protein banding profiles of culture filtrate samples harvested from individual *Phytophthora* species grown in clarified V8 broth.** All species were grown for seven days as static cultures at 22°C in the dark. Culture filtrates were harvested by filtration, freeze-dried and resuspended in 100 µL sterile water. A total of 20 µL was then mixed with 10 µL loading dye and resolved by sodium dodecyl sulfate–polyacrylamide gel electrophoresis (SDS-PAGE) on a 4–20% Mini-PROTEAN TGX gel. Lane 1, PageRuler Prestained Protein Ladder, with bands shown as kDa; Lane 2, *P. agathidicida* culture filtrate; Lane 3, *P. cinnamomi* culture filtrate; Lane 4, *P. multivora* culture filtrate. Each culture filtrate sample is representative of four biological replicates.

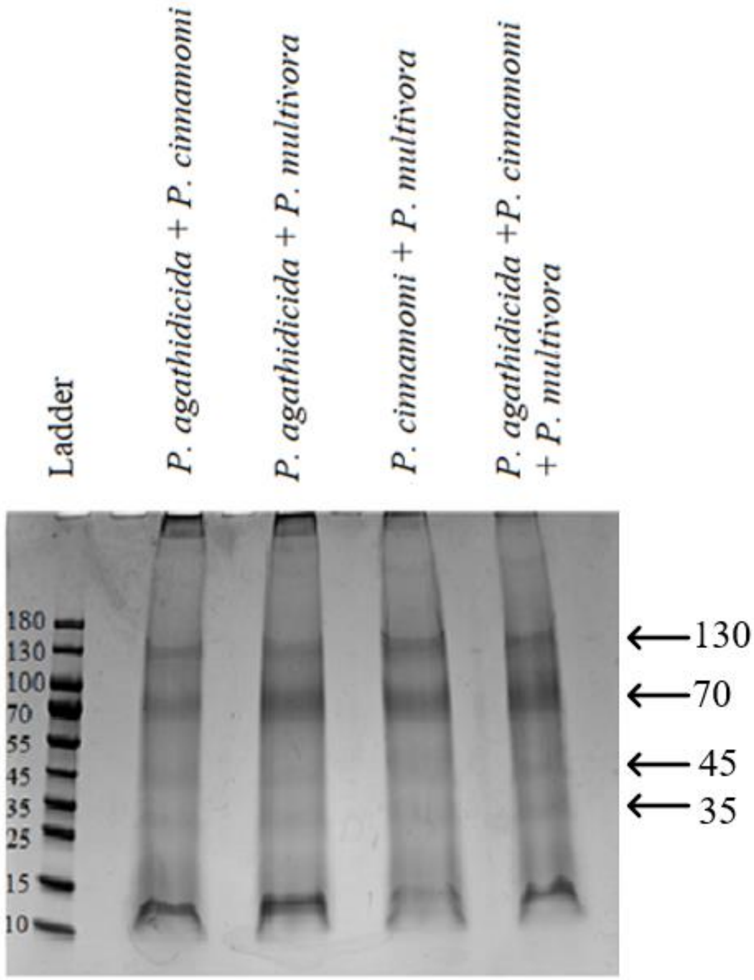

Figure 3. 8. **Protein banding profiles of culture filtrate samples harvested from co-inoculated *Phytophthora* species grown in clarified V8 broth.** All species were grown for seven days as static cultures at 22°C in the dark. Culture filtrates were harvested, freeze-dried and resuspended in 100 µL sterile water. A total of 20 µL was then mixed with 10 µL loading dye and resolved by sodium dodecyl sulfate–polyacrylamide gel electrophoresis (SDS-PAGE) on a 4–20% Mini-PROTEAN TGX gel. Lane 1, PageRuler Prestained Protein Ladder, with bands shown as kDa; Lane 2, *P. agathidicida* + *P. cinnamomi* culture filtrate; Lane 3, *P. agathidicida* + *P. multivora* culture filtrate; Lane 4, *P. cinnamomi* + *P. multivora* culture filtrate; Lane 5, *P. agathidicida* + *P. cinnamomi* + *P. multivora* culture filtrate. Each culture filtrate sample is representative of four biological replicates.

2.3: Identification of putatively secreted proteins in culture filtrate samples

Following SDS-PAGE in Section 2.2, the proteins present in each gel lane, representing each sample type, each with four biological replicates, were digested with trypsin and the resulting peptides identified by LC–MS. Here, peptides were mapped against the predicted proteome of each *Phytophthora* species present in the sample type. To minimise the risk of false discovery, the Proteome Discoverer software used in this analysis removed all predicted proteins that were not found in at least two of the four biological replicates. Based on the analysis of the single-species samples, *P. agathidicida* produced the most proteins, with 248 proteins identified, which was slightly more than *P. cinnamomi* with 217 and *P. multivora* with 200 (Table 3.1). To determine which of these proteins were likely to be secreted into the culture filtrate, and not simply the result of cytoplasmic contamination, each was analysed and screened using various webservers (Chapter 2, section 2.3.7). Following this, a total of 106, 110, and 104 putatively secreted proteins without a predicted transmembrane domain, but with a predicted signal peptide (secretion signal), were identified in the *P. agathidicida*-only, *P. cinnamomi*-only, and *P. multivora*-only sample types, respectively, representing 43%, 51% and 52% of the total protein pool in each individual dataset (Table 3.1).

For the sample types containing a combination of *Phytophthora* species, the number of *P. agathidicida* proteins identified were greater than in the single species alone, excluding the sample containing all three species of which the protein number was slightly lower (Table 3.1). However, for *P. cinnamomi* and *P. multivora* the number of proteins identified in the samples containing multiple species decreased compared to the number of proteins identified in the single species sample (Table 3.1). The number of proteins identified in a multi-species sample type were, for example, greater when *P. agathidicida* was present. Similar to the single-species samples, the number of proteins predicted to be secreted into the culture filtrate of multi-species samples was considerably lower than the total number of proteins identified, with 49% for *P. agathidicida* + *P. cinnamomi*, 45% for *P. agathidicida* + *P. multivora*, 54% for *P. cinnamomi* + *P. multivora*, and 53% for *P. agathidicida* + *P. cinnamomi* + *P. multivora*. As secreted proteins formed the focus of this study, all proteins without a predicted signal peptide or with a predicted transmembrane domain were not pursued further.

Table 3. 1. **Number of *Phytophthora* proteins identified in multi-species culture filtrate samples.**

Phytophthora **single- and multi-species combinations**	**Total number of proteins identified[2]**	**Total number of predicted secreted proteins identified[3]**
P. agathidicida	248	106
P. cinnamomi	217	110
P. multivora	200	104
P. agathidicida **+** ***P. cinnamomi***	432 (256, 176)	212 (128,84)
P. agathidicida **+** ***P. multivora***	459 (301, 158	209 (131, 78)
P. cinnamomi **+** ***P. multivora***	301 (143, 158)	164 (82,82)
P. agathidicida **+** ***P. cinnamomi*** **+** ***P. multivora***	368 (165, 94,109)	197 (96,46,55)

[1]*Phytophthora* species were grown in clarified V8 broth for seven days in the dark without shaking and the proteins identified in the resulting culture filtrate using liquid chromatography–mass spectrometry (LC–MS).

[2]Numbers in brackets represent the total number and secreted number of proteins identified from each species and are ordered according to their name order in the *Phytophthora* species combination column.

[3]Secreted proteins without a transmembrane domain were predicted using SignalP v3.0 (Bendtsen et al., 2004) and TMHMM v2. (Krogh etal., 2001), respectively.

Given that all three oomycete species investigated in this study were from the same genus (*Phytophthora*), it remained possible that some of the peptides derived from the putatively secreted proteins identified in the multi-species combinations were not mutually exclusive (i.e. they were identical peptides derived from orthologous proteins). This is not ideal, as the peptides could have been assigned to the wrong species. However, an investigation of the peptide data revealed that all putatively secreted proteins identified in this study possessed at least one peptide unique to the species in question, confirming that there was indeed no misassignment of proteins (Appendix 2). This is supported by the heatmap shown in Figure 3.10 (see below).

To investigate the presence/absence profile of putatively secreted proteins identified across the biological replicates of single- and multi-species samples, two heatmaps were prepared using R Studio. One of these contained only those putatively secreted proteins associated with the single-species samples (Figure 3.9), while the other contained these proteins, together with those putatively secreted proteins associated with the multi-species samples (Figure 3.10). For the single-species samples, the proteins grouped in accordance to which species they originated from. Furthermore, the majority of proteins were present in at least three of the four biological replicates (89% for *P. agathidicida*, 89% for *P. cinnamomi* and 86% for *P. multivora*), with very few proteins being only identified in two of the biological replicates (Figure 3.9). Additionally, the heatmap containing all sample types (Figure 3.10) showed a similar trend with between 83 to 88.5% of proteins from each respective sample found in three or more biological replicates. Additionally, the heatmap also highlighted that some proteins found in the single-species samples were also found in some and, in several cases, all of the multi-species sample types that contained the respective single species. Interestingly, the opposite was also shown with some proteins only produced when in combination with another species (31% of secreted proteins for *P. agathidicida*, 11.5% for *P. cinnamomi* and 2% for *P. multivora*), as indicated by the purple shading in the multi-species samples (presence) and the light blue shading (absence) in the single-species only columns (Figure 3.10). A full list of putatively secreted proteins identified from each species across each sample type, including what class of functional protein they belong to, where known, and their top protein hit in the non-redundant protein database present at the National Centre for Biotechnology Information (NCBI) using Basic Local Alignment Search Tool for protein (BLASTp), can be found in Appendix 3.

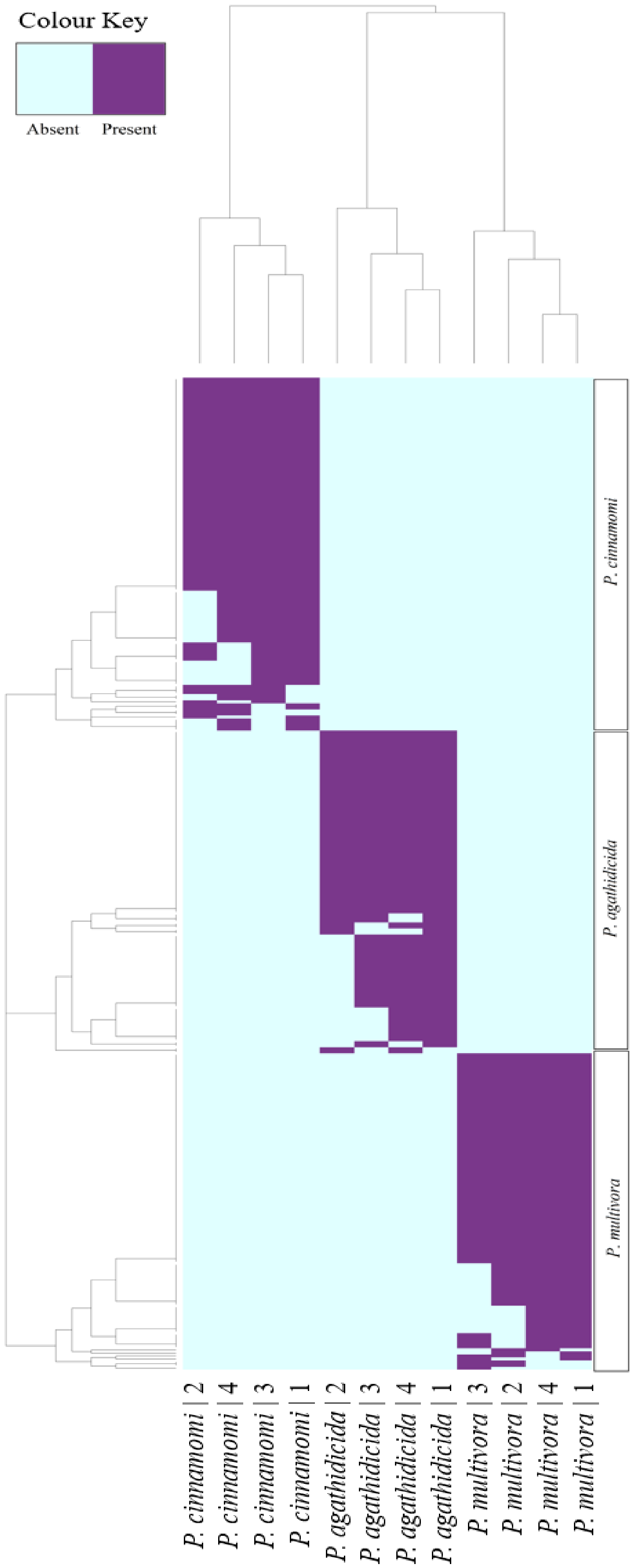

***Figure 3. 9.* Heatmap showing the presence/absence profile of putatively secreted proteins from *Phytophthora* species grown alone in static clarified V8 broth.** Proteins were identified from culture filtrate using liquid chromatography–mass spectrometry (LC–MS). Four biological replicates were included per species (1–4). Blue shading indicates protein absence and purple shading indicates protein presence. The tree on the left side of the heatmap shows the similarity of proteins based on their presence/absence profile. The tree on the top of the heatmap shows similarity between the protein presence/absence profile of sample biological replicates.

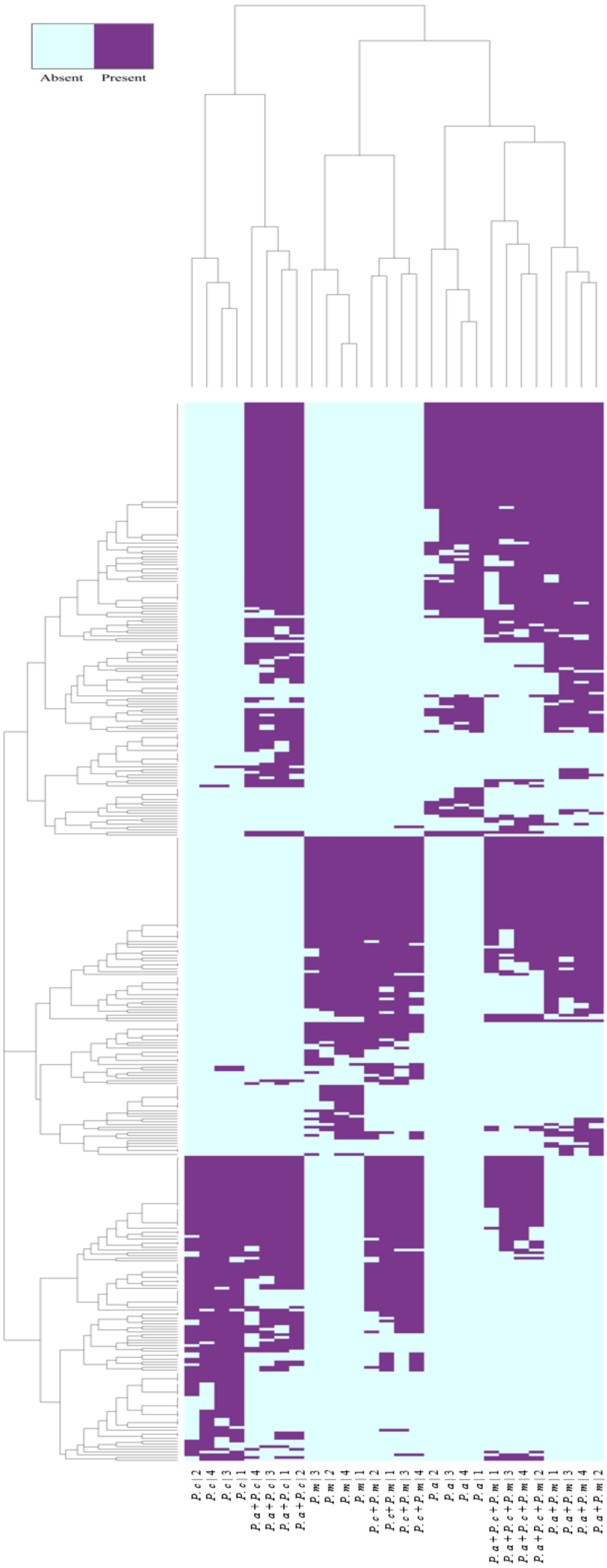

***Figure 3. 10*. Heatmap showing the presence/absence profile of putatively secreted proteins from *Phytophthora* species grown alone or in combination in static clarified V8 broth.** Proteins were identified from culture filtrate using liquid chromatography–mass spectrometry (LC–MS). Four biological replicates were included per individual species or species combination type (1–4). Blue shading indicates protein absence and purple shading indicates protein presence. *P. a* = *P. agathidicida*, *P. c* = *P. cinnamomi*, and *P. m* = *P. multivora*. The tree on the left side of the heatmap shows the similarity of proteins based on their presence/absence profile. The tree on the top of the heatmap shows similarity between the protein presence/absence profile of sample biological replicates.

Venn diagrams were then produced for each species to visualise the number of proteins present in each sample type (Figures 3.11–3.13). Figure 3.11 shows that 78 *P. agathidicida* proteins were present in all sample types, irrespective of whether this species was grown individually or in combination with another *Phytophthora* species, while nine proteins were produced when grown in every combination but not produced when grown alone , and eight proteins were produced only when grown alone. For *P. cinnamomi*, no combination-specific proteins were produced, however 23 proteins were produced only when *P. cinnamomi* was grown by itself (Figure 3.12). Finally, for *P. multivora*, only one protein was identified as being unique to multi-species samples. Like *P. cinnamomi*, *P. multivora* grown by itself resulted in a high number of unique proteins, with 17 (Figure 3.13).

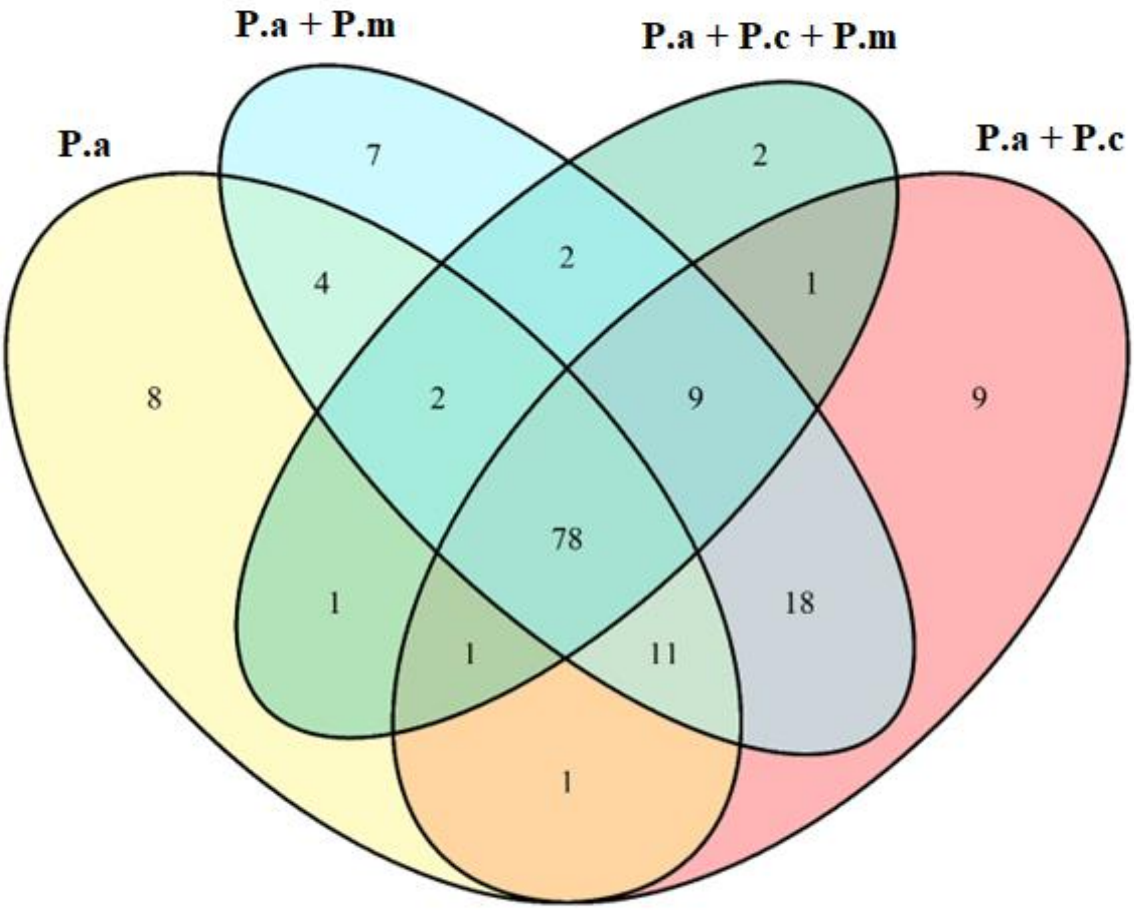

Figure 3. 11. **Venn diagram showing the numbers of putatively secreted proteins from *Phytophthora agathidicida* that are detected in culture filtrate when grown alone or in combination in with other *Phytophthora* species in static clarified V8 broth.** Proteins were identified in culture filtrates at seven days post-inoculation using liquid chromatography–mass spectrometry (LC–MS) and had to be present across at least two of four biological replicates to be regarded as a positive identification. Secreted proteins are shown in yellow for *P. agathidicida*, red for *P. agathidicida* + *P. cinnamomi*, blue for *P. agathidicida* + *P. multivora*, and green for *P. agathidicida* + *P. cinnamomi* + *P. multivora*. Crossover between two or more colours shows secreted proteins which are shared between sample types, with the centre showing the secreted proteins shared between all three sample types. P.a = *P. agathidicida*, P.c = *P. cinnamomi*, P.m = *P. multivora*.

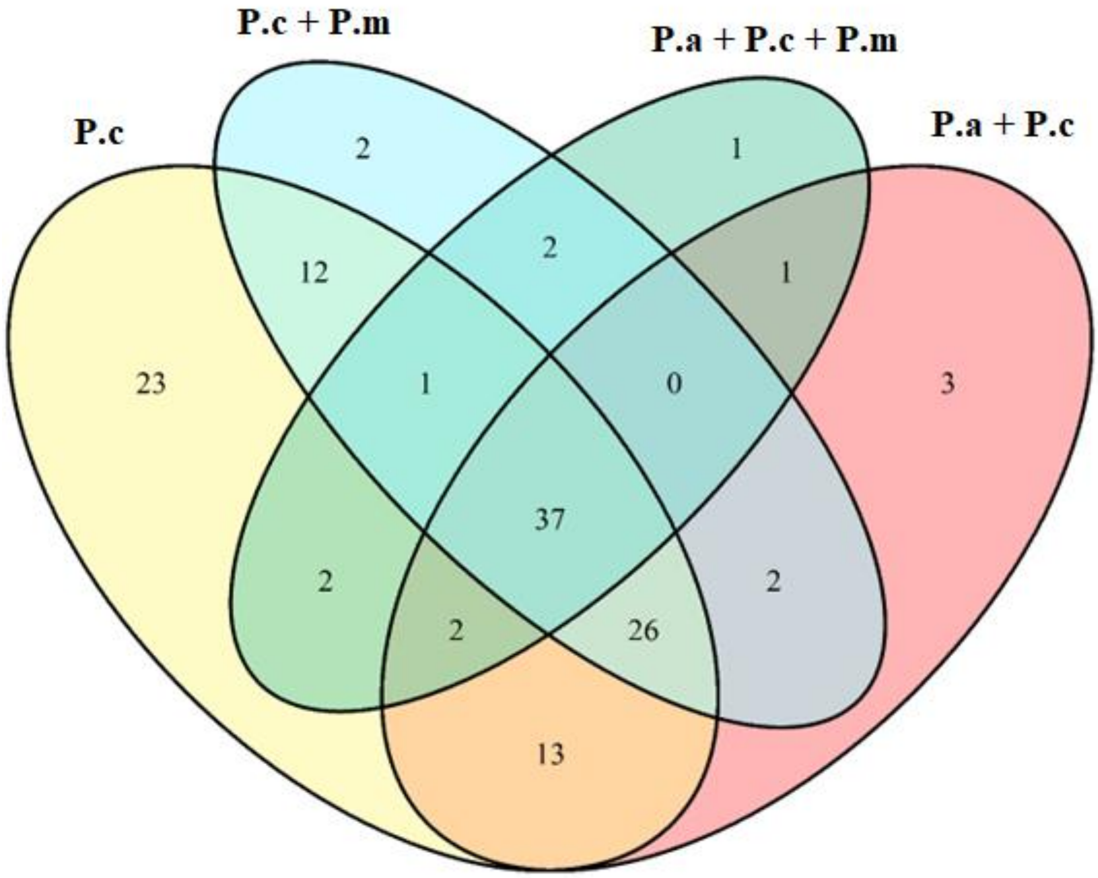

***Figure 3. 12*. Venn diagram showing the numbers of putatively secreted proteins from *Phytophthora cinnamomi* grown alone or in combination in with other *Phytophthora* species in static clarified V8 broth.** Proteins were identified in culture filtrates at seven days post-inoculation using liquid chromatography–mass spectrometry (LC–MS) and had to be present across at least two of four biological replicates to be regarded as a positive identification. Secreted proteins are shown in yellow for *P. cinnamomi*, red for *P. agathidicida* + *P. cinnamomi*, blue for *P. cinnamomi* + *P. multivora*, and green for *P. agathidicida* + *P. cinnamomi* + *P. multivora*. Crossover between two or more colours shows secreted proteins which are shared between sample types, with the centre showing the secreted proteins shared between all three sample types. P.a = *P. agathidicida*, P.c = *P. cinnamomi*, P.m = *P. multivora*.

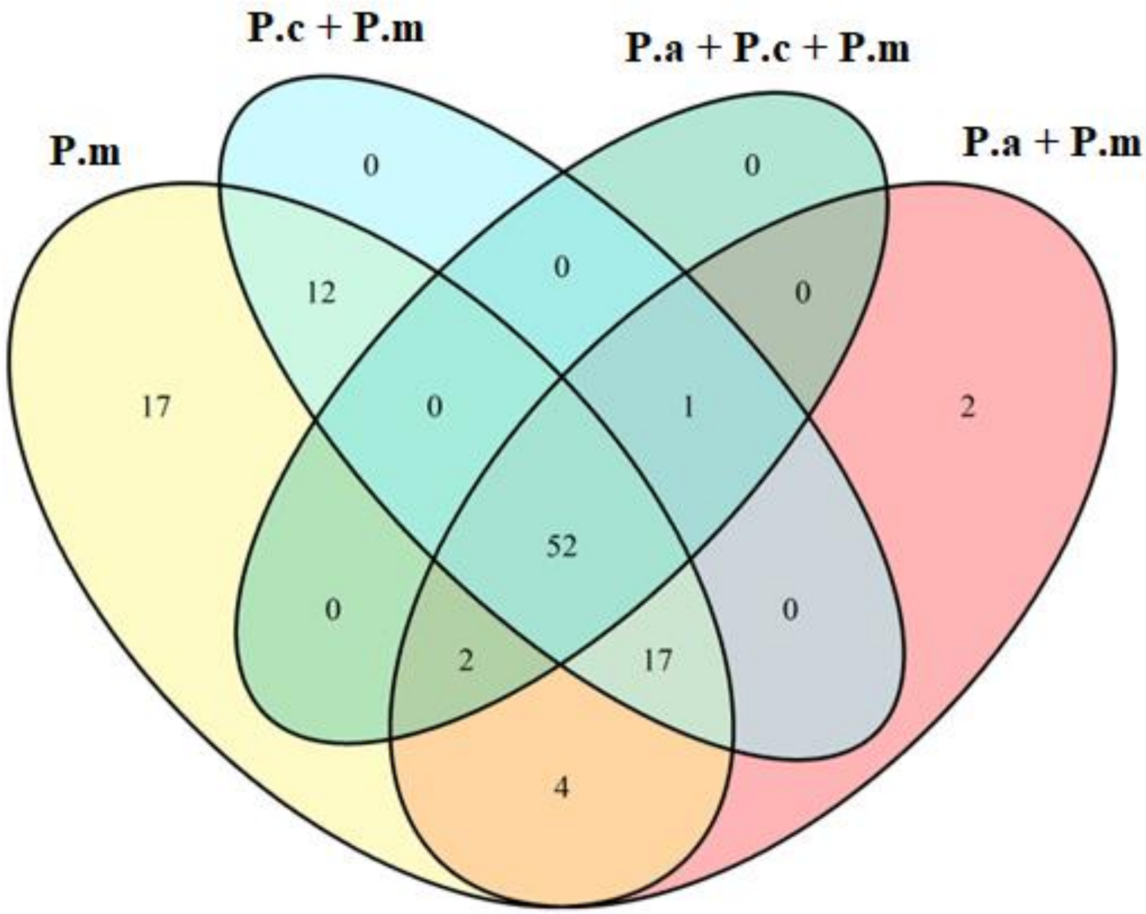

Figure 3. 13. **Venn diagram showing the numbers of putatively secreted proteins from *Phytophthora multivora* grown alone or in combination in with other *Phytophthora* species in static clarified V8 broth.** Proteins were identified in culture filtrates at seven days post-inoculation using liquid chromatography–mass spectrometry (LC–MS) and had to be present across at least two of four biological replicates to be regarded as a positive identification. Secreted proteins are shown in yellow for *P. multivora*, red for *P. agathidicida* + *P. multivora,* blue for *P. cinnamomi* + *P. multivora*, and green for *P. agathidicida* + *P. cinnamomi* + *P. multivora*. Crossover between two or more colours shows secreted proteins which are shared between sample types, with the centre showing the secreted proteins shared between all three sample types. P.a = *P. agathidicida*, P.c = *P. cinnamomi*, P.m = *P. multivora*.

2.4: Bioinformatic analysis of putatively secreted proteins exclusively produced in all combinations of co-cultured *Phytophthora* species

The putatively secreted proteins from Section 2.3 identified as only being produced in ALL sample types containing more than one *Phytophthora* species, but not in sample types containing an individual *Phytophthora* species, were selected as qualitative candidate effectors for modulating *Phytophthora–Phytophthora* interactions. Here, effector prediction programs like EffectorP v3.0 (Sperschneider & Dodds, 2022) were not applied, as it was reasoned that any secreted protein could theoretically function as an effector in modulating *Phytophthora–Phytophthora* interactions. In total, there were nine putatively secreted proteins identified in Section 2.3 from *P. agathidicida*, one from *P. multivora*, and none from *P. cinnamomi* that were only produced under all co-culturing conditions with one or two other *Phytophthora* species (Table 3.2). The protein sequences of identified qualitative candidate effectors were screened using dbCAN v2.0 and InterProScan to identify any functionally characterized domains or predicted functions (Table 3.2). Only two of the candidate effector proteins lacked functionally characterized domains and were classified as hypothetical proteins. Of the 10 qualitative candidates identified, three were identified as having auxiliary activities (KNV87_001091-T1, KNV87_013191-T1 and Pmult_s012298g00001.1). The two *P. agathidicida* proteins had Pfam domains described as PF08031 and PF07731 however, the *P. multivora* protein did not have a Pfam domain available. Two other proteins were identified as carbohydrate-active enzymes (CAZymes) that formed part of glycoside hydrolase (GH) families (KNV87_006685-T1 and KNV87_011472-T1).

Table 3. 2. **Putatively secreted qualitative candidate effector proteins produced by *Phytophthora agathidicida* and *Phytophthora multivora* when co-cultured with other *Phytophthora* species.**

Protein accession number	Predicted function[1]	Pfam number[2]
KNV87_000854-T1	Haloacid dehalogenase-like hydrolase	PF12710
KNV87_001091-T1	AA7	PF08031
KNV87_001706-T1	Lactonase	PF10282
KNV87_006685-T1	GH12	PF01670
KNV87_007317-T1	Unknown (hypothetical protein)	
KNV87_010604-T1	Unknown (hypothetical protein)	
KNV87_011472-T1	GH43	PF00135
KNV87_013191-T1	AA1	PF07731
KNV87_014053-T1	Calcineurin-like phosphoesterase	PF00149
Pmult_s012298g00001.1	AA17	

[1]AA1, Auxiliary Activity family 1; AA7, AA family 7; GH12, Glycoside Hydrolase family 12; GH43, GH family 43.

[2]Pfam, Protein family number (www.ebi.ac.uk/interpro).

[3]BLASTp, Basic Local Alignment Search Tool for protein (https://blast.ncbi.nlm.nih.gov/).

As two of the qualitative candidate effectors were hypothetical proteins that lacked known functional domains, AlphaFold2 (Jumper et al., 2021), in conjunction with ColabFold (Mirdita et al., 2022), was used to predict the tertiary structure of these proteins in the hope that the FoldSeek webserver (van Kempen et al., 2023) or DALI (Holm et al., 2023) would be able to identify structural homologs with characterized biological functions. Using DALI, the first hypothetical protein from *P. agathidicida*, KNV87_007317-T1, was predicted to adopt a fold with structural homology to chain B of the *Mycobacterium tuberculosis* MbcT-MbcA toxin-antitoxin complex, of which chain B corresponds to the toxin subunit (Freire et al., 2019) (PDB ID: 6fkg) (Figure 3.14). A FoldSeek webserver search on the other hand showed predicted structural homology to a *Phytophthora parasitica* apple domain-containing protein (FoldSeek ID: AF-A0A081AYV0) (Figure 3.15).

For the second hypothetical protein from *P. agathidicida*, KNV87_010604-T1, predicted structural similarity was observed to an uncharacterised protein from *Phytophthora sojae* using the FoldSeek server (FoldSeek ID: AF-G5AAV2-F1) (Figure 3.16), while no hit was identified using DALI. Notably, the first approximately 100 amino acids of the predicted mature protein (i.e. lacking their signal peptide) were predicted to be intrinsically disordered. This intrinsic disorder was supported by the PONDR VLXT webserver (Romero et al., 2001) (Figure 3.16D), which is a predictor of intrinsically disordered regions (IDRs) in protein sequences.

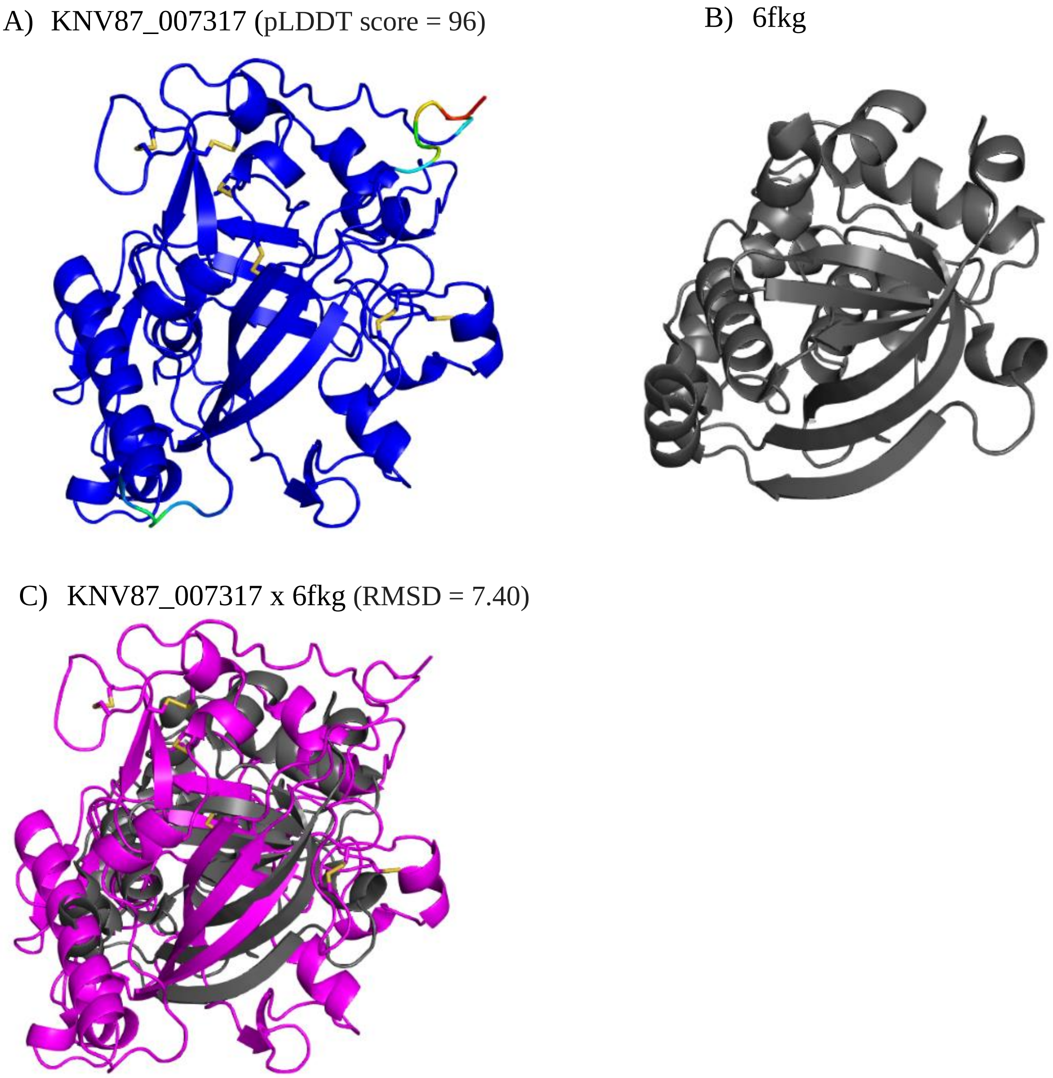

Figure 3. 14. **Predicted tertiary structure of the KNV87_007317-T1 protein from *Phytophthora agathidicida*.** A. Predicted structure of KNV87_007317-T1 using AlphaFold2 in conjunction with ColabFold. pLDDT, predicted Local Distance Difference Test score (0–100). A pLDDT score of 70–100 is indicative of medium to high confidence for the predicted tertiary structure of the protein. The structure was coloured according to the pLDDT score: high confidence = dark blue, confident to low confidence = light blue to yellow, very low confidence = red. B. Crystal structure of the chain B of the MbcT subunit of the MbcT-MbcA toxin-antitoxin complex from *Mycobacterium tuberculosis* (Protein Data Bank ID: 6fkg), which was the top DALI server hit for KNV87_007317-T1. C. Structural alignment of KNV87_007317-T1 with 6fkg using PyMol v2.5 in conjunction with the alignment plugin tool CEalign. KNV87_007317-T1 coloured grey and 6fkg coloured pink. Disulfide bonds coloured as yellow sticks. RMSD: root-mean-square deviation.

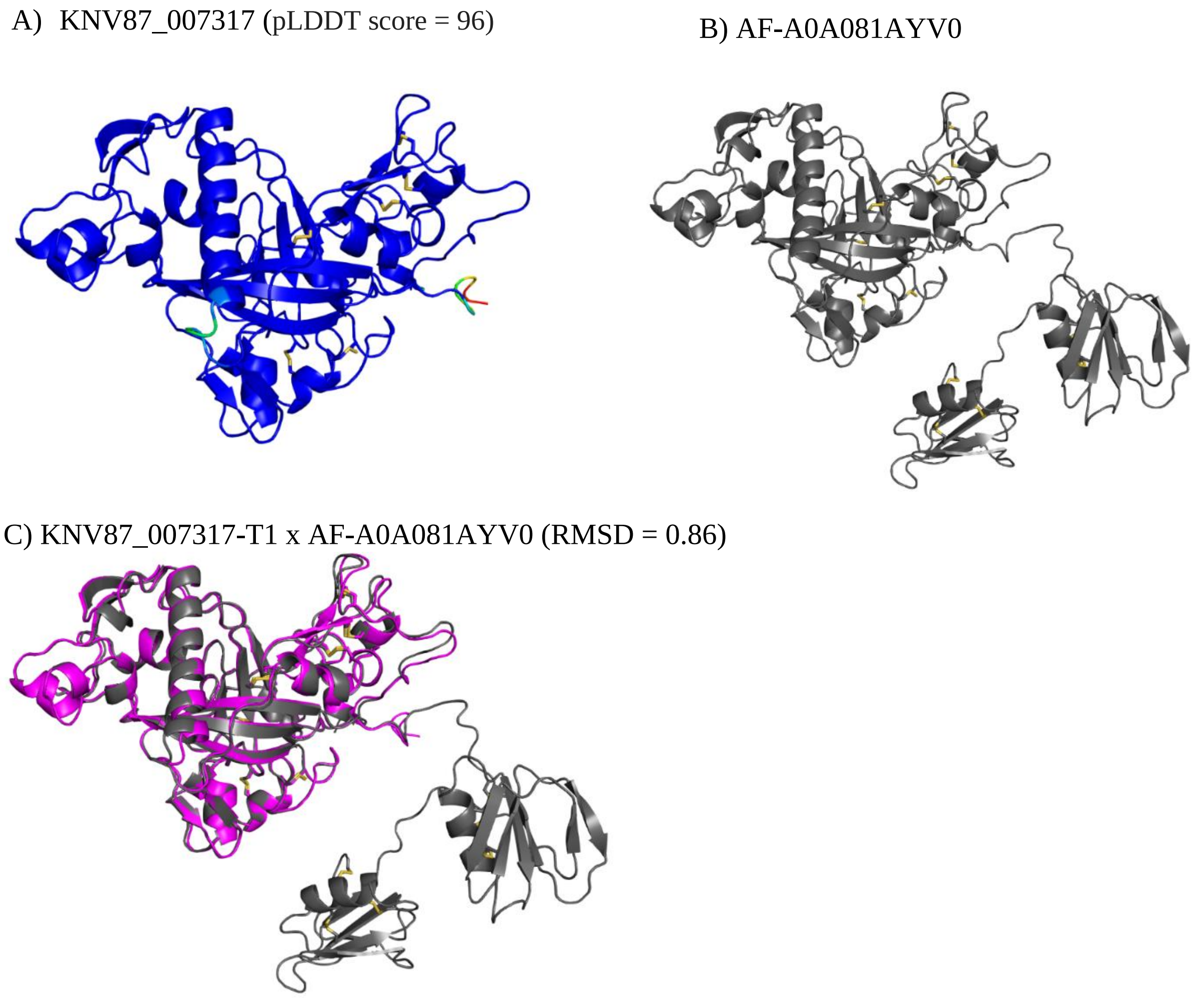

***Figure 3. 15*. Predicted tertiary structure of the KNV87_007317-T1 protein from *Phytophthora agathidicida*.** A. Predicted structure of KNV87_007317-T1 using AlphaFold2 in conjunction with ColabFold. pLDDT, predicted Local Distance Difference Test score (0–100). A pLDDT score of 70–100 is indicative of medium to high confidence for the predicted tertiary structure of the protein. The structure was coloured according to the pLDDT score: high confidence = dark blue, confident to low confidence = light blue to yellow, very low confidence = red. B. Predicted structure of *Phytopthora parasitica* AF-A0A081AYV0 (FoldSeek server top hit for KNV87_007317-T1). C. Structural alignment of KNV87_007317-T1 with AF-A0A081AYV0 using PyMol v2.5 in conjunction with the alignment plugin tool CEalign. KNV87_007317-T1 coloured grey and AF-A0A081AYV0 coloured pink. Disulfide bonds coloured as yellow sticks. RMSD: root-mean-square deviation.

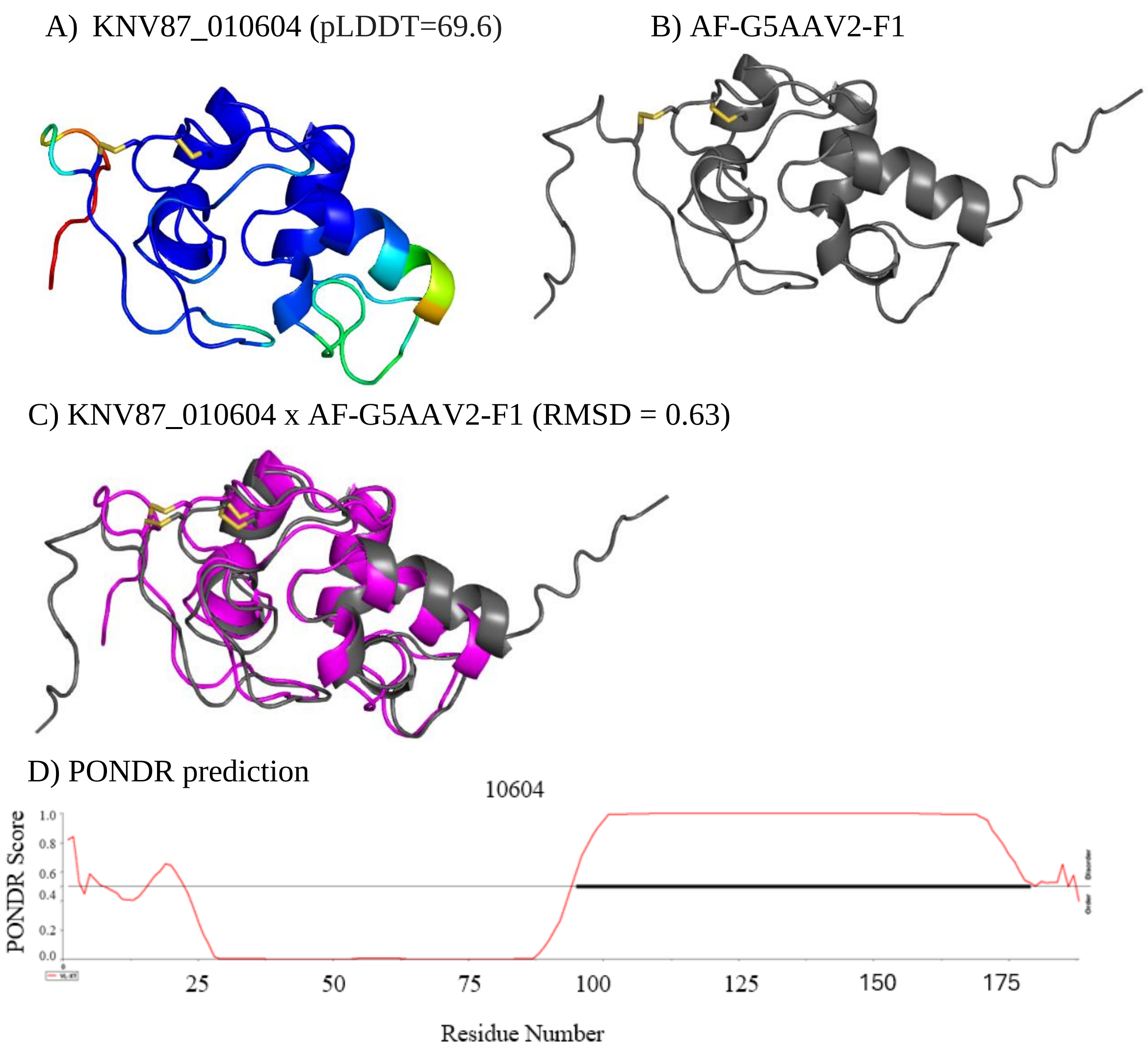

***Figure 3. 16.* Predicted tertiary structure of the KNV87_010604-T1 protein from *Phytophthora agathidicida*.** A. Predicted structure of KNV87_010604-T1 using AlphaFold2 in conjunction with Colabfold. pLDDT, predicted Local Distance Difference Test score (0–100). A pLDDT score of 70–100 is indicative of medium to high confidence for the predicted tertiary structure of the protein. The structure was coloured according to the pLDDT score: high confidence = dark blue, confident to low confidence = light blue to yellow, very low confidence = red. B. Predicted structure of *Phytophthora sojae* AF-G5AAV2-F1 (FoldSeek server top hit for KNV87_010604-T1). C. Structural alignment of KNV87_010604-T1 with AF-G5AAV2-F1 using PyMol v2.5 in conjunction with the alignment plugin tool CEalign. KNV87_007317-T1 coloured grey and AF-G5AAV2-F1 coloured pink. Disulfide bonds coloured as yellow sticks. D. Predicted intrinsically disordered region (IDR) in KNV87_010604 using PONDR VLXT. The region highlighted with a thick black bar is predicted to be an IDR. RMSD: root-mean-square deviation.

To understand the expression profiles of the genes encoding the nine candidate effector proteins from *P. agathidicida*, *in vitro* and *in planta* RNA-sequencing (RNA-seq) FPKM (fragments per kilobase of transcript per million mapped reads) values from a previous study by Cox et al. (2022) were investigated. These previous data were based on *P. agathidicida* isolate NZFS 3813 (which is almost identical to isolate NZFS 3770 at the genetic level) during growth in V8 broth at 22°C for five days without shaking (*in vitro* samples) or during growth in kauri leaves and roots at 6-, 12-, 24-, 48- and 72-hours post-inoculation (*in planta* samples), each with three biological replicates (Cox et al., 2022). For the current study, for each gene, the *in vitro* FPKM value, along with the peak *in planta* leaf and root FPKM value, were plotted in a bar graph (Figure 3.17). Only two of the genes that encode the nine candidate effectors showed *in vitro* expression with a FPKM value greater than 1 (KNV87_006685 and KNV87_010604). The genes encoding KNV87_013191 demonstrated the highest level of expression during infection of kauri leaf but was very minimally expressed during infection of kauri root. However, the genes encoding KNV87_001091 and KNV87_010604 displayed not only high expression in leaf but the highest expression in root out of the nine candidates (Figure 3.17)

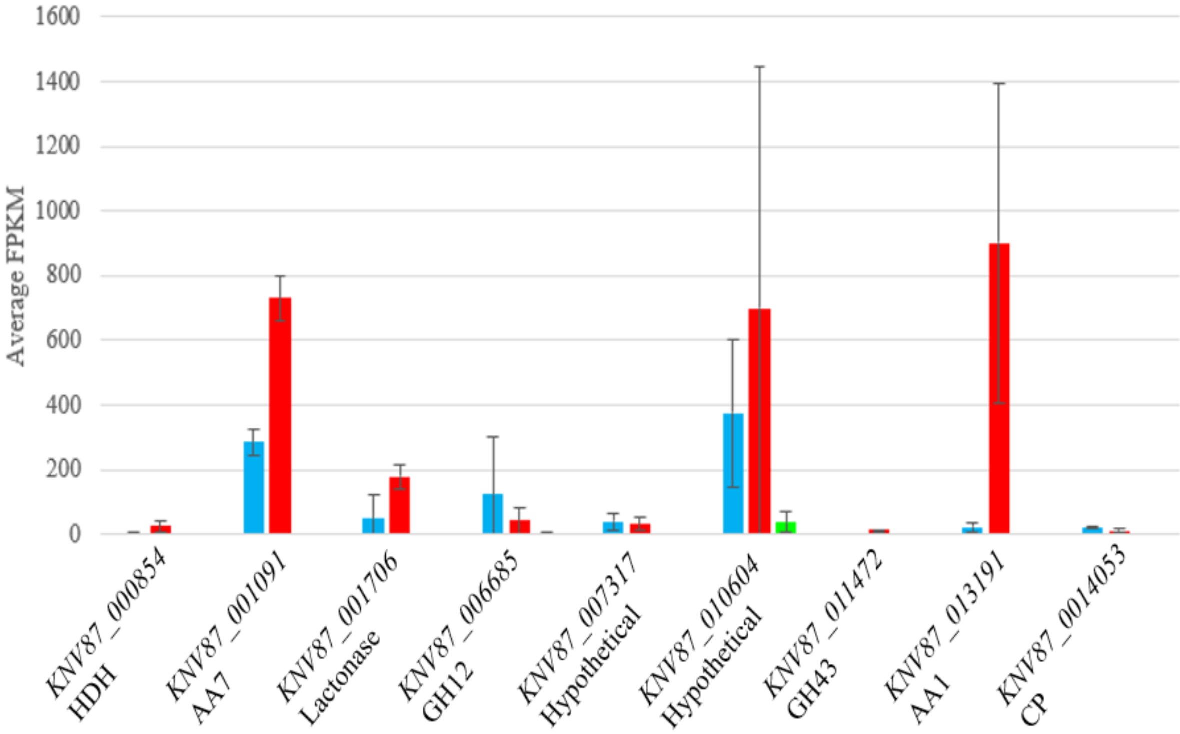

Figure 3. 17. **Bar graph showing average expression for genes encoding the qualitative candidate effector proteins of *Phytophthora agathidicida* during growth *in vitro* and in kauri leaves and roots.** Gene expression is based on RNA-sequencing (RNA-seq) data of *P. agathidicida* isolate NZFS 3813 from Cox et al. (2022), which is almost identical to isolate NZFS 3770 at the genetic level. In the study by Cox et al. (2022), *P. agathidicida* was grown in V8 broth at 22°C for five days without shaking (*in vitro* samples) or was inoculated onto kauri leaves and roots, with samples harvested at 6-, 12-, 24-, 48- and 72-hours post-inoculation (*in planta* samples), each with three biological replicates. RNAseq FPKM (fragments per kilobase of transcript per million mapped reads) values for the three biological replicates were averaged and the peak mean expression value for the *in planta* time course (both leaves and roots) shown. The bars are coloured according to the sample they originated from; root = blue, leaf = red and *in vitro* = green. Error bars represent standard deviation across the three biological replicates. HDH = haloacid dehalogenase-like hydrolase, AA7 = auxiliary activity family 7, GH12 = glycoside hydrolase family 12, GH43 = glycoside hydrolase family 43, AA1 = auxiliary activity family 1, CP = calcineurin-like phosphoesterase.

2.5: Identification of putatively secreted proteins in culture filtrates that differ quantitatively between sample types

In Section 2.3, a qualitative (presence/absence) analysis of proteins putatively secreted by individual and co-cultured *Phytophthora* species into V8 broth was performed. To determine whether the abundance of putatively secreted proteins identified in the single-species sample types changed when co-cultured with one or both of the other *Phytophthora* species, a quantitative analysis of the LC–MS data from Section 2.3 was performed using volcano plots. In the volcano plots, a $-\log_{10}$ probability value plotted on the y axis that is greater than 1.3 ($-\log_{10}(0.05)=1.3$) is considered statistically significant. The $\log_2$ values on the x axis indicate fold change in the multi-species sample protein relative to the single-species sample: a positive $\log_2$ value indicates higher abundance in a multi-species sample compared to the abundance for that same protein in the single-species sample. In the case of *P. agathidicida*, 148 of 154 proteins putatively secreted into the culture medium by this species were found to be significantly more abundant in the presence of at least one other species compared to when grown on its own (Figure 3.18). In contrast, there were only six putatively secreted proteins of *P. agathidicida* that were significantly less abundant in the presence of another species compared to individually grown *P. agathidicida* (Figure 3.18). However, the opposite was shown for both *P. cinnamomi* and *P. multivora*, with almost all significant proteins being less abundant, apart from one *P. multivora* protein which was significantly more abundant (Figures 3.18 and 3.19).

The *Phytophthora* proteins that had a $-\log_{10}$ value greater than 1.3 ($-\log_{10}(0.05)=1.3$) and a positive value (>0) for $\log_2$ fold change (ranging from 0.668 to 9.335), indicating significantly higher levels in mixed cultures, are shown in Table 3.4, with functions predicted by the dbCAN v2.0 or InterProScan webserver database. As with the proteins found only to be present in multi-species sample types in Section 2.3, the proteins found to be significantly more abundant in multi-species sample types were referred to as quantitative candidate effectors. *P. agathidicida* had ten proteins that were significantly more abundant in every multi-species sample type relative to when grown alone. These ten proteins were found to be significantly more abundant in the *P. agathidicida* + *P. cinnamomi*, *P. agathidicida* + *P. multivora* AND *P. agathidicida* + *P. cinnamomi* + P. *multivora* samples. These ten proteins are different to those identified in the qualitative analysis of Section 2.3, as these proteins were also produced in the *P. agathidicida*-only samples, but at a low abundance. Five of the ten proteins that were significantly more abundant in multi-species samples had a $-\log_{10}$ value (significance value) greater than 3 (indicated by pink shading in Table 3.3). For *P. cinnamomi* and *P. multivora*, there were three and four proteins, respectively, that had significant changes in protein abundance when co-cultured with another *Phytophthora* species. However, unlike those proteins identified from *P. agathidicida*, these were less abundant across every multi-species sample type and had a $-\log_{10}$ value no greater than 3. All raw data are shown in Appendix 1: Tables A1, A2 and A3.

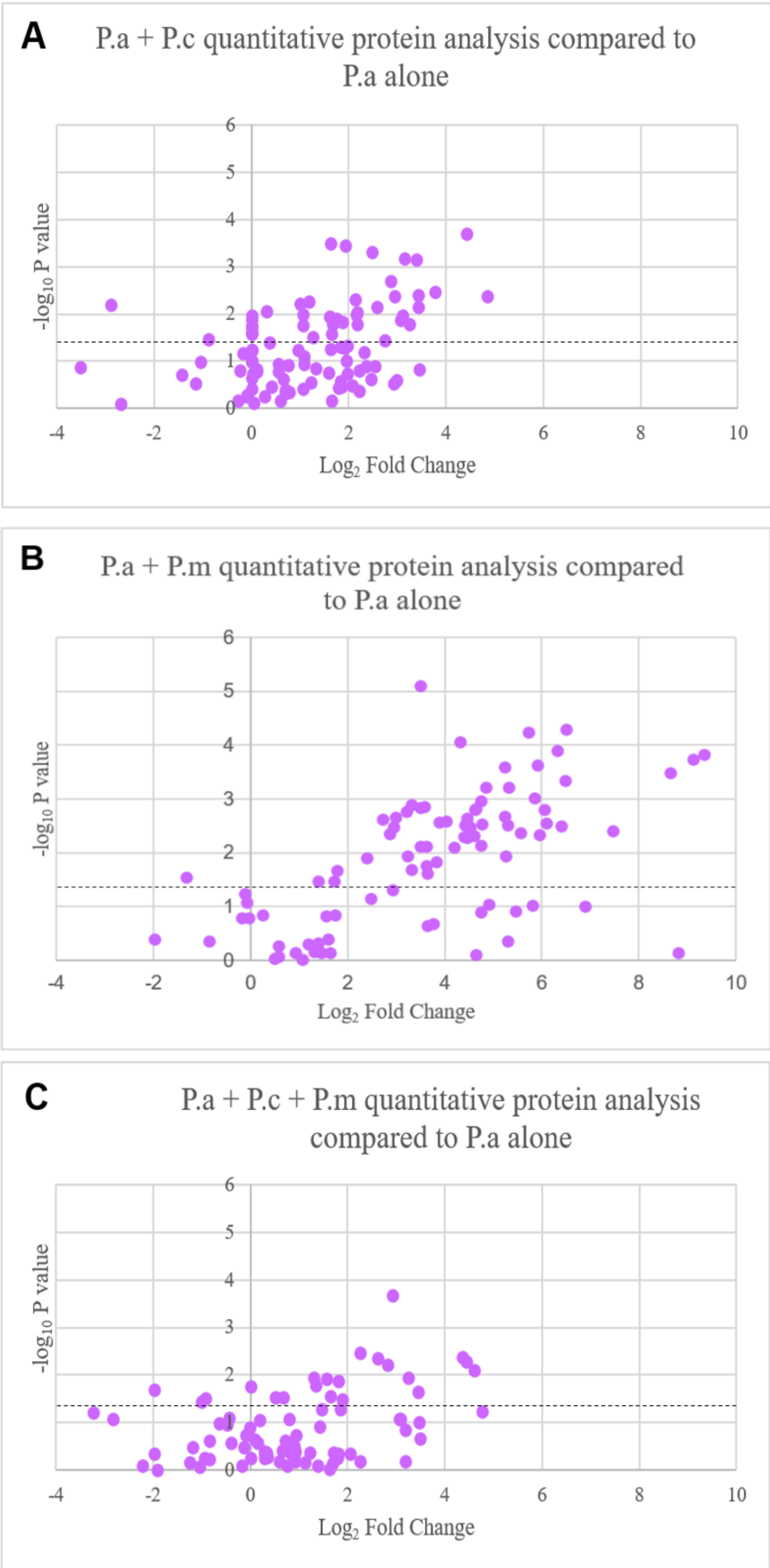

Figure 3. 18. **Volcano plot of putatively secreted proteins from *P. agathidicida* that are more or less abundant in the presence of other *Phytophthora* species when cultured in clarified V8 broth.** Proteins were identified in culture filtrates at seven days post-inoculation using liquid chromatography–mass spectrometry (LC–MS) and had to be present across at least two of four biological replicates to be regarded as a positive identification. X axis indicates negative or positive fold change in protein abundance for each protein across each multi-species sample type when compared to *P. agathidicida* grown alone. Y axis indicates statistical significance, with a $\log_{10}$ value of 1.3 or $\log_{10}(0.05)$ or higher indicative of statistical significance. Each purple dot represents an independent protein.

A = *P. agathidicida* + *P. cinnamomi* compared to *P. agathidicida* alone.

B = *P. agathidicida* + *P. multivora* compared to *P. agathidicida* alone.

C = *P. agathidicida* + *P. cinnamomi* + *P. multivora* compared to *P. agathidicida* alone.

P.a = *P. agathidicida*; P.c = *P. cinnamomi*; P.m = *P. multivora*.

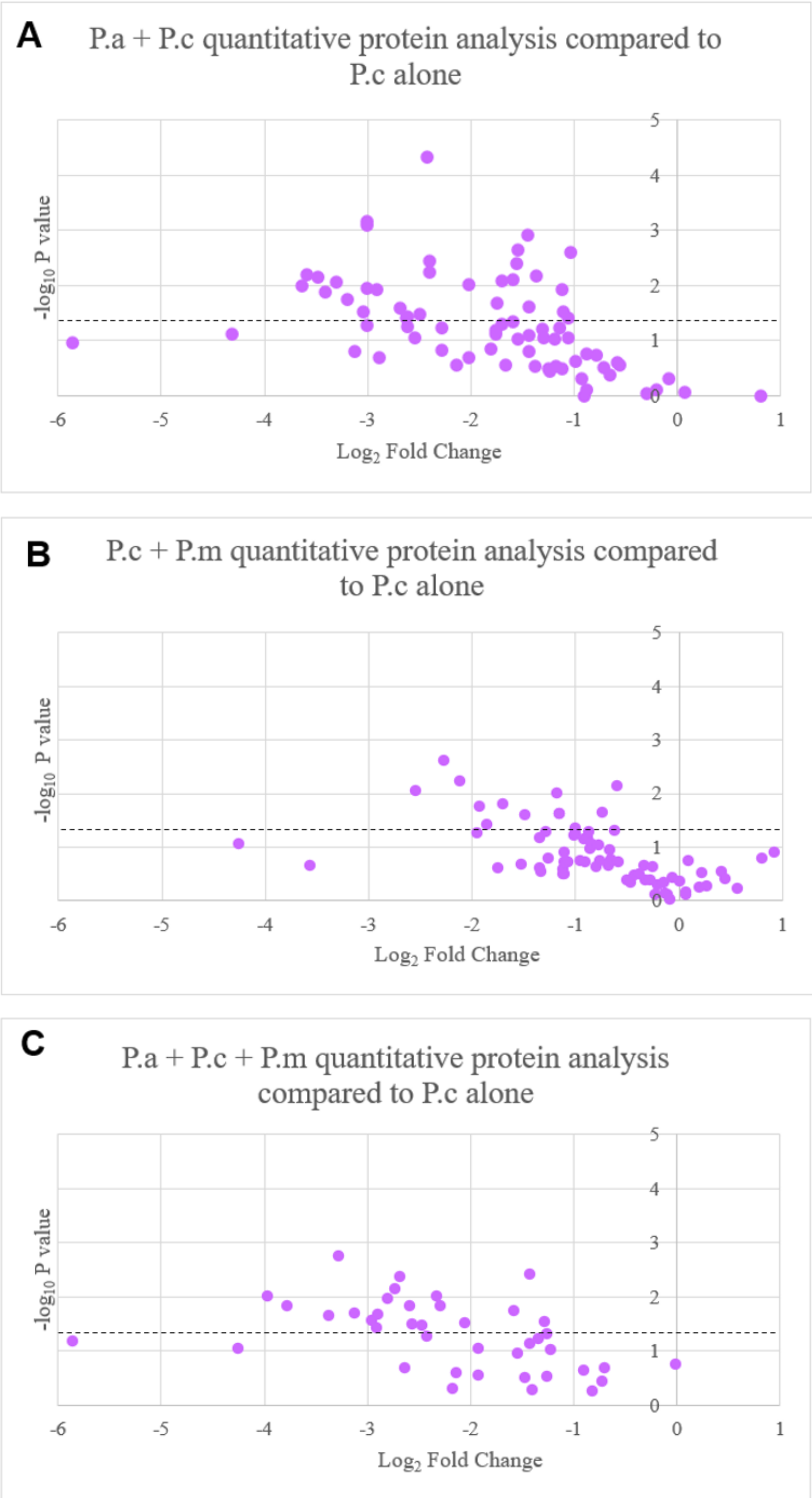

***Figure 3. 19.* Volcano plot of putatively secreted proteins from *P. cinnamomi* that are more or less abundant in the presence of other *Phytophthora* species when cultured in clarified V8 broth.** Proteins were identified in culture filtrates at seven days post-inoculation using liquid chromatography–mass spectrometry (LC–MS) and had to be present across at least two of four biological replicates to be regarded as a positive identification. X axis indicates negative or positive fold change in protein abundance for each protein across each multi-species sample type when compared to *P. cinnamomi* grown alone. Y axis indicates statistical significance, with a $\log_{10}$ value of 1.3 or $\log_{10}(0.05)$ or higher indicative of statistical significance. Each purple dot represents an independent protein.

A = *P. agathidicida* + *P. cinnamomi* compared to *P. cinnamomi* alone.

B = *P. cinnamomi* + *P. multivora* compared to *P. cinnamomi* alone.

C = *P. agathidicida* + *P. cinnamomi* + *P. multivora* compared to *P. cinnamomi* alone.

P.a = *P. agathidicida*; P.c = *P. cinnamomi*; P.m = *P. multivora*.

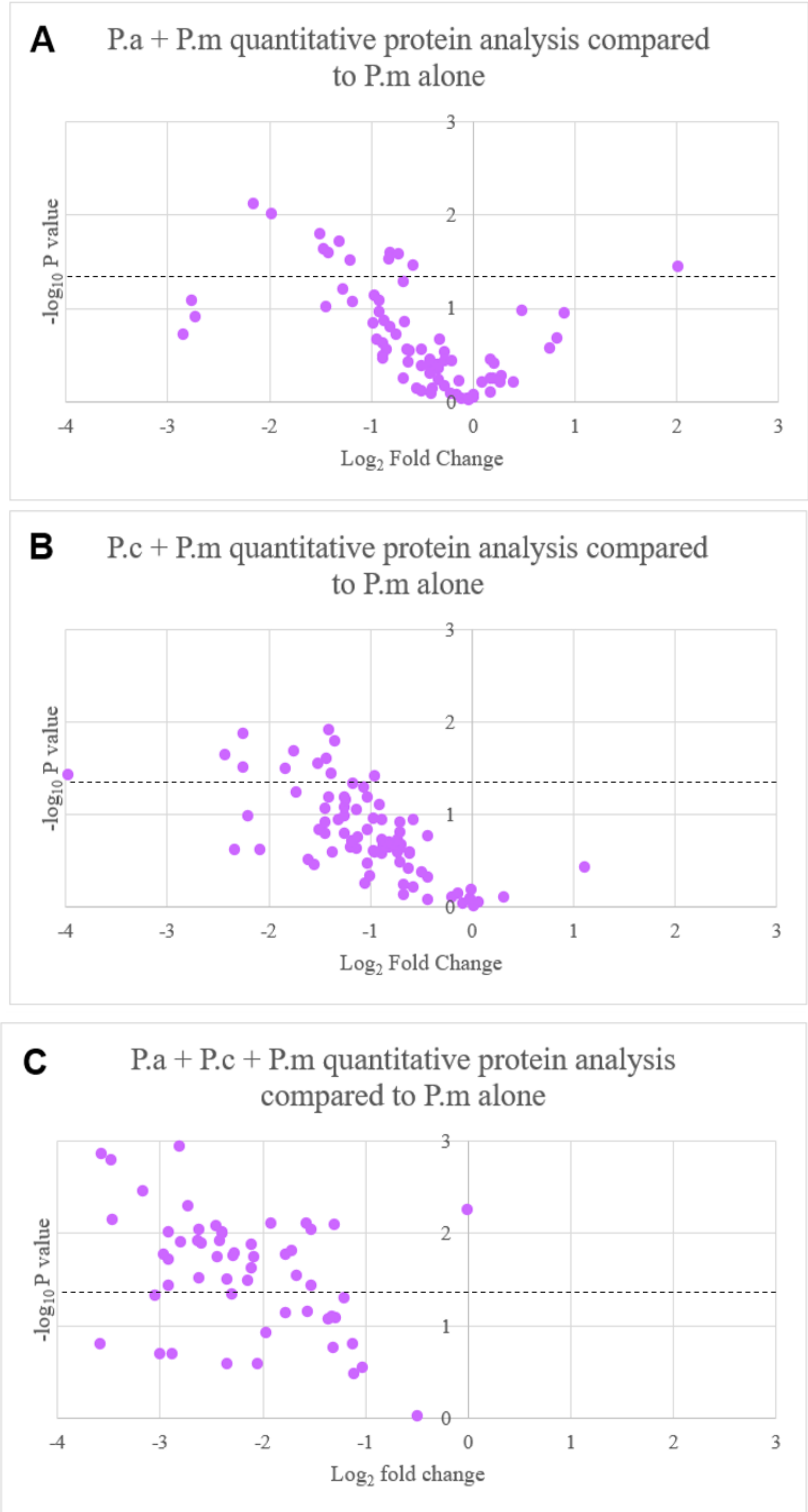

***Figure 3. 20.* Volcano plot of putatively secreted proteins from *P. multivora* that are more or less abundant in the presence of other *Phytophthora* species when cultured in clarified V8 broth.** Proteins were identified in culture filtrates at seven days post-inoculation using liquid chromatography–mass spectrometry (LC–MS) and had to be present across at least two of four biological replicates to be regarded as a positive identification. X axis indicates negative or positive fold change in protein abundance for each protein across each multi-species sample type when compared to *P. multivora* grown alone. Y axis indicates statistical significance, with a $\log_{10}$ value of 1.3 or $\log_{10}(0.05)$ or higher indicative of statistical significance. Each purple dot represents an independent protein.

A = *P. agathidicida* + *P. multivora* compared to *P. multivora* alone.

B = *P. cinnamomi* + *P. multivora* compared to *P. multivora* alone.

C = *P. agathidicida* + *P. cinnamomi* + *P. multivora* compared to *P. multivora* alone.

P.a = *P. agathidicida*; P.c = *P. cinnamomi*; P.m = *P. multivora*.

Of the ten *P. agathidicida* effector candidates identified in the quantitative analysis, only one protein lacked functionally characterized domains and was classified as a hypothetical protein (KNV87_015800-T1). Of the nine other quantitative effector candidates, four were identified as CAZymes: two glycoside hydrolases (KNV87_004012-T1 with a PF18271 Pfam domain and KNV87_017260-T1 with a PF00933 Pfam domain) and two auxiliary activity enzymes (KNV87_013190-T1 with a PF00394 Pfam domain and KNV87_017260-T1 with no Pfam domain but, instead, identified as an auxiliary activity enzyme using the dbCAN webserver).

Similarly to the three hypothetical proteins identified in Section 2.4, the tertiary structure of the hypothetical protein identified in the quantitative analysis, KNV87_015800, was predicted using AlphaFold2, in conjunction with ColabFold, to gain insights into its function, as no functional domains were predicted by InterProScan or dbCAN. AlphaFold2/ColabFold predicted a tertiary structure which matched an auxiliary activity family 15 protein from the insect *Thermobia domestica* on the DALI webserver (PDB ID: 5msz), while the top hit on the FoldSeek webserver was an uncharacterised protein from the fungus *Cladophialophora carrionii* (FoldSeek ID: AF-A0A1C1CP81-F1) (Figure 3.19).

***Table 3. 3.* Fold change and -log10 values for each candidate effector protein from *Phytophthora agathidicida* that significantly increased in abundance when co-cultured with another *Phytophthora* species, relative to growth alone.**

Protein ID/number	Description	Pfam number	P.a + P.m	P.a + P.c + P.m	P.a + P.c
KNV87_004012-T1	GH131	PF18271	**5.318**	**1.890**	**2.863**
KNV87_004047-T1	AA17		**6.475**	**4.436**	**1.607**
KNV87_004566-T1	Periplasmic substrate binding protein	PF133143	**3.207**	**4.604**	**1.666**
KNV87_008864-T1	Lipoxygenase	PF00305	**4.454**	**0.668**	**2.734**
KNV87_009659-T1	Non-lysosomal ceramidase	PF17048	**9.124**	**2.248**	**3.773**
KNV87_011474-T1	Carboxylesterase family 24	PF00135	**5.957**	**1.801**	**2.571**
KNV87_013190-T1	AA1	PF00394	**8.651**	**1.638**	**4.412**
KNV87_015800-T1	Unknown (hypothetical protein)		**7.454**	**3.245**	**2.948**
KNV87_016404-T1	Cyclophilin type peptidyl-prolyl isomerase	PF00160	**6.409**	**3.449**	**1.868**
KNV87_017260-T1	GH3	PF00933	**9.335**	**2.920**	**3.137**

1. AA1, Auxiliary Activity family 1; AA7, AA family 7; GH12, Glycoside Hydrolase Family 12; GH43, GH family 43; P.a = *P. agathidicida*; P.c = *P. cinnamomi*; P.m = *P. multivora*.
2. Coloured by -$\log_{10}$ P-value (values not shown in table) = the higher -$\log_{10}$ value, the more statistically significantly the increased abundance of the protein is. Light purple = -$\log_{10}$ value between 1.3 and 2; dark purple = -$\log_{10}$ value between 2 and 3; dark pink = -$\log_{10}$ value >3.
3. Values in each column represents the $\log_2$ fold change value (increase in protein abundance when co-cultured with another *Phytophthora* species, relative to growth alone).
4. Species were cultured as single-species samples or multi-species samples in clarified V8 broth for seven days without shaking and the proteins secreted into the culture medium assessed for differences in abundance using LC–MS data generated from the Proteome Discoverer program after searching against respective proteome databases.

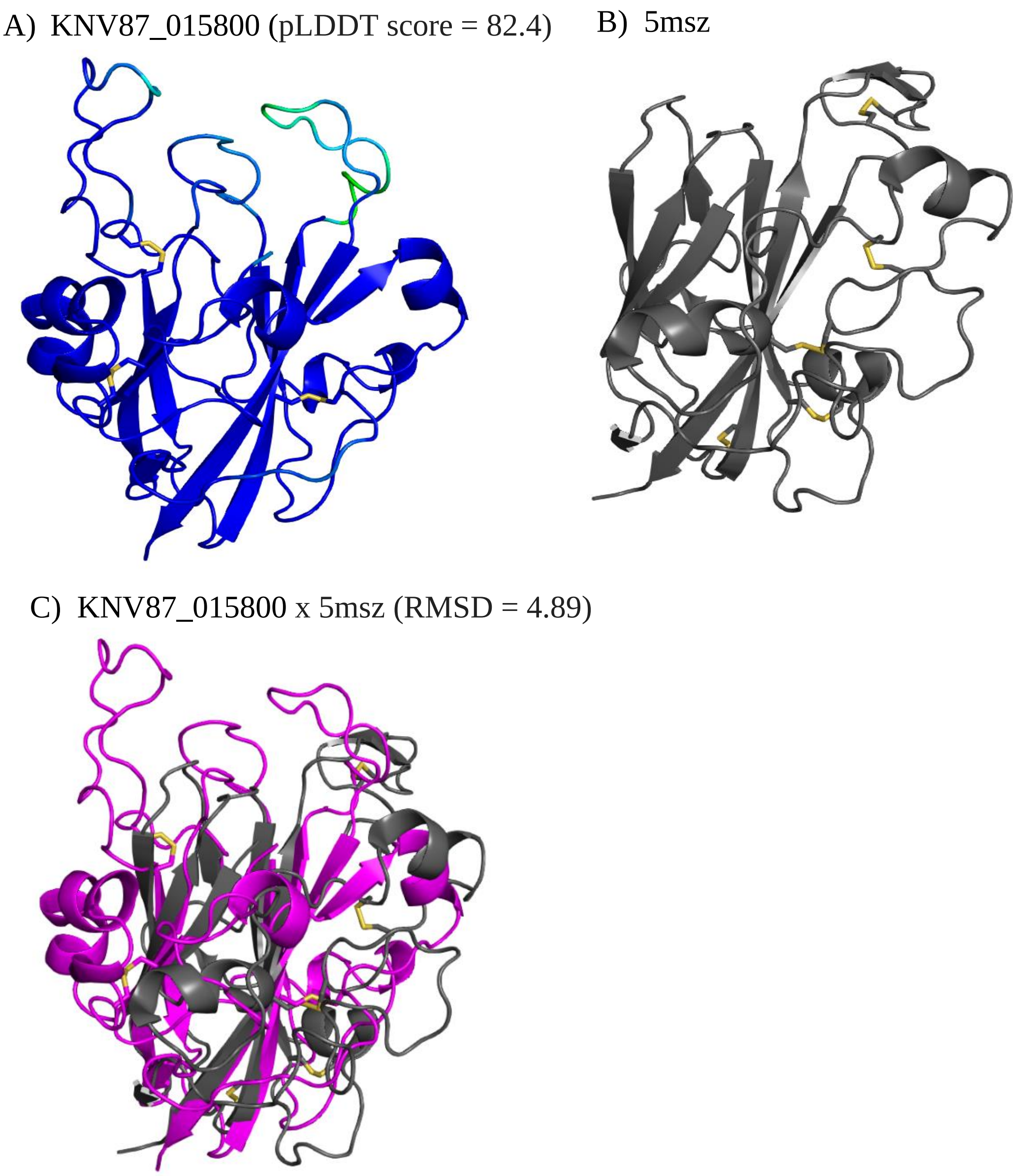

Figure 3. 21. **Predicted tertiary structure of the KNV87_015800-T1 protein from *Phytophthora agathidicida*.** A. Predicted structure of KNV87_015800-T1 using AlphaFold2 in conjunction with ColabFold. pLDDT, predicted Local Distance Difference Test score (0–100). A pLDDT score of 70–100 is indicative of medium to high confidence for the predicted tertiary structure of the protein. The structure was coloured according to the pLDDT score: high confidence = dark blue, confident to low confidence = light blue to yellow, very low confidence = red. B. Predicted structure of *Thermobia domestica* 5msz (Dali server top hit for KNV87_015800-T1). C. Structural alignment of KNV87_015800-T1 with 5msz using PyMol v2.5 in conjunction with the alignment plugin tool CEalign. KNV87_015800-T1 coloured grey and 5msz coloured pink. Disulfide bonds coloured as yellow sticks.

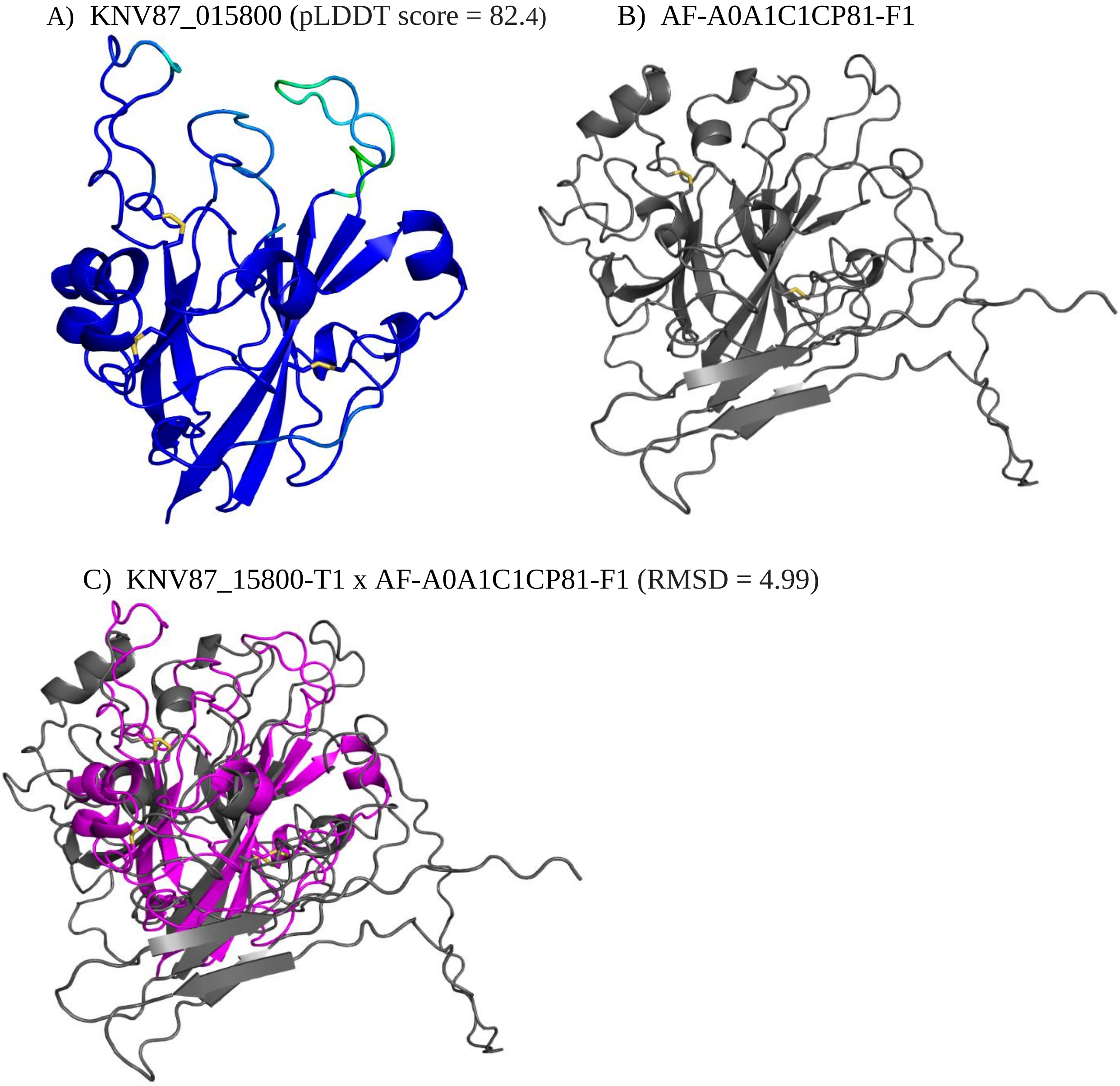

***Figure 3. 22.* Predicted tertiary structure of the KNV87_015800-T1 protein from *Phytophthora agathidicida*.** A. Predicted structure of KNV87_015800-T1 using AlphaFold2 in conjunction with ColabFold. pLDDT, predicted Local Distance Difference Test score (0–100). A pLDDT score of 70–100 is indicative of medium to high confidence for the predicted tertiary structure of the protein. The structure was coloured according to the pLDDT score: high confidence = dark blue, confident to low confidence = light blue to yellow, very low confidence = red. B. Predicted structure of *Cladophialophora carrionii* AF-A0A1C1CP81-F1 (FoldSeek server top hit for KNV87_015800-T1). C. Structural alignment of KNV87_015800-T1 with F-A0A1C1CP81-F1 using PyMol v2.5 in conjunction with the alignment plugin tool CEalign. KNV87_015800 coloured grey and AF- F-A0A1C1CP81-F1 coloured pink. Disulfide bonds coloured as yellow sticks.

To get a better understanding of how the 10 candidate effector proteins with statistically significant increases in abundance during production in co-culture looked relative to each other in terms of abundance across sample types, the normalised abundance from each sample was plotted (Figure 3.21). The *P. agathidicida* + *P. multivora* samples tended to produce proteins that had the highest normalised abundance values out of all sample types as shown by the green points. Of particular interest, proteins KNV87_004012-T1 (GH131) and KNV87_013190-T1 (AA1) had abundance values originating from the *P. agathidicida* + *P. multivora* samples between 10 to 15 times more than when *P. agathidicida* was grown by itself.

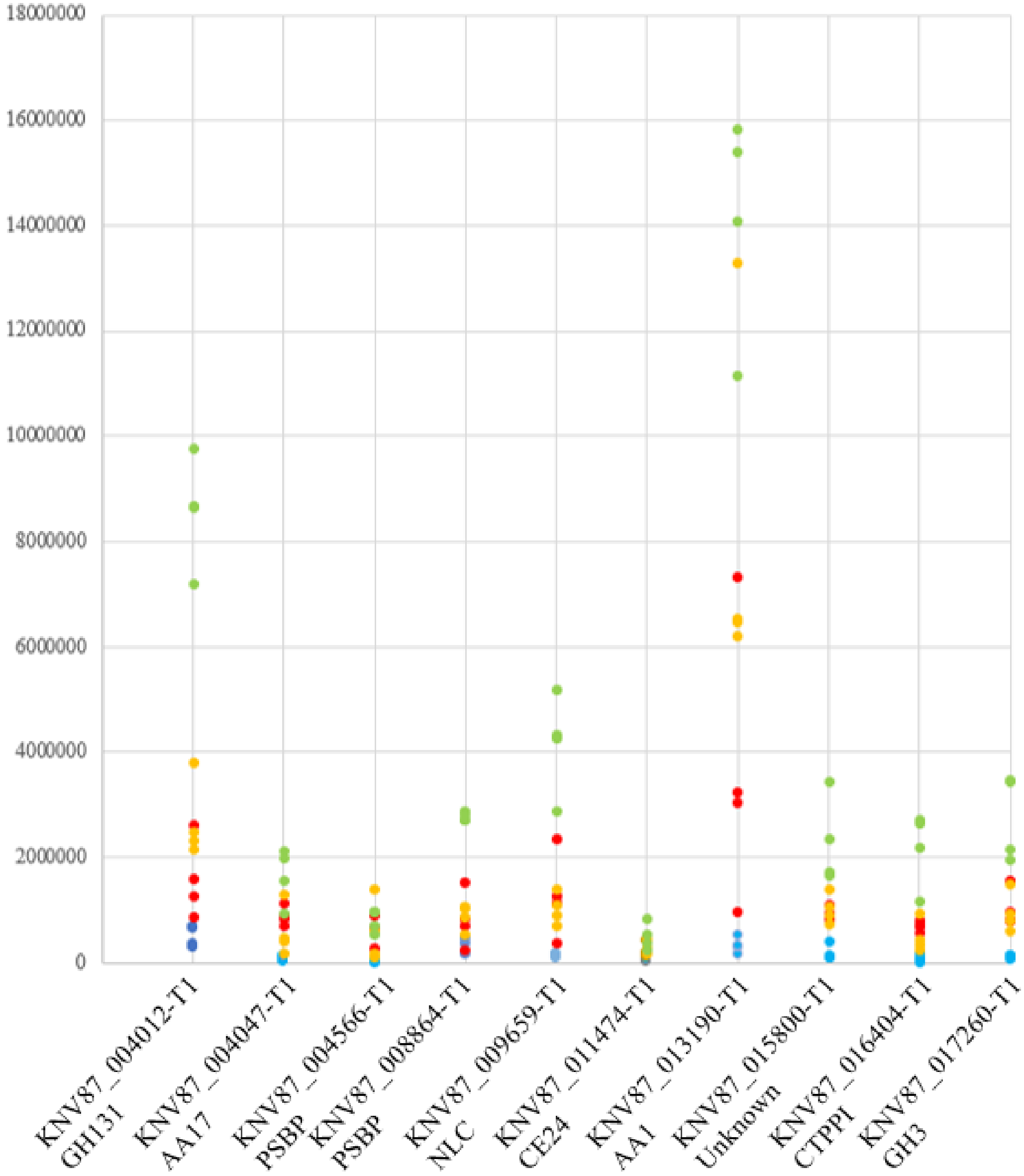

Figure 3. 23. **Dot plot of normalised abundance scores from each candidate protein identified as significantly increased abundance across all multi-species samples when compared to the single-species sample**. The dots are coloured according to which sample they originated from; blue = *P. agathidicida*, red = *P. agathidicida* + *P. cinnamomi* + *P. multivora*, orange = *P. agathidicida* + *P. cinnamomi*, green = *P. agathidicida* + *P. multivora*. Normalised abundance scores were calculated for each protein across each biological replicate according to Section 2.3.9 (Chapter 2). GH131 = glycoside hydrolase family 131, AA17 = auxiliary activity family 17, PSBP = periplasmic solute binding protein, NLC – non-lysosomal ceramidase, CE26 = carboxylesterase family 24, AA1 = auxiliary activity family 1, CTPPI = cyclophilin type peptidyl-prolyl isomerase, GH3 = glycoside hydrolase family 3.

To understand the expression profile of the genes encoding the ten *P. agathidicida* candidate effector proteins, the peak *in vitro* and *in planta* RNA-seq FPKM values from Cox et al. (2022) were once again investigated. This analysis revealed that, in all but one case (KNV87_004012), gene expression corresponding to each of the candidate effector proteins was detected both *in vitro* and *in planta*, with most more highly expressed *in planta* relative to growth *in vitro* (Figure 3.22). Of note, of the ten candidate effector proteins, the genes encoding KNV87_013190 (AA1) and KNV87_16404 (isomerase) demonstrated the highest peak level of expression during infection of kauri leaves, with the latter also demonstrating the highest expression during infection of kauri roots (Figure 3.22).

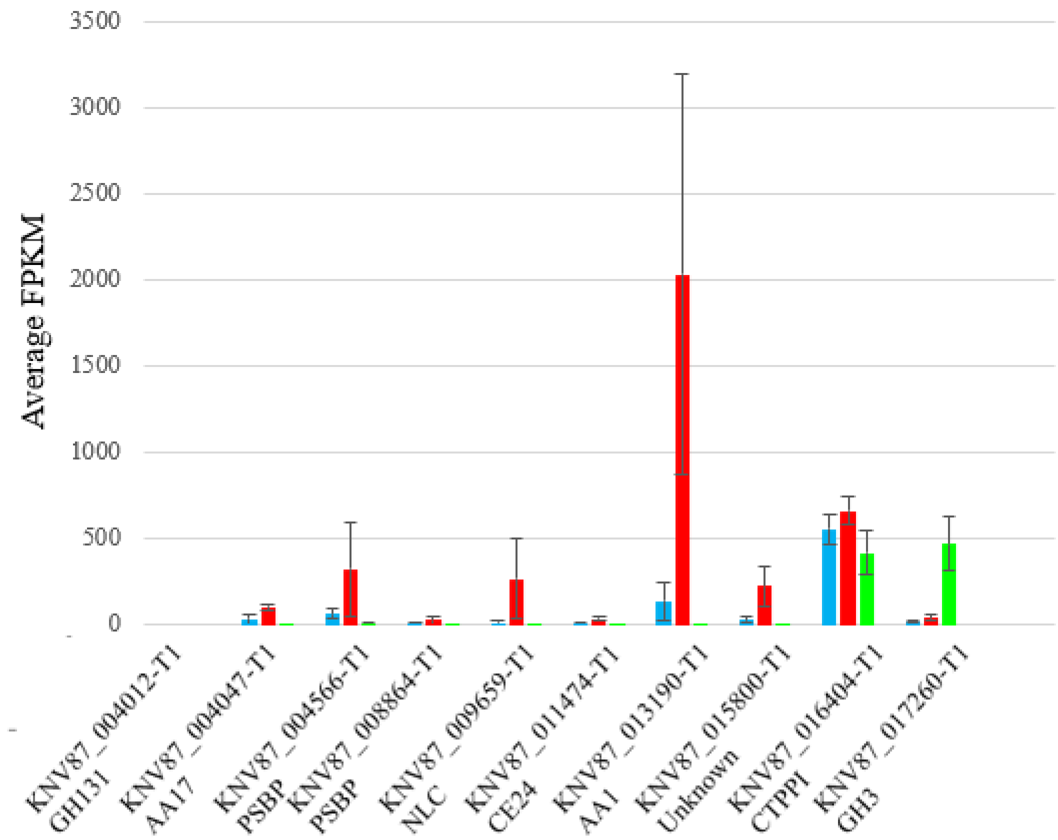

***Figure 3. 24*. Bar graph showing average expression for genes encoding the quantitative candidate effector proteins of *Phytophthora agathidicida* proteins *in vitro* and in kauri leaves and roots.** Gene expression is based on RNA-sequencing (RNA-seq) data of *P. agathidicida* isolate NZFS 3813 from Cox et al. (2022), which is almost identical to isolate NZFS 3770 at the genetic level. In the study by Cox et al. (2022), *P. agathidicida* was grown in V8 broth at 22°C for five days without shaking (*in vitro* samples) or was inoculated onto kauri leaves and roots, with samples harvested at (6-, 12-, 24-, 48- and 72-hours post-inoculation), each with three biological replicates. RNAseq FPKM (fragments per kilobase of transcript per million mapped reads) values for the three biological replicates were averaged and the peak mean expression value for the *in planta* time course (both leaves and roots) shown. The bars are coloured according to the sample they originated from; root = blue, leaf = red and *in vitro* = green. Error bars represent standard deviation across the three biological replicates. GH131 = glycoside hydrolase family 131, AA17 = auxiliary activity family 17, BESBP = bacterial extracellular solute binding protein, NLC – non-lysosomal ceramidase, CE26 = carboxylesterase family 24, AA1 = auxiliary activity family 1, CTPPI = cyclophilin type peptidyl-prolyl isomerase, GH3 = glycoside hydrolase family 3.

3: Infection assays involving Phytophthora species and the model plant Nicotiana benthamiana

To determine whether the three *Phytophthora* species modulate the growth of each other *in planta*, it first must be determined whether the species used in this study can all infect the test plant species in question. Furthermore, it must be determined whether any of these species are naturally more aggressive that the others in terms of lesion formation, as a dominant species may colonise the entire plant tissue prior to lesions being formed by the other species, which means that differences in lesion size cannot be easily assessed upon co-inoculation. Unfortunately, due to cultural agreements not being in place at the time of experiments, infection tests could not be performed on kauri tissue. With these points in mind, wildtype *Nicotiana benthamiana*, which is known to be a host for *P. agathidicida* (Mesarich and Bradshaw lab, unpublished data) and *P. cinnamomi* (Belisle et al., 2019), was chosen for this experiment. Here, as roots are not an easy tissue to perform experiments of this nature on, plants were grown for five weeks before the detached leaves from independent plants were inoculated independently with each of the three *Phytophthora* species (i.e. one species per leaf on both sides of the major leaf vein).

All species were able to infect wildtype *N. benthamiana* plants derived from seed stored at Massey University. However, with the exception of *P. multivora*, a large amount of variation occurred between the biological replicates. *P. multivora* was found to be an aggressive pathogen of *N. benthamiana* with lesions consistently visible by 24 hours post-inoculation (hpi) and complete destruction of the leaf by four dpi (Figure 3.27). *P. agathidicida* showed the most amount of variation in lesion size with some points of inoculation resulting in visible lesions (Figure 3.25) while, on other leaves, no lesions were observed (Appendix 1: Table A4). This pathogen seemed to be affected by the age and morphology of the leaves: the older the leaf, the better the infection, and the fact that it needed to be flat without crinkled edges. *P. cinnamomi* could infect *N. benthamiana*, but with difficulty and high variability (Figure 3.26). Small lesions, the size of the five mm agar plug, formed at around three dpi. Furthermore, *P. agathidicida* took a similar timeframe to infect *N. benthamiana* as that shown by *P cinnamomi*, however the lesion size increased much faster. By this time *P. multivora* had disseminated in the leaves as they could form lesions this size one to two days prior. Due to differences between the species in the rates of infection of the leaves, detached leaf assays with differing species combinations were not undertaken. A table indicating when lesions exceeded the size of the five mm agar plug is described in Table A4 (Appendix 1).

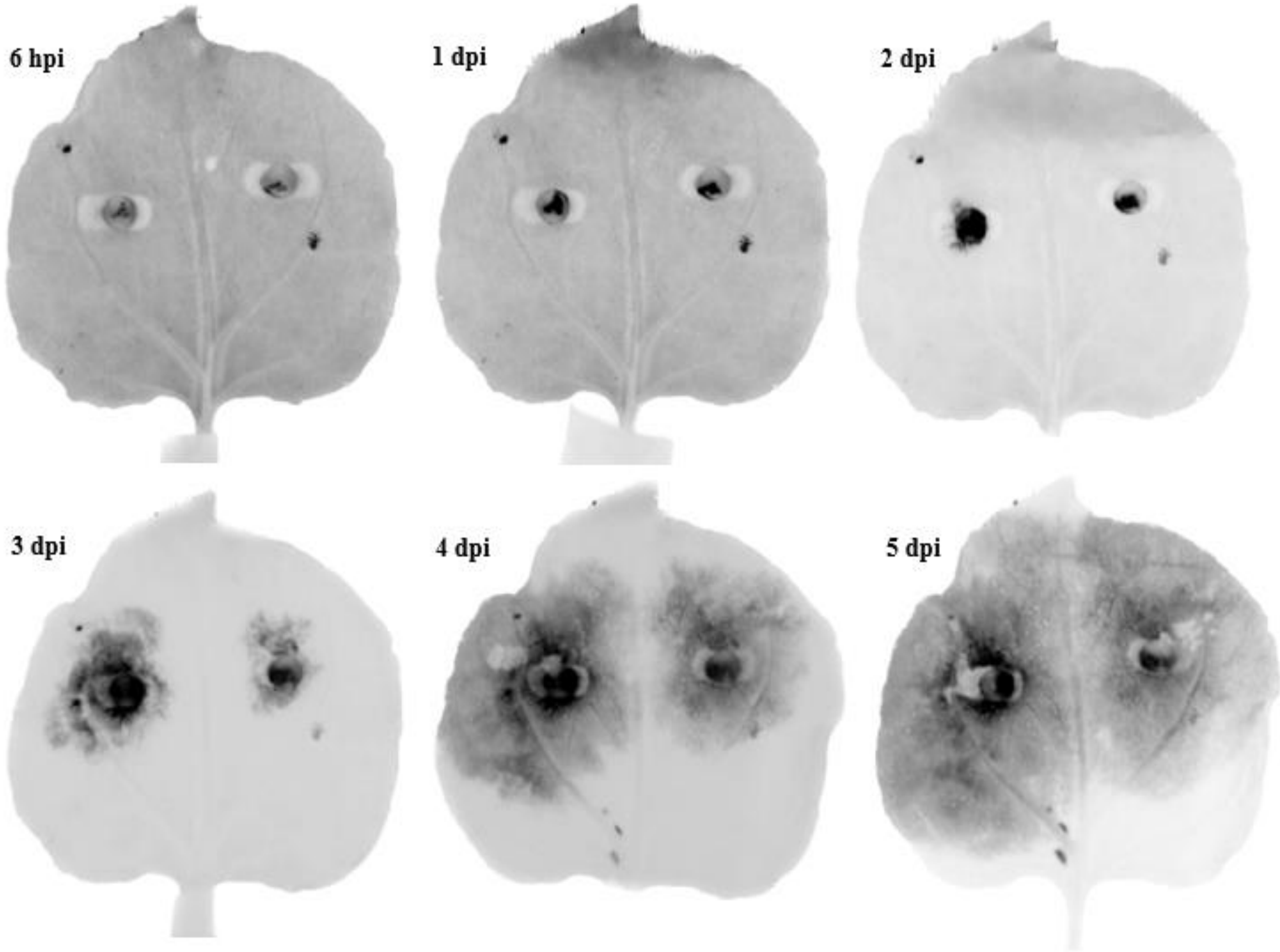

***Figure 3. 25. Phytophthora agathidicida* infection assay time course on detached leaves of wildtype *Nicotiana benthamiana* plants.** Leaves were inoculated with a five mm agar plug of mycelium extracted from the leading edge of a growing colony on clarified V8 agar. Detached leaves were photographed with infrared light every day post-inoculation (dpi), inclusive of a 6-hour post-inoculation (hpi) image. Dark shading indicates infection lesion. Circular shadow represents the five mm agar plug.

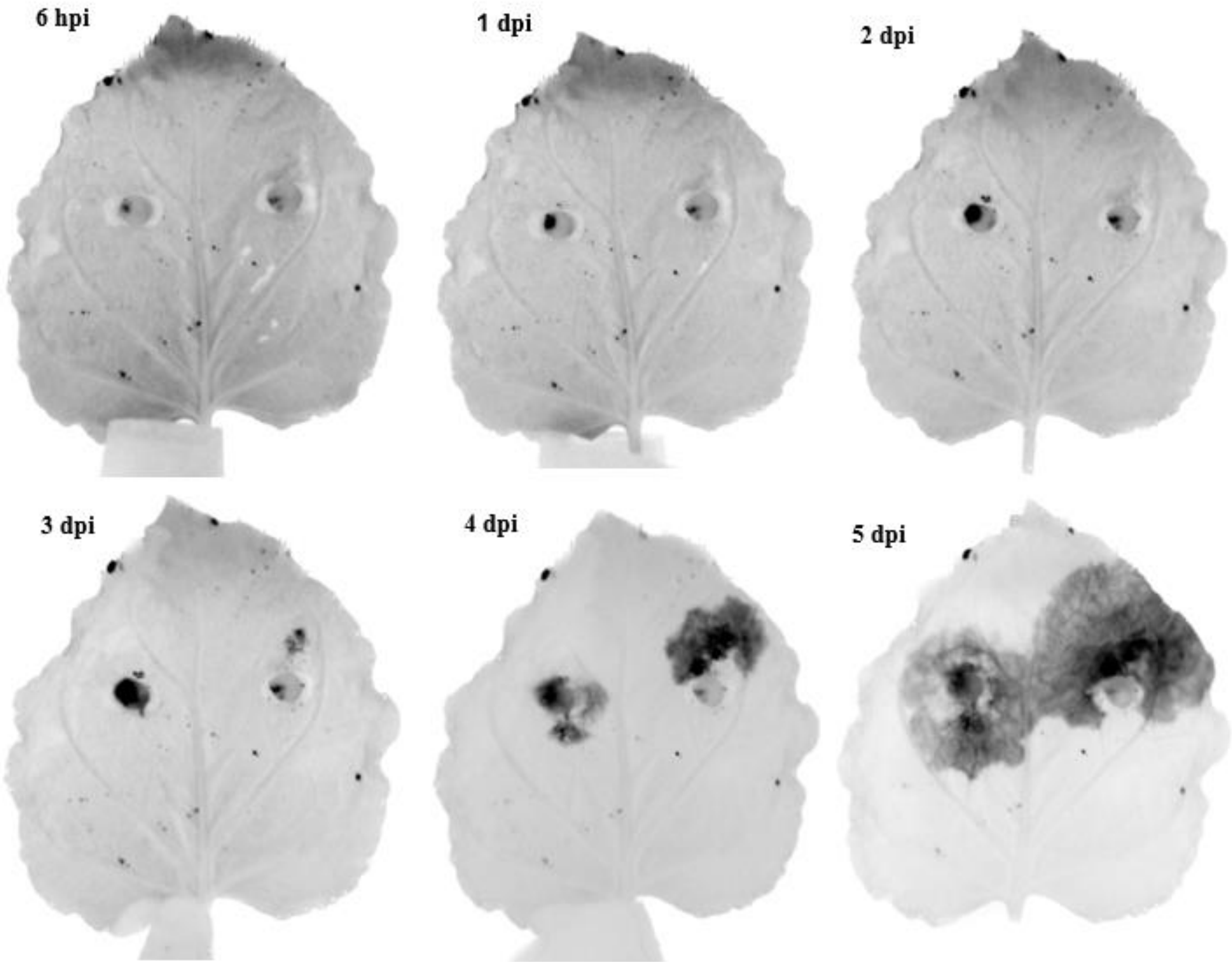

Figure 3. 26. Phytophthora cinnamomi **infection assay timeline in** ***Nicotiana benthamiana*** **wildtype detached leaves.** Leaves were inoculated with a five mm agar plug of mycelium extracted from the leading edge of a growing colony on clarified V8 agar. Detached leaves were photographed with Infrared light every day post-inoculation (dpi), inclusive of a 6-hour post-inoculation image. Dark shading indicates infection lesion. Circular shadow represents the five mm agar plug.

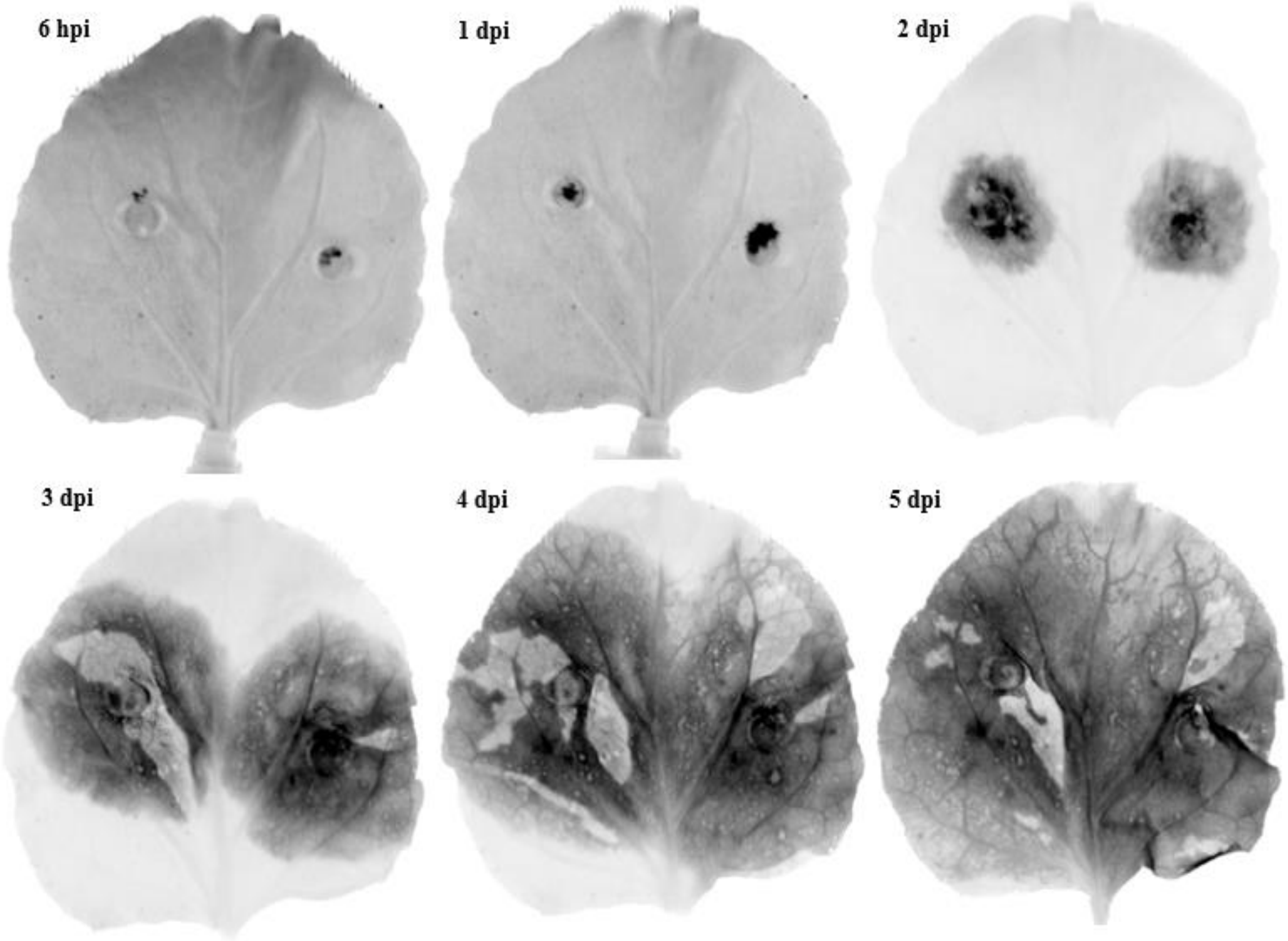

3 d

Figure 3. 27. Phytophthora multivora **infection assay timeline in *Nicotiana benthamiana* wildtype detached leaves.** Leaves were inoculated with a five mm agar plug of mycelium extracted from the leading edge of a growing colony on clarified V8 media. Detached leaves were photographed with Infrared light every day post-inoculation (dpi), inclusive of a 6-hour post-inoculation image. Dark shading indicates infection lesion. Circular shadow represents the five mm agar plug. Water present on leaves visible as light shading in lesion area.

Due to large differences in the infectivity of *N. benthamiana* by *P. agathidicida*, *P. cinnamomi* and *P. multivora*, it was suspected that extracellular plant immunity had a role to play in restricting lesion formation. To investigate this possibility, detached leaves of *N. benthamiana* with a knockout of the extracellular immunity-associated gene *SOBIR1* (Δ*sobir1*), as well as the equivalent isogenic wildtype sourced from the same laboratory that generated the mutant, were inoculated with each *Phytophthora* species and lesion formation monitored over four days. This experiment included four biological replicates of the Δ*sobir1* and corresponding isogenic wildtype plants, with each biological replicate from an independent plant. Similar to the original *in planta* experiment, *P. multivora* was readily and consistently able to infect both the isogenic wildtype and Δ*sobir1* leaves, with large lesions already visible at two dpi (Figure 3.28). However, for *P. agathidicida*, infection only rapidly and consistently progressed in the Δ*sobir1* leaves, with lesions also already visible at two dpi, and progressing in size at a similar rate to those of *P. multivora* (compare Figures 3.28 and 3.29). Indeed, on the isogenic wildtype leaves, lesions were not observed for *P. agathidicida* throughout the experiment (Figure 3.29). This is a stark contrast to the infection observed of wildtype *N. benthamiana* leaves in Figure 3.25. Interestingly, *P. cinnamomi* showed no differences in the ability to form lesions on the isogenic wildtype and Δ*sobir1* plants, as lesions were not formed on either (Figure 3.30). Again, this is a stark contrast to the infection observed of wildtype *N. benthamiana* leaves in Figure 3.26.

Quantification of lesion size (area) was undertaken manually using ImageJ at two and three dpi for *P. agathidicida* and *P. multivora* wildtype and Δ*sobir1* leaves. After three dpi, the lesions had reached the edge of the leaf and thus full lesion sizes could not be quantified. *P. cinnamomi* was excluded as there were no visible lesions. The area of each lesion was averaged across the four biological replicates (Figure 3.31A and Figure 3.31B). A T-test showed that *P. agathidicida* lesions on Δ*sobir1* leaves were significantly larger than those on the corresponding wildtype leaves at both two dpi ($p=0.0238$) and three dpi ($p = 0.0009$) (Figure 3.31), as a P value less than 0.05 is considered statically significant. Similarly, *P. multivora* showed a significant increase in lesion size on the Δ*sobir1* knockout compared to the wildtype at three dpi ($p = 0.0061$) (Figure 3.31B).

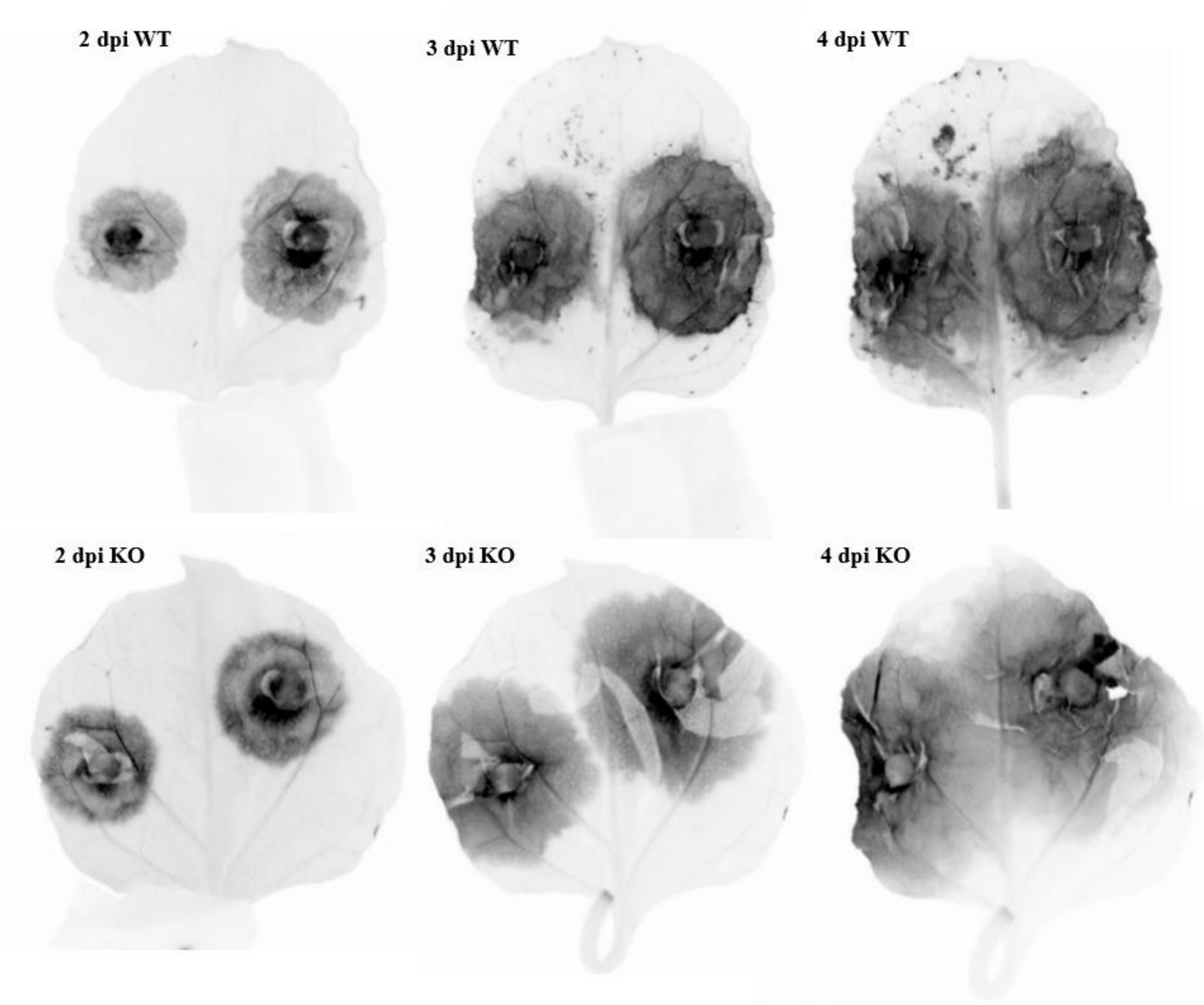

Figure 3. 28. Phytophthora multivora **infection assay timeline on *Nicotiana benthamiana* detached leaves with isogenic wildtype and *Δsobir1* background.** Leaves were inoculated with a five mm agar plug of mycelium extracted from the leading edge of a growing colony on clarified V8 agar. Detached leaves were photographed with Infrared light every day post-inoculation (dpi), inclusive of a 6-hour post-inoculation image. Top row = wildtype (WT), Bottom row = Δ*sobir1* (KO). Dark shading indicates infection lesion. Circular shadow represents the five mm agar plug.

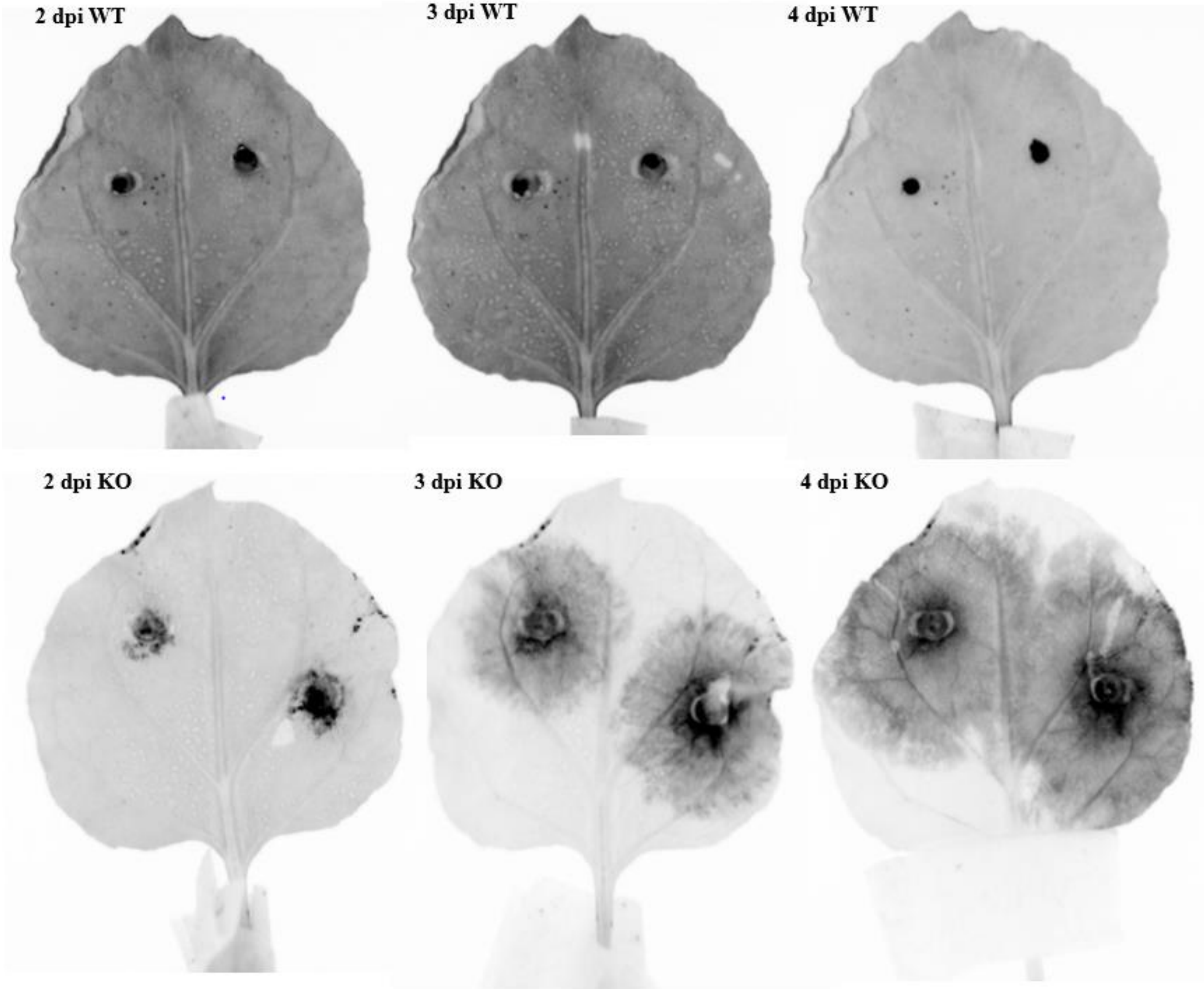

Figure 3. 29. Phytophthora agathidicida **infection assay timeline on *Nicotiana benthamiana* detached leaves with isogenic wildtype and *Δsobir1* background.** Leaves were inoculated with a five mm agar plug of mycelium extracted from the leading edge of a growing colony on clarified V8 agar. Detached leaves were photographed with Infrared light every day post-inoculation (dpi), inclusive of a 6-hour post-inoculation image. Top row = wildtype (WT), Bottom row = Δ*sobir1* (KO). Dark shading indicates infection lesion. Circular shadow represents the five mm agar plug.

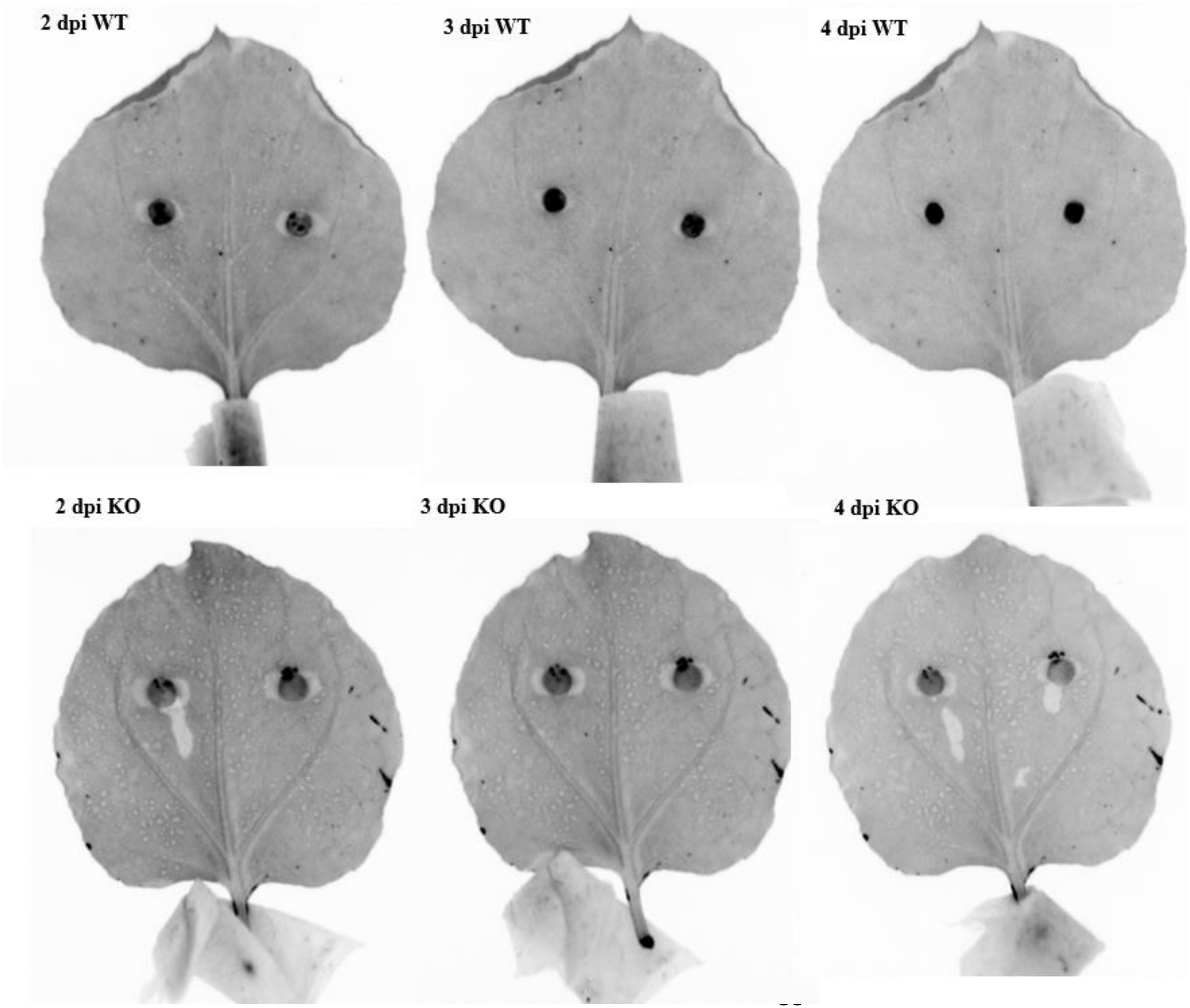

***Figure 3. 30. Phytophthora cinnamomi* infection assay timeline on *Nicotiana benthamiana* detached leaves with isogenic wildtype and *Δsobir1* background.** Leaves were inoculated with a five mm agar plug of mycelium extracted from the leading edge of a growing colony on clarified V8 agar. Detached leaves were photographed with Infrared light every day post-inoculation (dpi), inclusive of a 6-hour post-inoculation image. Top row = WT, Bottom row = Δ*sobir1* (KO). Dark shading indicates infection lesion. Circular shadow represents the five mm agar plug.

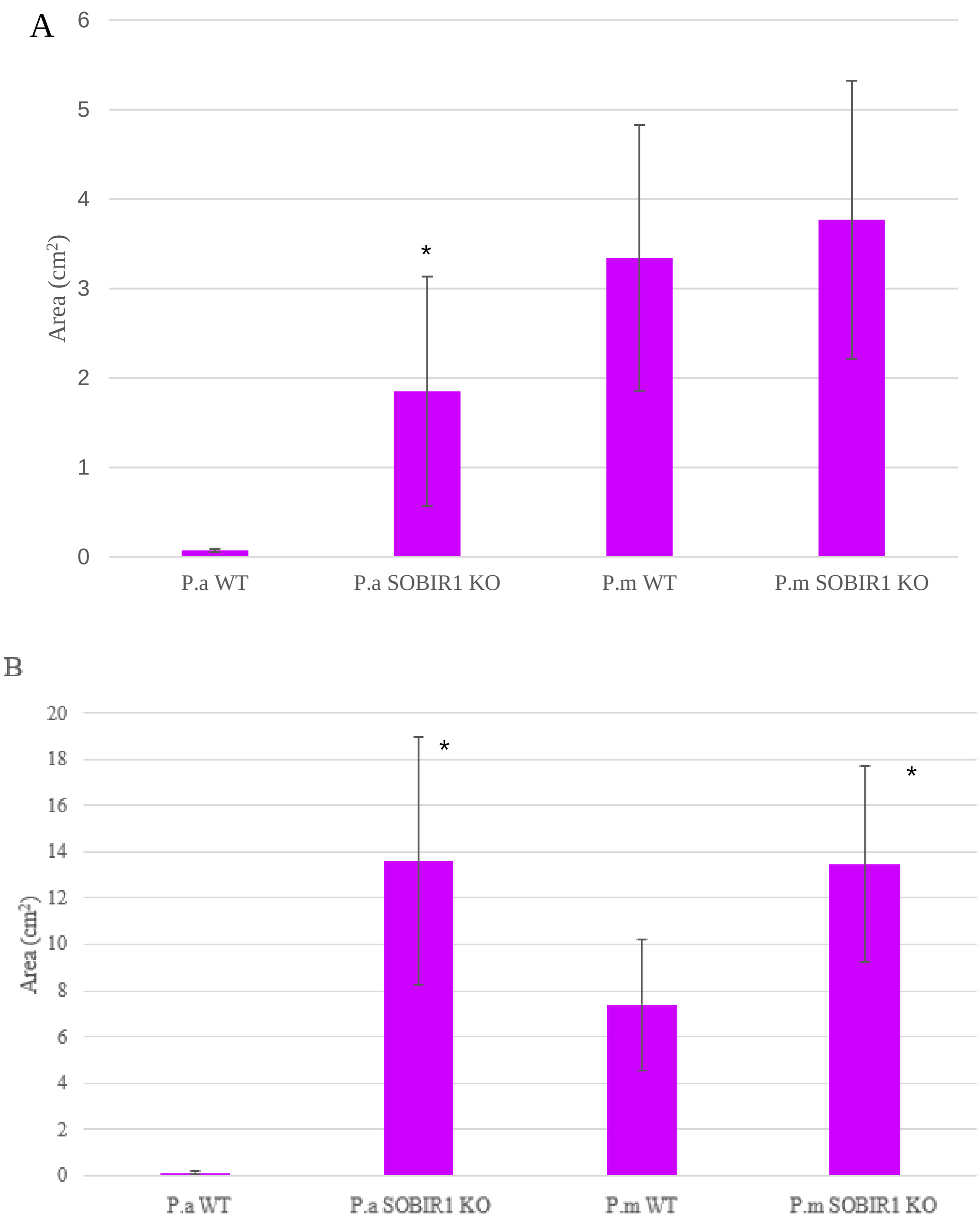

***Figure 3. 31.* Bar graph showing average lesion size (area) of *Phytophthora agathidicida* and *Phytophthora multivora* on detached leaves of *Nicotiana benthamiana* with isogenic wildtype and *Δsobir1* backgrounds.** Lesion area calculations were completed on ImageJ using Infrared photos at two and three days post inoculation (dpi). A = lesion calculations at two dpi. B = lesion calculations at three dpi. Error bars represent the standard deviation across the four biological replicates. P.a = *P. agathidicida*; P.m = *P. multivora*; WT = wildtype; KO = Δ*sobir1* knockout, * = statistically significant increase in lesion size on Δ*sobir1* background leaves.

Chapter Four: Discussion

Kauri dieback, caused by the soil-borne oomycete *Phytophthora agathidicida*, is a disease that threatens the long-term survival of *Agathis australis* (kauri), one of Aotearoa New Zealand's largest, longest living, and most culturally significant tree species (Bradshaw et al., 2020). Alongside *P. agathidicida*, two other *Phytophthora* species, *Phytophthora cinnamomi* and *Phytophthora multivora*, which are pathogenic on a wide range of host plant species (Hardham & Blackman, 2018; Tsykun et al., 2022), had previously been found to co-occur in the soils surrounding affected kauri trees, with glasshouse trials showing that they are capable of causing disease lesions on kauri seedling leaves (Horner & Hough, 2014). Whether *P. agathidicida*, *P. cinnamomi* and *P. multivora* cooperate to cause kauri dieback disease or, alternatively, are antagonistic towards each other in the soil environment or during kauri colonization, currently remains unknown. Such knowledge is vital because it could mean that kauri dieback disease control strategies need to target all three *Phytophthora* species to be effective.

In an attempt to start filling this knowledge gap, the current study had three objectives. These were to: determine whether colonies of *P. agathidicida*, *P. cinnamomi* and *P. multivora* interact with or repel each other during growth on solid growth media (Objective 1), determine whether the secreted protein profiles of *P. agathidicida*, *P. cinnamomi* and *P. multivora* change upon co-culturing with another *Phytophthora* species, relative to growth alone, in liquid growth media (Objective 2), and investigate whether the angiosperm plant *Nicotiana benthamiana* can be used as a model host for studying antagonistic or disease-promoting interactions between *P. agathidicida*, *P. cinnamomi* and *P. multivora* (Objective 3).

4.1: Macroscopic *Phytophthora* interaction assays on solid growth media (Objective 1)

For Objective 1, to determine whether colonies of *P. agathidicida*, *P. cinnamomi* and *P. multivora* interact with or repel each other at the macroscopic level in culture, both intraspecies and interspecies colony interaction assays were carried out on nutrient-rich (clarified V8 and carrot) and nutrient-poor (plich and cornmeal) agar media types. Colony interaction assays were chosen for use in this study, as they are routinely used in the field of microbiology to show different types of interaction between microorganism colonies, whether antagonistic or otherwise (Royse & Ries, 1978; Skidmore & Dickinson, 1976). For instance, based on observations obtained from colony interaction assays by Porter (1924) and Dickinson and Boardman (1970), Skidmore and Dickinson (1976) described four different types of interaction commonly observed between fungal colonies. These four interaction types were described as: Mutual intermingling, where colonies grow into each other and in some cases growth is halted after initial contact. Intermingling, where one colony grows over another, irrespective of whether this is detrimental to the other colony. Slight inhibition, where colony growth is halted within close proximity to the other colony. Lastly, inhibition at a distance, where growth is halted at a distance greater than two mm. These descriptions are useful as they can be applied to all other filamentous microorganisms, such as *Phytophthora* species which look and behave like fungi but do not belong to the fungal kingdom.

In the current study involving *P. agathidicida*, *P. cinnamomi* and *P. multivora*, all intraspecies and interspecies interaction assays resulted in a zone of growth inhibition between the three colonies tested, regardless of the media type used. These results align with the descriptions described above for slight inhibition and inhibition at a distance. A subsequent study by Esser and Meinhardt (1984), described another class of mutual intermingling, where growth is halted after initial contact, which notably has been termed a barrage zone. In these zones, cytoplasmic contact between hyphae is made, but no nuclear transfer occurs and a distinct line of often dead hyphal material is formed; no growth is observed past this point (Esser & Meinhardt, 1984). In the current study it was observed that there were distinct colonies present, but it was not determined whether the hyphae of adjacent colonies were intermingling at the microscopic level. As a future experiment, microscopic visualisation of the zone of growth inhibition between the *Phytophthora* colonies should be carried out to determine whether this zone is free from hyphae or whether there is interaction that cannot be observed macroscopically. Additionally, given that only one isolate of each *Phytophthora* species was tested in the current study, it would be interesting to test whether genetically distinct isolates of the same *Phytophthora* species result in the formation of the same types of inhibition zone or whether merging would occur.

There are multiple reasons why microbial colonies avoid each other. A commonly studied phenomenon in fungi and oomycetes is incompatibility. Hyphae are constantly surveying their surrounding environment, not only for competing species, space and nutrients, but also for compatible mating partners (Money, 2021; Turrà et al., 2016). In some cases, vegetative fusing of hyphae from colonies can occur (Leeder et al., 2011). Similarly, hyphae from colonies of species that are genetically distinct grow towards each other and fuse freely due to the possession of opposite mating-type genes, leading to compatibility (Leeder et al., 2011). However, in some instances upon contact, hyphal merging does not occur, resulting in programmed cell death (PCD) (Caten, 1972; Uwamori et al., 2015). This has been shown in species such as the chestnut blight fungus, *Cryphonectria parasitica* (Anagnostakis, 1987). In the case of *C. parasitica*, a distinct barrage zone that was visually darker than the active colony was formed between strains of incompatible mating types (Rigling & Prospero, 2018). In a study on *Phytophthora megasperma*, agar plugs carrying strains with different mating-type genes, *A1* and *A2*, were co-inoculated on agar media to see if compatibility was observed (Ho, 1978). In all crossings involving strains with opposite mating-types genes, inhibition at a distance was observed. Like in the current study, it was noted that separation between the colonies was widest in the centre of the agar plate. However, an interesting observation was made by Ho (1978) in that all colony interaction assays involving *P. megasperma* strains of the same mating type resulted in merging. Although the observations made by Ho (1978) for strains of opposite mating types align with what was shown in the current study in terms of inhibition, the possibility of incompatibility for zones of inhibition is unlikely for *P. agathidicida* and *P. multivora*, as these species are homothallic and therefore are capable of producing sexual spores without the need for the union between opposite mating-type strains (Bellgard & Probst, 2018). An explanation as to why colonies of the same species did not fuse despite being homothallic remains unclear however, has been noted by Lucas et al. (1990) that hyphae fusion in *Phytophthora* species is relatively rare.

An alternative explanation for the zone of growth inhibition observed in the current study is that the colonies have produced antagonistic or inhibitory molecules. Inhibition as described by Esser and Meinhardt (1984) states that the excretion of inhibitory substances can lead to the formation of a zone free of hyphae between the approaching colonies on agar, which may be one-sided or mutual. This is commonly shown in fungi as they produce bioactive molecules known as secondary metabolites which play a critical role in shaping the surrounding microbial environment as well as during fungal development (Keller, 2019). For example, approximately 750 compounds with anti-fungal, -microbial or -tumour activity were isolated from fungi within a nine year time period from 1993 to 2001 (Pela, 2004). These types of metabolites have been a focus for biocontrol of detrimental pathogens as some have shown an ability to inhibit and prevent infection (Vey et al., 2001). An example is provided by *Trichoderma* species, which can cause narrow lines of growth inhibition between themselves and the fungus *Erratomyces patelii*, which causes leaf smut of cowpea (Adejumo et al., 1999). In all plate confrontation assays with *Trichoderma* fungi, radial growth of *E. patelii* was restricted. This was not due to hyphal distortion or coiling away from the approaching colonies but, rather, it was suspected to be due to secreted metabolites.

Since oomycetes do not have a large capacity to produce secondary metabolites (Soanes et al., 2007), it is predicted that antagonistic interactions with other microbes may be due to the secretion of proteinaceous molecules termed effectors. While most microbial effectors characterized to date have been shown to promote host colonization through modulation of the plant immune system, it has recently been determined that a subset have anti-microbial activity (Gómez-Pérez et al., 2023). For example, as mentioned in the introduction, a study has recently shown the inhibitory effects of effector proteins in oomycete–bacteria interactions involving *Albugo canidida* (the oomycete) and phyllosphere bacteria. In this example, *Albugo* was found to produce antimicrobial effector proteins in the leaf apoplast that decreased microbial diversity of bacteria typically found in the phyllosphere *in vitro* (Gómez-Pérez et al., 2023).

4.2: Proteomic analysis of secreted proteins produced in single-species and multi-species *Phytophthora* liquid cultures (Objective 2)

Given that in the current study there was an apparent lack of physical interaction between colonies of *Phytophthora*, irrespective of whether they were from the same or a different species, no species-specific conclusions about these interactions could be drawn. It remained possible, however, that species-specific interactions were occurring at the molecular level. To determine whether *P. agathidicida*, *P. cinnamomi* and *P. multivora* interact at the molecular level, a proteomic analysis of culture filtrate following growth in clarified V8 liquid broth at seven days post-inoculation (dpi) was carried out using liquid chromatography–mass spectrometry (LC–MS). Co-culturing was a logical choice for dissecting such interactions, as previous studies had shown that such experiments can lead to the identification of proteins that are produced only when in co-culture or show a significant increase in expression when grown in the presence of another species (Zhong et al., 2018). A study by Zhong et al. (2018), for example, found that when three different fungal species of the division Basidiomycota, each capable of causing white rot (*Trametes versicolor*, *Pleurotus ostreatus* and *Dichomitus squalens*), were co-cultured for nine days, an increase in abundance of proteins relating to stress and energy responses were observed. Additionally, it was found that *Trametes veriscolour* produced 381 unique proteins when grown in co-culture compared to that of growth in single cultures.

In the current study, both qualitative (presence/absence) and quantitative (abundance) differences in the secreted protein profiles of the three species when cultured in the presence of one or both of the other species, relative to when cultured alone, were investigated. In total, 154, 127 and 107 putatively secreted proteins were identified from *P. agathidicida*, *P. cinnamomi* and *P. multivora*, respectively. Notably, this was the first study of its kind to complete an interaction-based proteomic analysis of co-cultured *Phytophthora* species.

Other studies with a central focus or component of proteomics have, however, been carried out on individual *Phytophthora* species. The first published proteomics-based studies on *Phytophthora* species focussed on the discovery of proteins associated with specific life phases or processes. These included, for example, studies on *Phytopthora infestans* appressoria and cyst formation *in vitro* (Ebstrup et al., 2005) and appressoria formation and subsequent infection processes *in planta* (Grenville-Briggs et al., 2005). In the palm pathogen, *Phytopthora palmivora*, appressoria development was investigated (Shepherd et al., 2003). Recently, of more relevance to the current study, full proteomic profile experiments, including those on extracellular proteins or secretomes, have been carried out. *P. infestans* was the first *Phytophthora* species to have its full repertoire of secreted and extracellular proteins investigated during mycelial growth, with a proteomic analysis performed on culture filtrates involving undiluted and different dilutions of clarified V8, non-clarified V8, Henniger and plich broth media types, each at a ten dpi time point (Meijer et al., 2014). In this example, an *in silico*-predicted secretome was used as a database to identify peptides by LC–MS. In total, 283 secreted or extracellular proteins were found across almost 200 different protein groups, of which 227 were found to be classically secreted, which is consistent with the number of total proteins found in the current study in *P. agathidicida*.

In terms of the species included in the current study, a comprehensive proteomic analysis has already been completed on *P. cinnamomi*, albeit on a different strain (MU94-48), which was obtained from the centre of *Phytophthora* science and management (Murdoch University, Australia) (Andronis et al., 2022). In the study by Andronis et al. (2022), the mycelia, zoospore and extracellular (secretome) sub-proteomes were analysed following growth on V8 agar for five days before the mycelia was transferred to Ribeiros minimal media broth for a further three days, resulting in the identification of 4635 proteins in total with 340 predicted to have a signal peptide. It should be noted here that, in the current study, it was not determined to what extent these 340 proteins overlapped with the secretome of strain NZFS 3750, as this was outside of the scope of this project.

For *P. multivora*, to my knowledge, only one study with a proteomics component has been performed, which was recently published by Berka et al. (2020). Here the authors used strains 159/07, 242/08 and 355/09, from the Czech collection of phytopathogenic oomycetes. This study was undertaken to aid in the identification of different *Phytophthora* species from closely related clades using the proteins identified from the extracts of crushed mycelia grown on malt extract agar for between seven to 14 days. A small proportion of the total proteins found were characterised, however those that mapped back to the reference proteome of *P. multivora* available on the UniProt database specifically corresponded to unknown/hypothetical proteins or proteins that formed part of major biochemical pathways, including enzymes involved in ATP synthesis or part of ribosomal subunits. In any case, secreted proteins did not form a focus of their study.

As for *P. agathidicida*, a proteomics analysis of the same strain used in the current study, strain NZFS 3770, was recently completed by Bradley (2022). In this study, the full secretome of *P. agathidicida* was analysed from culture filtrates of the microorganism grown in kauri apoplastic wash fluid, or one of clarified and non-clarified V8, henniger, plich or potato dextrose liquid media, for ten days. This analysis identified 986 proteins across all media types, of which 355 were predicted to be secreted.

Notably, in the current study, a total of 20 proteins were identified as candidate effectors for the modulation of interactions between different *Phytophthora* species. Of these, ten were present in all species combinations tested that involved a specific species, but not when this species was cultured alone (i.e. as part of the qualitative analysis). A further ten demonstrated a significant increase in abundance in all species combinations tested that involved a specific species, relative to this species was cultured alone (i.e. as part of the quantitative analysis). Curiously, none of the 20 candidate proteins were from *P. cinnamomi,* while only one of the qualitative proteins was from *P. multivora*.

Upon classification of the 20 proteins with bioinformatic tools, whether based on primary amino acid sequence or predicted tertiary structure, several major groupings could be made based on predicted function. The first grouping was those that belong to the Auxiliary activity (AA) family. Auxiliary activity (AA) family members are catalytic proteins which include lytic polysaccharide monooxygenases (LPMOs) and redox enzymes that have a role in degrading the plant cell wall (Levasseur et al., 2013). This group of carbohydrate-active enzymes (CAZymes) was created when glycoside hydrolase family 61 (GH61) and non-catalytic carbohydrate-binding module family 33 (CBM) were reclassified as LPMOs. Currently, 17 families of AA proteins have been identified through structural and sequence similarity. In the current study, five AA proteins were identified in the set of 20 candidate effector proteins, of which all belonged to either AA family 1 (KNV87_013190-T1, KNV87_013191-T1), 7 (KNV87_001091-T1) or 17 (KNV87_,004047-T1, Pmult_s012298g00001.1). The two *P. agathidicida* proteins identified as AA1 (KNV87_013190-T1, KNV87_013191-T1) were found to be encoded by genes that are highly expressed during infection of kauri leaves and in the quantitative study were found to have a found $\log_2$ fold change of 8.6.

AA Family 1 (AA1) proteins are multi-copper oxidases that can be categorized into three subfamilies; laccases, ferroxidases and laccase-like multicopper oxidases (CAZy database). AA1 proteins are commonly associated with fungal and bacterial interactions and their activity can be involved in self-protection and/or antagonism. It has been discovered that a fungus, specifically *Pyconoporus cinnabarinus*, is capable of using a laccase to metabolise 3-hydroxyanthranilic acid into other products such as cinnabarinic acid or to catalyse the iodination of phenolic compounds which in turn creates anti-microbial products (Eggert et al., 1998; Ihssen et al., 2014). These compounds can inhibit bacteria such as *Streptococcus* and *Klebsiella*, as well as various wood-decaying fungi. Furthermore, in pathogenic fungi, laccase activity has been associated with melanin synthesis, which can aid in virulence, and it has been discovered that melanin is capable of binding and inhibiting antimicrobial compounds secreted by surrounding microbes (Kaliszan et al., 1993; Kaur et al., 2019). Antagonism has also been observed on solid media between fungal species *Trichoderma longibrachiatum* and *Pleurotus ostreatus*, where it was found that *P. ostreatus* inhibits the growth of *T. longibrachiatum* to form a barrage zone that has visual discolouration of the surrounding mycelia, likely from the production of pigment which could be linked to laccase-mediated oxidation of various aromatic compounds (Velázquez-Cedeño et al., 2007). An expression analysis showed that transcription of laccase-encoding genes was greatly upregulated in culture when *T. longibrachiatum* was co-cultured with *P. ostreatus* compared to when *P. ostreatus* was grown alone (Velázquez-Cedeño et al., 2007).

AA Family 7 (AA7) proteins are gluco-oligosaccharide oxidases that, like AA1 proteins, can be characterized into subfamilies (Haddad Momeni et al., 2021). These subfamilies have been termed clades, with each clade generally referring to AA7 proteins from a different kingdom of life. Those from oomycetes tend to cluster into clade 2b. In a study by Bashyal et al. (2017), the genome of *Fusarium fujikuroi* isolate F250 was sequenced and annotated, with 16% of all predicted secretory proteins found to be AA proteins, of which most were AA7. AA7 proteins have been predicted to trigger the action of LPMOs (Haddad Momeni et al., 2021). The AA7 proteins found by Haddad Momeni et al. (2021) were determined as having a crucial role in pathogenesis as they can produce hydrogen peroxide which is an important product required for lignin-degrading enzymes such as laccases (AA1) (Nekiunaite et al., 2016). Hydrogen peroxide is required to depolymerise lignin as the first step of degradation. However, like in Nekiunaite et al. (2016), no lignin was present in the co-cultures of the *Phytophthora* species and, as such, they may therefore have another function that has yet to be characterised.

Taken together, this suggests that AA1 and AA7 may not only be important for pathogenesis *in planta*, but also have roles in antagonism if oomycetes are capable of performing the roles described for AA1 in fungi and bacteria.

AA Family 17 (AA17) is relatively new, having been created in 2021 after the identification of enzymes in *P. infestans* that had sequence homology to other AA proteins but no known functional domains (Sabbadin et al., 2021). This homology included two conserved histidine residues that form a "histidine brace" associated with LPMOs (Quinlan et al., 2011; Sabbadin et al., 2021). The AA17 family has only been found in oomycetes, including 46 different species of the *Phytophthora* genus. This includes *P. infestans*, which has 31 AA17 protein-encoding genes. During *in planta* experiments, it was determined through dsRNA-mediated transient gene silencing that an AA17 protein, PiAA17C, is essential for successful infection by *P. infestans* in tomato leaves, with silenced transformants producing smaller lesions compared to the controls (Sabbadin et al., 2021).

Another group of proteins that predominated in the list of 20 candidate effectors of the current study were the glycoside hydrolase (GH) family, which constitute the largest group of CAZymes (Zhao et al., 2013). To date, there are currently 183 families of GH proteins, which are organised by functional and sequence similarity (CAZy database). Of the 183 families, four had representatives in the list of 20 candidate effectors; families 3 (KNV87_017260-T1), 12 (KNV87_006685-T1), 43 (KNV87_011472-T1) and 131 (KNV87_004012-T1). The GH3 protein was found to be the protein with the most significant increase in abundance across every sample type as each sample had a $\log_{10}$ value greater than 3.

GH family 3 (GH3) proteins have been found to have β-glucosidase activity and have since been characterised in a number of bacteria and eukaryotes (CAZy database). A GH3 example from the fungus *Septoria lycopersici*, a pathogen that causes leaf spot of tomato, encodes a tomatinase enzyme capable of degrading α-tomatine (Sandrock et al., 1995). A-tomatine is a saponin compound in tomato that, upon binding to 3β-hydroxy sterols, can promote anti-fungal effects due to its effects on membrane permeability. The GH3 enzyme produced by *S. lycopersisi* can convert the saponin to a less toxic form, therefore promoting fungal pathogenicity. While no GH3 proteins have been functionally characterised in oomycetes to date, genes that encodes GH3 proteins have been found in a wide number of oomycetes (Cantarel et al., 2008). This suggests that oomycete GH3 proteins may have a similar role in promoting the detoxification of toxic plant- (or even microbe-derived) secondary metabolites and that this activity may aid in achieving efficient infection.

GH family 12 (GH12) proteins are xyloglucanases which play a role in breaking down the plant cell wall. In the abovementioned study by Bradley (2022), six GH12 proteins with proteomic support were identified from *P. agathidicida* culture filtrate samples and found to induce rapid cell death when heterologously expressed in the model host plant *Nicotiana benthamiana*. This cell death is anticipated to be the result of plant immune system activation following their recognition by the RXEG1 immune receptor in this plant (Wang et al., 2018). In the current study, the identified GH12 (KNV87_006685-T1) is the same as one of the six cell death-eliciting GH12 proteins (Pag009588) identified by Bradley (2022), however the protein ID differs due to the secretome of strain NZFS 3770 being updated since the study by Bradley (2022) was completed. This protein was shown to have xyloglucanase activity using an *in vitro* xyloglucanase enzymatic activity assay (Bradley, 2022). It is possible that the identified GH12 protein, as a function of its xyloglucanase activity, plays a role in nutrient acquisition *in planta* but is recognized as a microbe-associated molecular pattern (MAMP) by XEG1 in *N. benthamiana* (Bradley, 2022; Ma et al., 2015). What role the protein plays in culture in the presence of other *Phytophthora* species remains to be determined.

GH family 43 (GH43) enzymes, like the various AA proteins discussed above, have been grouped into subfamilies (Mewis et al., 2016). More specifically, there are four major enzymes amongst 37 subfamilies (α-L-arabinofuranosidases, β-D-xylosidases, α-L-arabinanases, and β-D-galactosidases), which act to break down hemicellulose and pectin in the plant cell wall. GH family 131 (GH131) enzymes function in a similar way in that they degrade the plant cell wall, specifically cellulose, in this case with β-glucosidase activity (Anasontzis et al., 2019). These enzymes are highly abundant across oomycetes and are extremely important in the early stages of infection as they aid in getting through the initial physical defences of the plant (Anasontzis et al., 2019).

Aside from the CAZymes mentioned above, of the list of 20 proteins, most others had a predicted enzymatic function. These included a dehalogenase hydrolase, lactonase, a calcineurin-like phosphatase, isomerase, carboxyesterase and a ceramidase. Of these enzymes, many had previously described roles in anything from pathogenicity, including adhesion, host immune system modulation (Zhang et al., 2020) and plant cell wall penetration (Zhi & Wang, 2022), to physiological processes (Judelson, 2017) involving metabolism. All of the enzymes mentioned above were encoded by genes that were expressed during *in planta* infection, however these were to a relatively low level except for the gene that encodes the lactonase which showed good expression in kauri leaves (KNV87_001706). In the quantitative analysis, the ceramidase protein (KNV87_009659-T1) was one of the proteins with the greatest increases in abundance, specifically when co-cultured with *P. multivora*. While it is possible that these roles may also hold true for the corresponding enzymes identified from *P. agathidicida*, specific roles during co-culture with other *Phytophthora* species are not as obvious.

Of particular note, KNV87_008864-T1, which was described as a lipoxygenase, was the only protein out of the 20 candidate effectors identified in the current study that was not also identified by Bradley (2022) when *P. agathidicida* was cultured alone at ten dpi in various media types. Lipoxygenases have been described in *Trichoderma atroviride*, a fungus that produces an antifungal secondary metabolite, 6-pentyl-α-pyrone. Interestingly, lipoxygenase activity was shown to be required for the formation of this secondary metabolite (Speckbacher et al., 2020). In another study involving the fungus *Podospora anserina*, a knockout of the *cox* and *lox* genes, that encode a lipoxygenase and cyclooxygenase enzyme respectively, resulted in the inhibition of volatile organic compound (VOC) production, which reduced antagonism with the nematode *Caenorhabditis elegans* (Ferrari et al., 2018). Another study also found that lipoxygenases aid in the formation of oxylipins which have signalling properties that have shown to be involved in cross kingdom signalling by pathogenic fungi to modify plant immune responses (Bärenstrauch et al., 2020). Not only that, but the genes that encode lipoxygenases are upregulated in co-culture. This suggests that lipoxygenases may not only be important for signalling but may also have a role in producing toxic compounds towards other species present in the co-culture as it suggests these genes may be upregulated to aid in self-protection.

Not all proteins identified in the list of 20 candidate effectors had a predicted functional domain or sequence similarity to proteins of characterized function. In these cases, their tertiary structures were predicted using AlphaFold2 and then screened against a database of characterized and predicted protein tertiary structures to gain insights into possible function. While for one of the hypothetical proteins, no further insights into function were provided, for another (KNV87_007317-T1), structural similarity to the toxin subunit of the MbcT-MbcA toxin-antitoxin complex produced by the bacterium *Mycobacterium tuberculosis* was observed (Freire et al., 2019). The MbcT component of the complex produces a bactericidal toxin in the bacterium through degradation of NAD+, however under favourable conditions such as high nutrients or limited competition, the MbcA antitoxin is produced which inhibits the function of the toxin. When the environment becomes stressful, for example due to the presence of antibiotics, the antitoxin is degraded and the toxin targets important activities (e.g. DNA replication) to reduce the growth of the bacteria and in some cases can aid in persistence (Page & Peti, 2016). Toxin-antitoxin complexes are abundant in prokaryotes, however they have only been predicted in some unicellular fungi through BLAST searches and genome sequences. These searches revealed a potential homolog of the *Escherichia coli* Doc toxin in some unicellular fungi (Yamaguchi et al., 2011). Toxin-antitoxin complexes have yet to be described in oomycetes, however if the predicted structural similarity is any indication of function, then KNV87_007317-T1 may form part of a toxin-antitoxin complex in *P. agathidicida* or, potentially, function as a distinct effector protein in antagonism against other *Phytophthora* (or other microorganism) species. It would be interesting to see if any of the other putatively secreted proteins from the current study have predicted structural similarity to the antitoxin subunit mentioned above or whether a similar functioning protein is produced at an earlier time point when environmental conditions were favourable.

Overall, the candidate effectors mentioned above appear to be important in not only the initial host infection stages and general metabolism functions, but some may also be beneficial in promoting antagonistic relationships in stressful situations. These types of effectors being produced in co-culture provide insights as to why they were identified as part of both the qualitative and quantitative analysis. It would be interesting to test whether competing microbes is the cause for these candidate effectors to be produced by *P. agathidicida* by testing whether they are present at three dpi or earlier when nutrients are less depleted. If *Phytophthora* species are capable of these antagonistic mechanisms such as toxin production that does not inhibit self, it could provide a reason as to how they co-exist in solid or liquid media.

As mentioned above, in the previous proteomic study carried out on *P. agathidicida* in liquid culture by Bradley (2022), 18 out of the 19 candidate effectors of interest were identified when the oomycete was grown alone for ten days in various liquid media. This may suggest that these proteins are not involved specifically in promoting antagonistic or beneficial interactions between *P. agathidicida* and both *P. cinnamomi* and *P. multivora*. However, this conclusion cannot be drawn, as the media type used and/or the time point sampled was different in the study by Bradley (2022). Indeed, in Bradley (2022), a later time-point was sampled (ten dpi vs. seven dpi). It could therefore be that many of the candidate effectors identified in the current study are secreted more generally under stressful conditions, as a form of stress management, such as during the presence of another microbial species, during nutrient exhaustion (e.g. at later time points like ten dpi), or during media acidification. This is expected to occur as oomycetes and fungi share similar feeding strategies and fungi readily produce hydrogen ions as a result of ATP synthesis (Latijnhouwers et al., 2003; Nelson, 1994). In this way, there could be many overlapping cues associated with stress for the production of these proteins, with nutrient exhaustion and acidification of media potentially enhanced in the presence of a competing microorganism to help secure the nutrients still available or reduce the competition.

It should also be pointed out that proteins can have more than one function, and thus some proteins with a role in modulating microbe–microbe interactions could have an additional related or unrelated function with additional cues for their production. One such example is the Zt6 effector protein from the fungal pathogen of wheat, *Zymoseptoria tritici*, which is a secreted ribonuclease that has both potent phytotoxic and antimicrobial activities (Kettles et al., 2018). Concomitant with its expression profile, it is thought that Zt6 first clears the zone surrounding germinating *Z. tritici* spores of competing microorganisms, but then later in infection may contribute to the fungus' necrotrophic lifestyle by simultaneously killing host tissue and preventing the colonization of this nutrient-rich necrotic tissue by opportunistic saprophytic microorganisms (Kettles et al., 2018) (Kettles et al., 2016). With this in mind, it could be possible that some of the candidate effectors identified in the current study could have other roles related or unrelated to modulating *Phytophthora–Phytophthora* interactions.

The *P. agathidicida* gene expression data analysed by Cox et al. (2022) highlighted that genes encoding some of the candidate effector proteins identified in the current study were not expressed highly during infection of kauri leaves or roots, or during growth *in vitro* in clarified V8 broth. It should be noted that the strain (NZFS 3813) used for the expression study in Cox et al. (2022) differed from that used in the present study (NZFS 3770), although they are fairly similar genetically (Cox et al., 2022). Of course, another explanation may be that these particular proteins play a role in modulating *Phytophthora–Phytophthora* interactions or that they are only produced when the pathogen is in a more stressful environment (e.g. when other *Phytophthora* species are present) and, as such, did not have the appropriate cues for their expression *in vitro* in the Cox et al. (2022) study. Along the same lines, the fact that some candidate effectors were not highly expressed *in planta* may reflect strain differences. A replicate *in planta* experiment to that carried out by Cox et al. (2022) would need to be carried out with strain NZFS 3770 to investigate this possibility further. Furthermore, the time point investigated by Cox et al. (2022) was earlier (five dpi) than that used in the current study (seven dpi). Together, the different strains and time points may help explain why some candidate effector genes were not expressed at all *in vitro* in the Cox et al. (2022) study, but the corresponding proteins were produced in the current study. It could also be that in the study by Cox et al. (2022), their expression peaks at a time point not investigated such as a later stage or before infection in the soil surrounding kauri roots. However, the expression of the genes that encode the candidate proteins could be investigated in the future using soil samples and qRT-PCR as described in Than et al. (2013).

While the current study has identified a set of interesting effector candidates for future investigation in roles associated with modulating interactions between *P. agathidicida* and other *Phytophthora* species, it remains possible that other effector candidates involved in these interactions have been missed. For example, the media composition used may have differentially selected for certain proteins to be produced. In Bradley (2022), each media type, whether nutrient-poor or nutrient-rich, produced putatively secreted proteins that were unique. Of note, culture filtrate from a replicate experiment, but using the nutrient-poor medium, plich, is currently stored at –20°C at Massey University for future analysis and could be investigated by proteomics to determine whether a similar repertoire of putatively secreted proteins and thus, candidate effectors, are produced. Indeed, it could be that the plich medium results in additional antagonistic effector candidates as the cultures will be under a greater level of nutrient stress than when grown in the nutrient-rich clarified V8 medium at the time point investigated. Furthermore, since this experiment investigated *in vitro* interactions in liquid media, it remains possible that proteins that are only expressed during *in planta* infection or in the soil surrounding kauri roots could have been missed as there was no *in planta* or in-soil cue for these proteins to be produced. Additionally, it is possible that certain interactions at the protein level between the different *Phytophthora* species could have occurred at an earlier time point in the experiment and, therefore, when the culture filtrates were harvested at seven dpi, were no longer present. Again, clarified V8 culture filtrate from an earlier time point is currently stored at –20°C at Massey University for future analysis and could be analysed by proteomics to investigate this possibility further.

The scope of the current project also meant that a strict set of criteria had to be applied to identify putatively secreted effector candidates for future testing. As such, a relaxation of the selection criteria (or a different set of criteria) may have resulted in different or additional candidate effectors being identified. For example, for the qualitative analysis, only those putatively secreted proteins that were present in all multi-species samples but not in the single-species samples were analysed. Similarly for the quantitative analysis, only those that were found in every sample with a significant increase in abundance found in the multi-species sample in comparison to the single-species sample were selected. These strict selection criteria therefore did not take into account those putatively secreted proteins that were only found in one or two of the multi-species sample types, but not the corresponding single-species samples.

Based on the literature, a sample type that could be beneficial for further analysis is the multi-species sample *P. agathidicida* + *P. multivora*. There are several reasons for this. Firstly, *P. multivora* has commonly been found at sites of kauri dieback disease (Waipara et al., 2013). Secondly, it was found that of the 34 kauri trees in the Waitakere Ranges sampling sites were undergoing rapid death with symptoms consistent with *Phytophthora* infection, of which *P. multivora* was isolated from 11 (Waipara et al., 2013). Thirdly, *P. multivora* has been hypothesized to exacerbate symptoms of dieback in another New Zealand native species, *kawakawa* (*Macropiper excelsum*) (Ho et al., 2010). Taken together, this information suggests that interactions between *P. multivora* and *P. agathidicida* are more common or biologically relevant than interactions between *P. agathidicida* and *P. cinnamomi*. Therefore, the strict criterion of a candidate effector protein from *P. agathidicida* needing to be in the *P. agathidicida* + *P. cinnamomi* sample type may not be warranted. Considering no candidate effector proteins of interest were identified from *P. cinnamomi* in the qualitative and quantitative analyses carried out in the current study, this suggests that *P. cinnamomi* may not interact with *P. agathidicida* to the same level as *P. multivora* does.

Another factor related to the strict set of criteria used in this study was the need to only retain those proteins with a signal peptide for secretion through the classical endoplasmic reticulum–Golgi secretory pathway. Ultimately, this meant that non-classically secreted proteins (i.e. proteins secreted by extracellular vesicles) were overlooked in this study (Nickel & Rabouille, 2009). The reason for this omission is that there is currently no accurate tool for their prediction and therefore they cannot be easily differentiated from proteins that result from cytoplasmic contamination – a feature of all large-scale proteomics-based studies to date (Gómez-Pérez et al., 2023). In the *P. cinnamomi* proteomics study (Andronis et al., 2022), it was found that 724 proteins that mapped back to the secretome database lacked a signal peptide, and therefore could potentially be proteins that are non-classically secreted. As such, proteins involved in modulating *Phytophthora–Phytophthora* interactions that are directed through the non-classical secretion pathway would have been missed. It should also be pointed out that the SignalP webserver is only a prediction tool for signal peptide identification, and it therefore cannot be guaranteed that every protein was correctly predicted to be secreted. A future non-biased approach could involve using RNA-seq to identify genes that are upregulated in certain sample types, irrespective of whether they encode a putatively secreted protein or not. For this purpose, the mycelia from each sample type investigated in the current study has been stored at –80°C at Massey University to enable further insight into the interactions occurring between the three *Phytophthora* species.

Lastly, a caveat to this study is that the qualitative and quantitative differences between co-cultures of the same species were not investigated. Although smaller satellite colonies formed off the main colony in many of the static cultures and likely mimicked the environment of multiple same-species colonies, they were treated as one sample and analysed as a whole. A replicate experiment involving discrete colonies of the same species in the same liquid culture could therefore also be investigated by proteomics in the future.

Future experiments are now needed to determine whether any of the 20 candidate effector proteins identified in the current study play a role in modulating interactions between the different *Phytophthora* species. A logical next step would be to test the 20 identified candidates for their ability to influence lesion development by either *P. agathidicida* (for the one candidate belonging to *P. multivora*) or *P. multivora* (for the 19 candidates belonging to *P. agathidicida*) on *N. benthamiana*. Here, each candidate effector could be heterologously expressed in *N. benthamiana* using an *Agrobacterium tumefaciens*-mediated transient transformation assay (ATTA), with an agar plug of either *P. agathidicida* or *P. multivora* placed on top to see if the effector candidate affects lesion area development relative to a no-protein (empty vector) control, as performed for GH12 proteins by Bradley (2022). Additionally, each candidate effector could be heterologously produced by the yeast *Pichia pastoris*, purified, and then tested to see whether it inhibits or enhances, for example, mycelial growth or zoospore germination of the three different species when added to pure cultures *in vitro*. The same candidate effectors could be infiltrated into kauri leaves, and a plug placed on top, as described above, to look for influences on lesion area development. It is possible that some candidate effectors may act to enhance the growth of other *Phytophthora* species. It has been shown in *Albugo laibachii* that it is able to antagonise some microbes while promoting the growth of others and this modulation is anticipated to be achieved through effector proteins (Agler et al., 2016).

4.3: *Nicotiana benthamiana* leaf infection assays

To determine whether the three *Phytophthora* species modulate the growth of each other *in planta*, infection assays based on lesion area were first carried out on detached leaves of wildtype *N. benthamiana*. In addition to determining whether the three species could infect the leaves of this plant, these assays were needed to determine whether any of these species are naturally more aggressive that the others in terms of lesion formation. If this is the case, a dominant species might colonise the entire leaf prior to lesions being formed by the other species, meaning that differences in lesion size could not be easily assessed upon co-inoculation. Unfortunately, due to cultural agreements not being in place at the time of these experiments, infection tests could not be performed on kauri tissue.

These initial assays revealed that the degree of lesion formation on *N. benthamiana* was highly variable between the three *Phytophthora* species. *P. multivora* could more rapidly infect the leaf than *P. agathidicida*, and *P. agathidicida* could more rapidly infect than *P. cinnamomi*. Furthermore, *P. multivora* could consistently produce lesions from each inoculation point (agar plug), whereas this was not always the case for *P. agathidicida* and even less so for *P. cinnamomi*. As the three species differed so greatly in their ability to infect as well as in the amount of leaf area they were able to colonize over a set time period, it was therefore unfortunately not possible to perform co-inoculation experiments on *N. benthamiana*. Ultimately, this may reflect that *N. benthamiana* is a better host for *P. multivora* than *P. agathidicida* and *P. cinnamomi*. Interestingly, a previous study showed that *P. cinnamomi* readily infects *N. benthamiana* (Belisle et al., 2019). However, in that study, different isolates, collected from a different host (avocado), were used rather than the isolate used in this current study. Furthermore, zoospore suspensions were used to initiate infection on *N. benthamiana* detached leaves rather than agar plugs containing actively growing mycelia, which may explain the variation seen between the infectivity of *P. cinnamomi* between these two studies. It would be beneficial to repeat this experiment using zoospores as it is more likely to represent the natural inoculum.

Due to large differences in the infectivity of *N. benthamiana* by *P. agathidicida*, *P. cinnamomi* and *P. multivora*, it was suspected that extracellular plant immunity in the form of pattern-triggered immunity (PTI) had a role to play in restricting lesion formation. To investigate this possibility, detached leaves of *N. benthamiana* with a knockout of the extracellular immunity-associated gene *SOBIR1* (Δ*sobir1*), as well as the equivalent isogenic wildtype, were inoculated with each *Phytophthora* species and lesion areas measured. In the Δ*sobir1* knockout, the gene that encodes the SOBIR1 co-receptor, which is required for receptor-like protein (RLP)-mediated immunity in plants (Liebrand et al., 2013), has been deleted. This co-receptor is of great importance to RLP-mediated immunity because, unlike RLPs, it possesses a kinase domain that, in conjunction with the kinase domain of another co-receptor, BAK1, transfers signals of most RLP-mediated invasion pattern recognition to defence (Liebrand et al., 2014). As such, in the absence of SOBIR1, RLP-mediated immunity is, for the most part, no longer active (Liebrand et al., 2013).

Intriguingly, *P. agathidicida* produced significantly larger lesions on leaves of the Δ*sobir1* plants by three dpi, with no lesions observed on leaves of the isogenic wildtype equivalent, indicating that RLP-mediated immunity does indeed play a significant role in slowing infection by *P. agathidicida*. This may mean that, on isogenic wildtype leaves, *N. benthamiana* is able to initiate an immune response faster than *P. agathidicida* is able to deploy effectors to suppress or prevent PTI, or that *P. agathidicida* does not have the appropriate repertoire of effectors to suppress or prevent RLP-mediated PTI in this plant. The finding that RLP-mediated immunity is important for protection of *N. benthamiana* against *P. agathidicida* is in line with previous research by Bradley (2022), who showed that extracellular candidate effector proteins of the GH12 family from *P. agathidicida* triggered immunity-related cell death responses in *N. benthamiana*, likely upon recognition by the endogenous RLP, RXEG1 (Wang et al., 2018). Interestingly, in *Phytophthora sojae*, it was found that a cytoplasmic RXLR effector was able to suppress cell death triggered by its own GH12 proteins, and therefore prevent the subsequent immune response initiated by RXEG1 (Ma et al., 2015). In line with that described above, *P. agathidicida* does not contain a homolog of this effector (Carl Mesarich, personal communication). It does, however, possess an intracellularly-targeted effector, RXLR40, which is able to suppresses cell death initiated by both intracellular and extracellular effectors (Guo et al., 2020), including one of the GH12 protein identified by Bradley (2022). This effector is upregulated during colonisation of *N. benthamiana*/kauri leaves and roots by

P. agathidicida (Jason Shiller, Unpublished results), but it remains unclear to what extent it can suppress other elicitors of RLP-mediated immunity.

P. multivora was also able to produce significantly larger lesions on leaves of the Δ*sobir1* knockout plants, relative to those on the wildtype equivalent after three dpi, although the difference in lesion size was not so pronounced as with *P. agathidicida*. This indicated that RLP-mediated immunity also plays a significant role in providing *N. benthamiana* with protection against *P. multivora*. *P. cinnamomi*, however, was not able to produce lesions on either the wildtype background or Δ*sobir1* knockout plants. This may indicate that this particular accession of *N. benthamiana* was not an effective host for *P. cinnamomi*. In any case, the fact that both *P. agathidicida* and *P. multivora* infect Δ*sobir1* plants well suggests that these plants could be used to assess whether the 20 candidate effectors mentioned above modulate the growth of *P. agathidicida* and *P. multivora* following ATTAs.

Curiously, differences in the ability of *P. agathidicida* and *P. cinnamomi* to infect wildtype *N. benthamiana* were observed between the two experiments discussed above, in which different wildtype accessions of *N. benthamiana* were used. It must be noted, however, that the exact accession and genetic characteristics of the two *N. benthamiana* lines used above are unknown. Furthermore, they were sourced from different labs. Therefore, is it possible that genetic differences between the accessions led to differences in the ability of *P. agathidicida* and *P. cinnamomi* to infect *N. benthamiana* (Goodin et al., 2008).

Differences in susceptibility of different wildtype accessions of *N. benthamiana* provide good reasoning for future experiments to include kauri. However, it is possible that between the different kauri lines there could be differences in susceptibility or resistance. This may enable the identification of kauri with increased tolerance to these *Phytophthora* pathogens. Although the *Phytophthora* species investigated were not able to infect *N. benthamiana* in some cases, they may all be able to infect kauri leaves. However, as was discussed above for *N. benthamiana*, the *Phytophthora* strains would first need to be tested for differences in their ability to infect and the size of lesions they produce. For such future experiments, it would be best to use strains of each species that have been co-isolated from the same soil sample. If the isolates of each species are found to infect kauri leaves and grow at the roughly same rate, then real-time quantitative polymerase chain reaction (RT-qPCR) experiments could be performed with species-specific primers to determine how the biomass of each *Phytophthora* species changes when another species is present. However, while species-specific primers are available for *P. agathidicida* (Than et al., 2013) and *P. cinnamomi* (Kong et al., 2003; Kostov et al., 2016), there are currently none for *P. multivora*, and so these would need to be developed.

Another future experiment of interest would be to determine whether the *SOBIR1* gene of kauri has the same ability to restrict *P. agathidicida* and *P. multivora* growth in *N. benthamiana*. This could be achieved by expressing the kauri *SOBIR1* gene in Δ*sobir1* plants of *N. benthamiana* using an ATTA and then looking at lesion area following inoculation with the *Phytophthora* species, as described above. However, cultural agreements need to be in place before this can be achieved with kauri *SOBIR1*. Thus, it should first be completed with another gymnosperm species such as *Pinus taeda*, which has a publicly available genome sequence, to determine if the *SOBIR1* gene from this species can functionally replace the *SOBIR1* gene in *N. benthamiana*. Such an experiment would provide a good indication that this experiment could work for the *SOBIR1* gene from kauri.

4.4: Conclusions

This study begins to explore interactions that occur between three different *Phytophthora* species that are commonly co-isolated from soil surrounding kauri trees with kauri dieback disease: *P. agathidicida*, *P. cinnamomi* and *P. multivora*. These species were initially cultured onto various solid media to observe interactions at a macroscopic level through colony interaction assays. The results of this assay suggested that no physical contact was occurring, however, it remained likely that they were interacting at the molecular level. To investigate this, an interaction-based approach was then used to determine if the secreted protein repertoire changed between samples containing single species and those that were co-cultured in multi-species samples. This was the first experiment of its kind to be completed with *Phytophthora* species. Furthermore, the proteomics component was among the first studies to look at the secretome of *P. multivora* in depth. It revealed 20 candidate *Phytophthora* effector candidates that were identified through quantitative analysis (significant increase in abundance when co-cultured) or qualitative analysis (present only when co-cultured). Finally, an *in-planta* experiment using a Δ*sobir1* plants of *N. benthamiana* was the first time *P. agathidicida* and *P. multivora* have been inoculated onto these plants and showed that lesions sizes were significantly larger than on the wildtype, suggesting the importance of RLP-immunity in suppressing these infections. This are intriguing results that warrant further work.

This study sets an excellent foundation for further testing of the 20 candidate effectors identified in this study. It would be advantageous to test all 20. However, those that should be prioritized are the CAZymes, the lipoxygenase and the hypothetical protein KNV87_007317-T1 as they all showed interesting insights into their potential function, with many having similarities to antagonistic or antimicrobial roles based on the literature of similar proteins from other fungal or oomycete species. Furthermore, most of these candidates were encoded by genes that were highly expressed in kauri, suggesting an importance in infection. Those that were identified in the quantitative study of this thesis were also highly abundant. The role for *SOBIR1* in immunity against *P. agathidicida* in *N. benthamiana* highlights that there is now a need to look into this further, especially by examining *SOBIR1* from kauri to see if RLP-mediated immunity in kauri plays as a significant role as it does in *N. benthamiana*. Furthermore, these results suggested that *Phytophthora*–candidate effector interactions involving these two *Phytophthora* species could be carried out in *N. benthamiana* plants lacking SOBIR1. Going forward, a study similar to this should be undertaken with the three species again, however it should use the species with the specific strains that are actually co-isolated together to gain further insights into their interactions.

Appendices

Appendix 1

1.1 Recipes for media

Carrot agar

200 g carrot

milli Q water to 1 L

15 g bacteriological agar (PureScience, New Zealand)

Combine carrot and 250 mL milliQ water in blender and blend at high speed until smooth. Strain with of two layers Miracloth to maintain carrot juice. Add milliQ water until 1 L total volume. Add 15 g agar before autoclaving at 121°C for 15 min. Pour plates aseptically in biohazard hood when agar cooled. Store plates at 4°C until required.

Clarified V8 concentrate

1.25 L V8 vegetable juice (Campbell's, Camden, New Jersey, USA)

1.25 g $CaCO_2$ (BDH Chemicals Ltd, New Zealand)

MilliQ water to 1 L

Combine V8 vegetable juice and $CaCO_2$ and stir until dissolved. Separate into centrifuge tubes and centrifuge (Heraeus Megafuge 16R Centrifuge (ThermoFisher Scientific, Waltham, Massachusetts, USA)) at 4,000 rpm for 20 min. Pour supernatant into 50 mL Falcon tubes and store at –20°C until required.

20% clarified V8 media

4 x 50 mL clarified V8 stock concentrate

15 g bacteriological agar (if making agar, ignore if making broth) (Acumedia®, Michigan, USA)

MilliQ water

Melt contents of frozen clarified V8 concentrate in Falcon tubes and add milliQ water up to 1 L. Add 15 g of agar (if required) and autoclave at 121°C for 15 min. Pour plates aseptically when cooled. Store agar plates at 4°C until required.

Cornmeal agar

17 g cornmeal agar (Difco Laboratories, Michigan, USA)

5 g bacteriological agar

1 mL ampicillin (Sigma-Aldrich) 250 mg/mL

0.6 mL rifampicin (Duchefa Biochemie, Haarlem, The Netherlands) 20 mg/mL

0.4 mL pimaricin (Sigma-Aldrich) 10 mg/mL

2.5 mL pentachloronitrobenzene (Sigma Aldrich) 40 mg/mL in DSMO

Combine cornmeal agar powder and bacteriological agar powder with milliQ water up to 1 L before autoclaving at 121°C for 15 min. When cooled, add antibiotics and pour plates aseptically. Store plates at 4°C until required.

Plich agar

0.5 g KH_2PO_4 (J.T.Baker®, Phillipsburg, New Jersey, USA)

0.25 g $MgSO_4.7H_2O$ (Scharlau, Barcelona, Spain)

0.1 g asparagine (Sigma-Aldrich)

0.001 g thiamine (Sigma-Aldrich)

0.5 g yeast extract (Sigma-Aldrich)

0.01 g β–sitosterol (Sigma-Aldrich)

25 g D-glucose (Sigma-Aldrich)

Combine all ingredients in a Schott bottle with milliQ water up to 1 L. Sterilise by autoclaving at 121°C for 15 min. Pour plates aseptically in biohazard hood when agar is cooled. Store plates at 4°C until required.

1.2 Buffer Recipe

1 x SDS Running Buffer

25 mM Tris

192 mM glycine

0.1% (v/w) SDS, pH 8.3

1.3. Tables and Figures

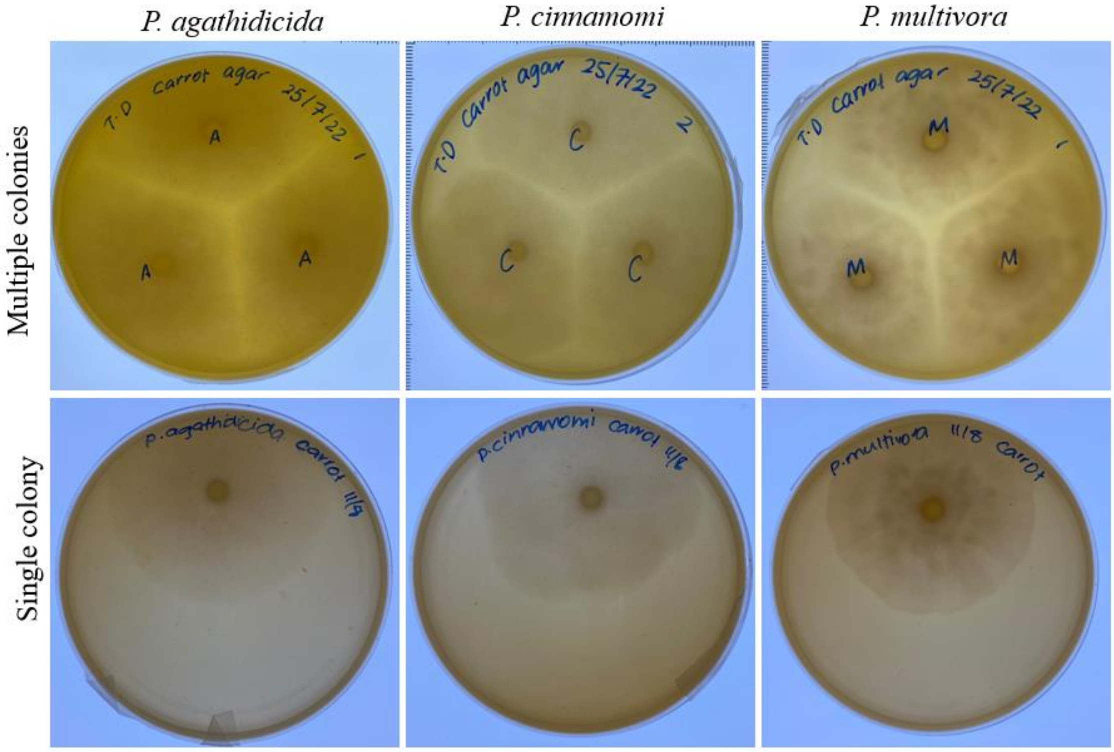

***Figure A1.* Intraspecific colony interaction assays of *Phytophthora* species on nutrient-rich carrot agar plates.** The top three images show three colonies each of *P. agathidicida*, *P. cinnamomi* and *P. multivora* initiated from agar plugs of five mm in diameter (small darker circles), that have grown towards each other until zones of growth inhibition (gaps) between them have been formed. The bottom three images show single-colony-only plates to illustrate that growth of a single colony from each of *P. agathidicida*, *P. multivora* and *P. cinnamomi* is not restricted in the absence of other colonies from the same species, and that they grow out past the point where a zone of inhibition is typically formed. Colonies were cultured on nine cm plates at 22°C for seven days and are representative of what was observed across four independent biological replicates. In blue marker pen: A = *P. agathidicida*; C = *P. cinnamomi*; M = *P. multivora*.

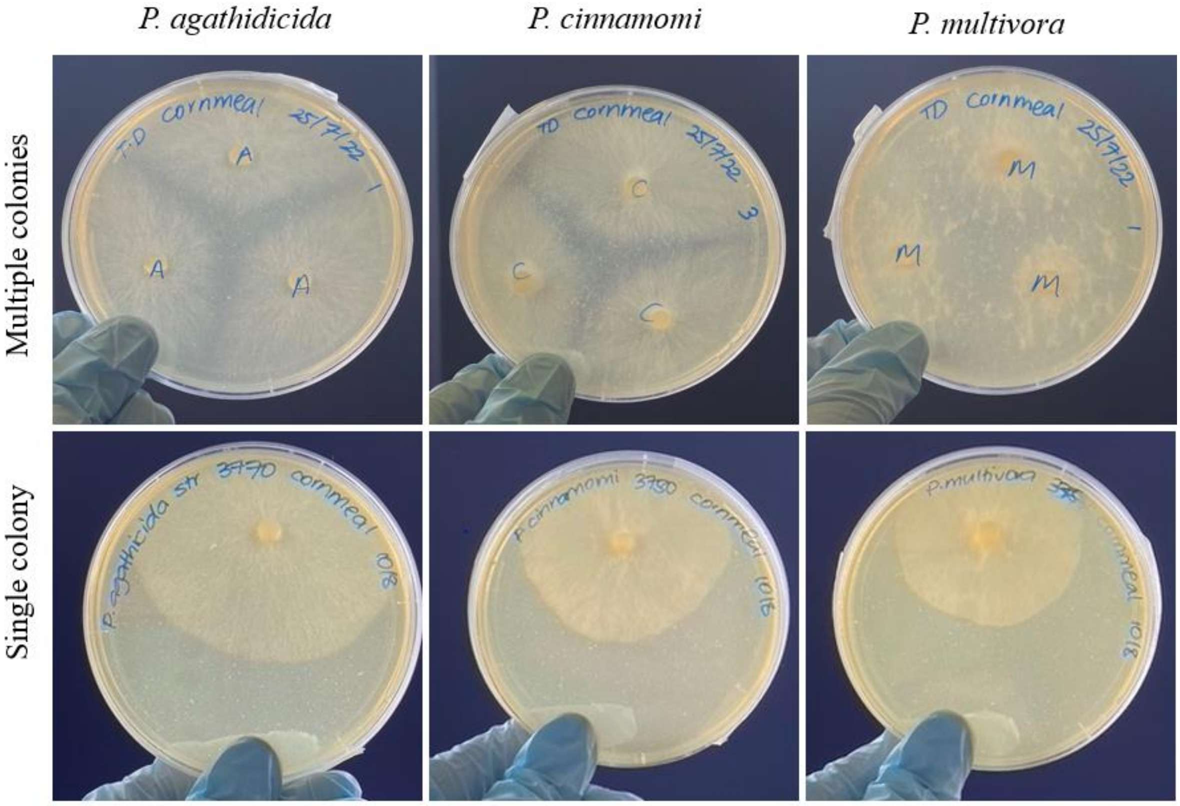

Figure A2. **Intraspecific colony interaction assays of *Phytophthora* species on nutrient-poor cornmeal + PARP antibiotic plates.** The top three images show three colonies each of *P. agathidicida*, *P. cinnamomi* and *P. multivora* initiated from agar plugs of five mm in diameter (small darker circles), that have grown towards each other until zones of growth inhibition (gaps) between them have been formed. The bottom three images show single-colony-only plates to illustrate that growth of a single colony from each of *P. agathidicida*, *P. multivora* and *P. cinnamomi* is not restricted in the absence of other colonies from the same species, and that they grow out past the point where a zone of inhibition is typically formed. Colonies were cultured on nine cm plates at 22°C for seven days and are representative of what was observed across four independent biological replicates. In blue marker pen: A = *P. agathidicida*; C = *P. cinnamomi*; M = *P. multivora*.

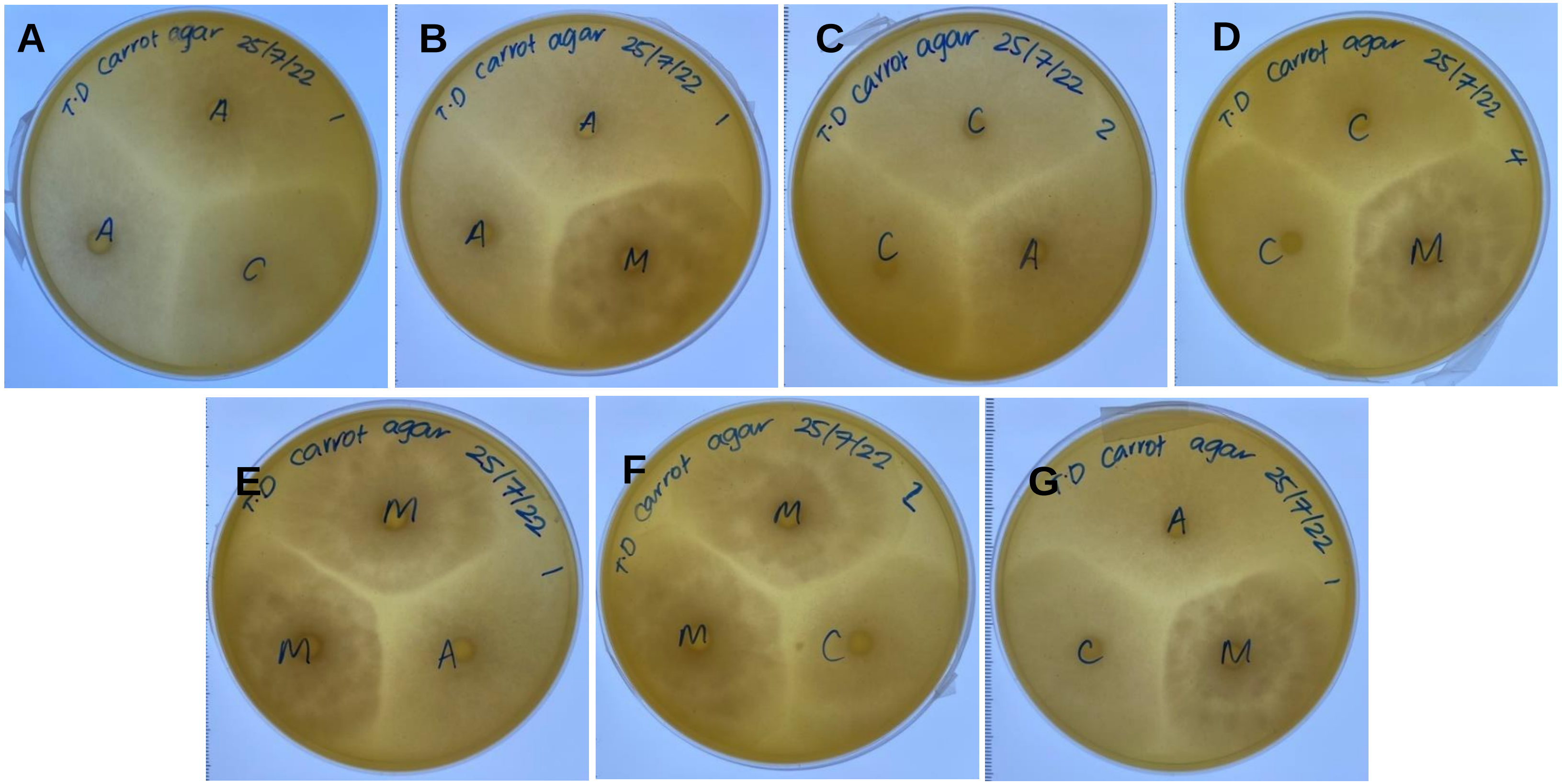

Figure A3. **Interspecific colony interaction assays of *Phytophthora* species on nutrient-rich carrot agar plates.** All plates show three colonies of *Phytophthora* (*P. agathidicida*, *P. cinnamomi* and *P. multivora*) in differing species combinations, initiated from an agar plug five mm in diameter (small darker circles), that have grown towards each other until zones of growth inhibition (gaps) between them have been formed. Colonies were cultured on nine cm plates at 22°C for six days and are representative of what was observed across four independent biological replicates. Combinations of each agar plate are indicated by letters in blue marker pen: A = *P. agathidicida*; C = *P. cinnamomi*; M = *P. multivora*.

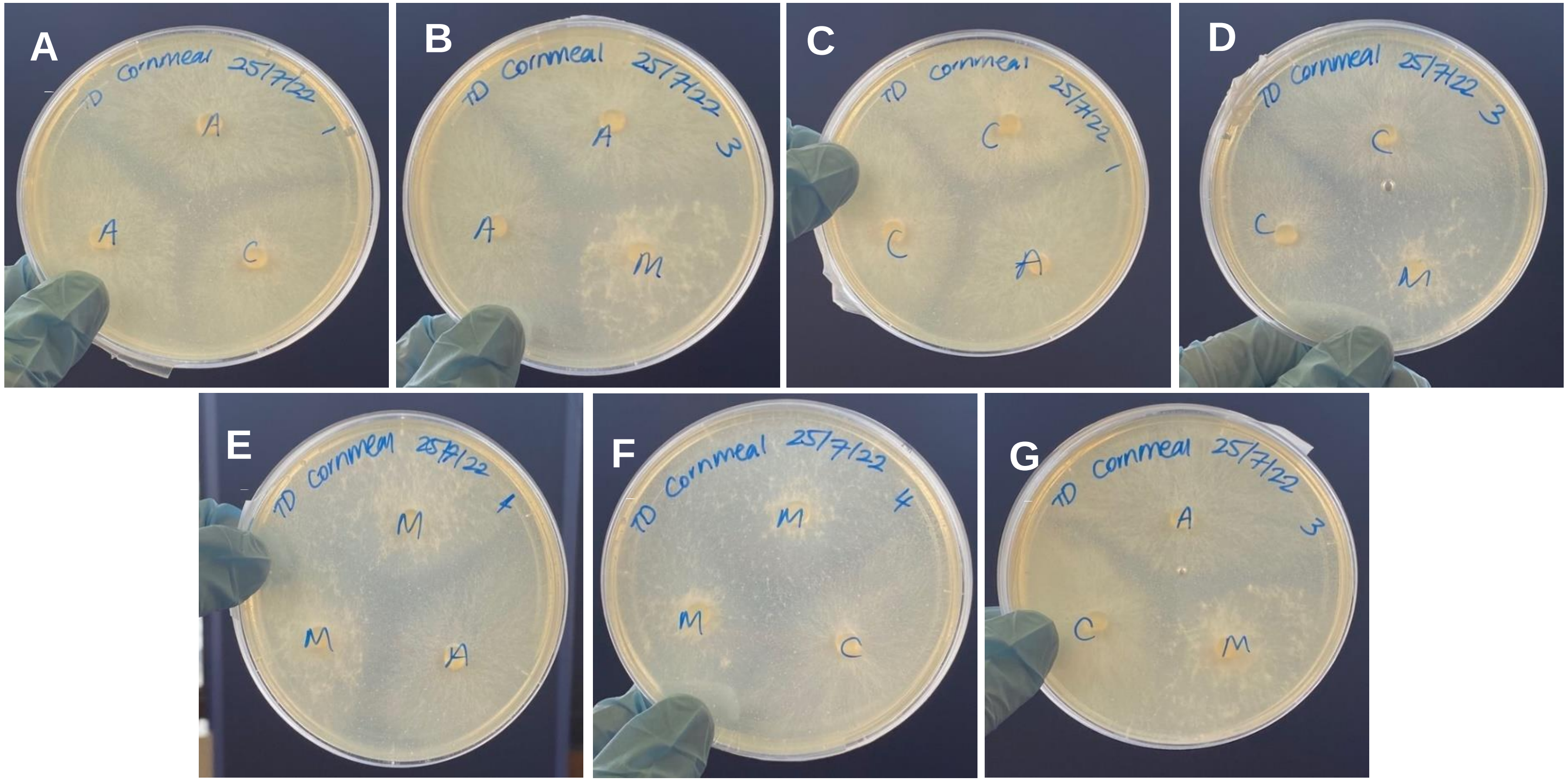

***Figure A4.* Interspecific colony interaction assays of *Phytophthora* species on nutrient-poor cornmeal + PARP antibiotics agar plates.** All plates show three colonies of *Phytophthora* (*P. agathidicida*, *P. cinnamomi* and *P. multivora*) in differing species combinations, initiated from an agar plug five mm in diameter (small darker circles), that have grown towards each other until zones of growth inhibition (gaps) between them have been formed. Colonies were cultured on nine cm plates at 22°C for six days and are representative of what was observed across four independent biological replicates. Combinations of each agar plate are indicated by letters in blue marker pen: A = *P. agathidicida*; C = *P. cinnamomi*; M = *P. multivora*.

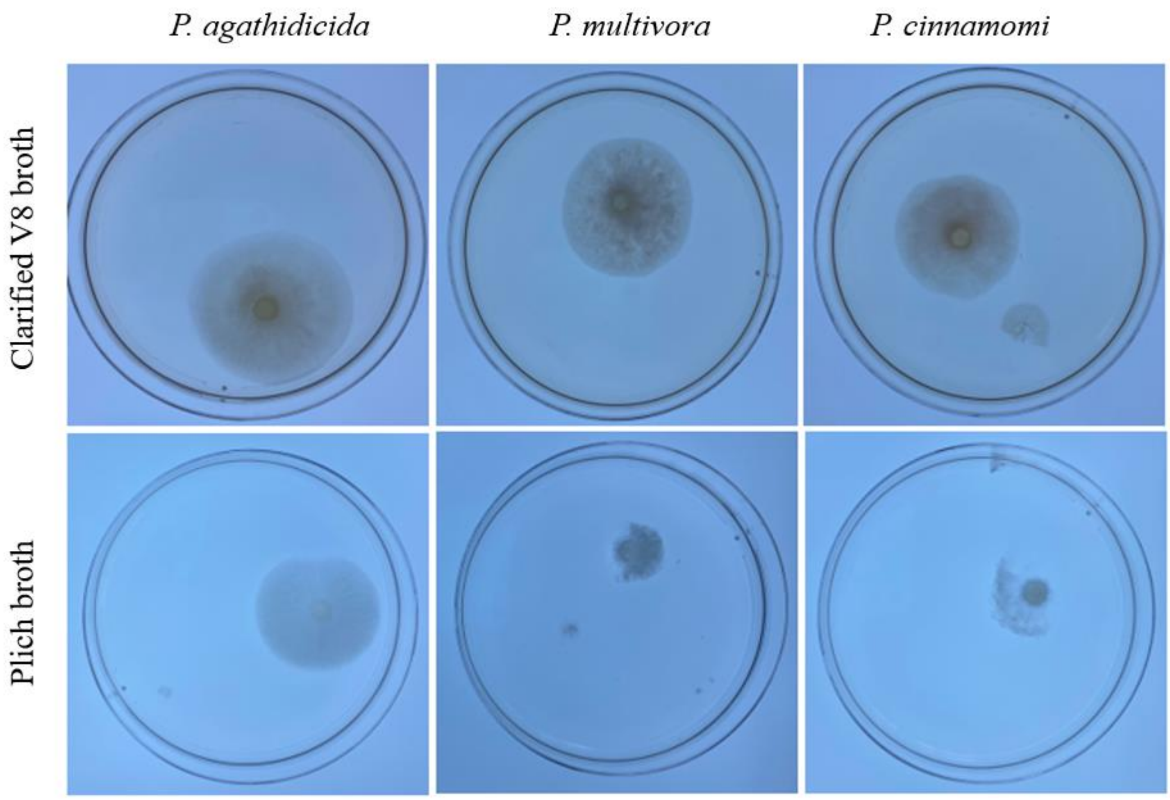

Figure A5. **Growth of single *Phytophthora* species in clarified V8 broth and plich broth media.** *P. agathidicida*, *P. multivora* and *P. cinnamomi* were each grown from a single five mm agar plug (extracted from the outer edge of an actively growing colony on clarified V8 agar) in 10 mL of clarified V8 broth in nine cm Petri dishes for three days in the dark at 22°C without shaking (i.e. as static cultures). The Petri dishes are representative of four independent biological replicates.

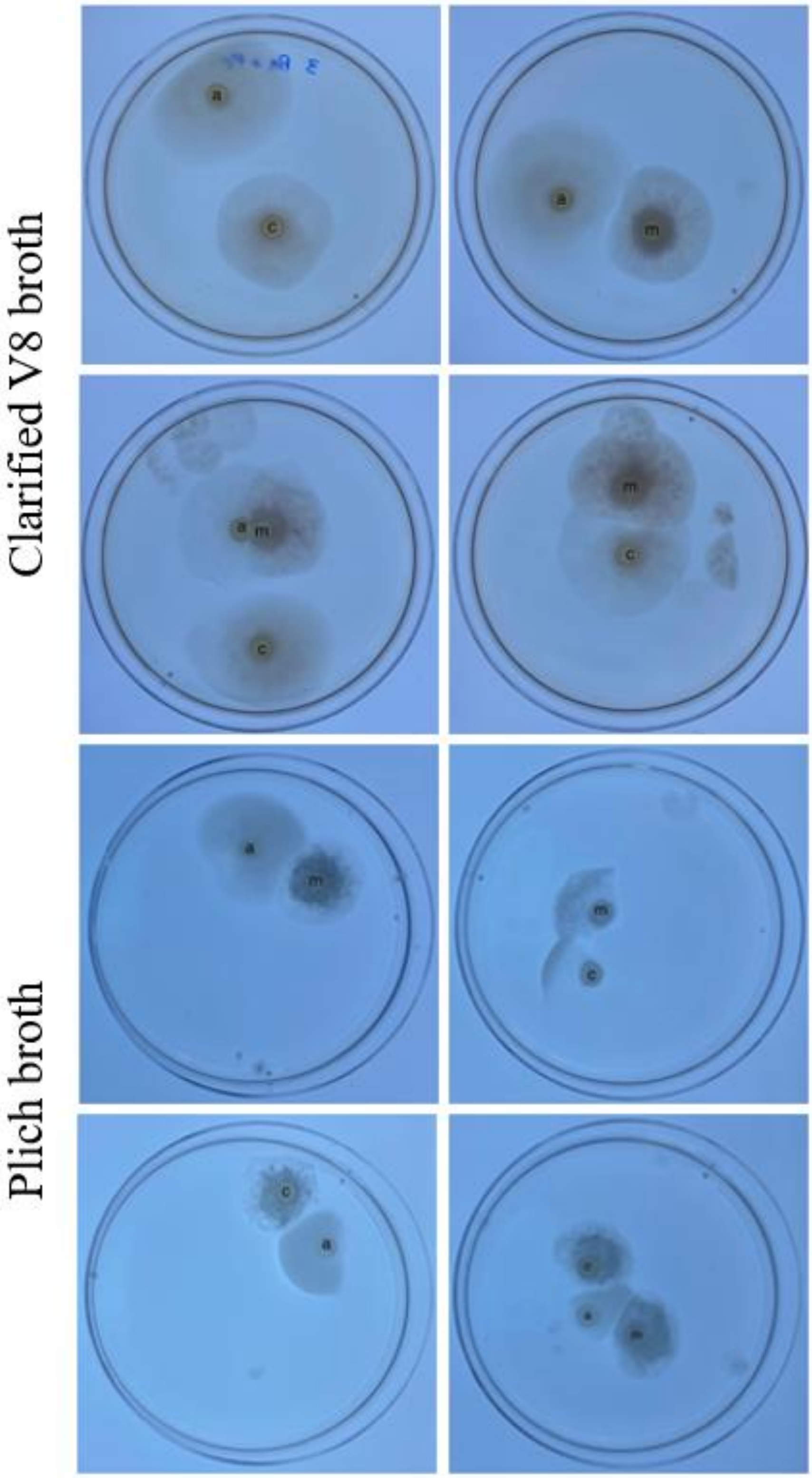

Figure A6. **Growth of multiple *Phytophthora* species in clarified V8 broth and plich broth media.** *P. agathidicida* (a), *P. cinnamomi* (c) and *P. multivora* (m) were each grown from a single five mm agar plug (extracted from the outer edge of an actively growing colony on clarified V8 agar) in 10 mL of clarified V8 broth in nine cm Petri dishes for three days in the dark at 22°C without shaking (i.e. as static cultures). The Petri dishes are representative of four independent biological replicates.

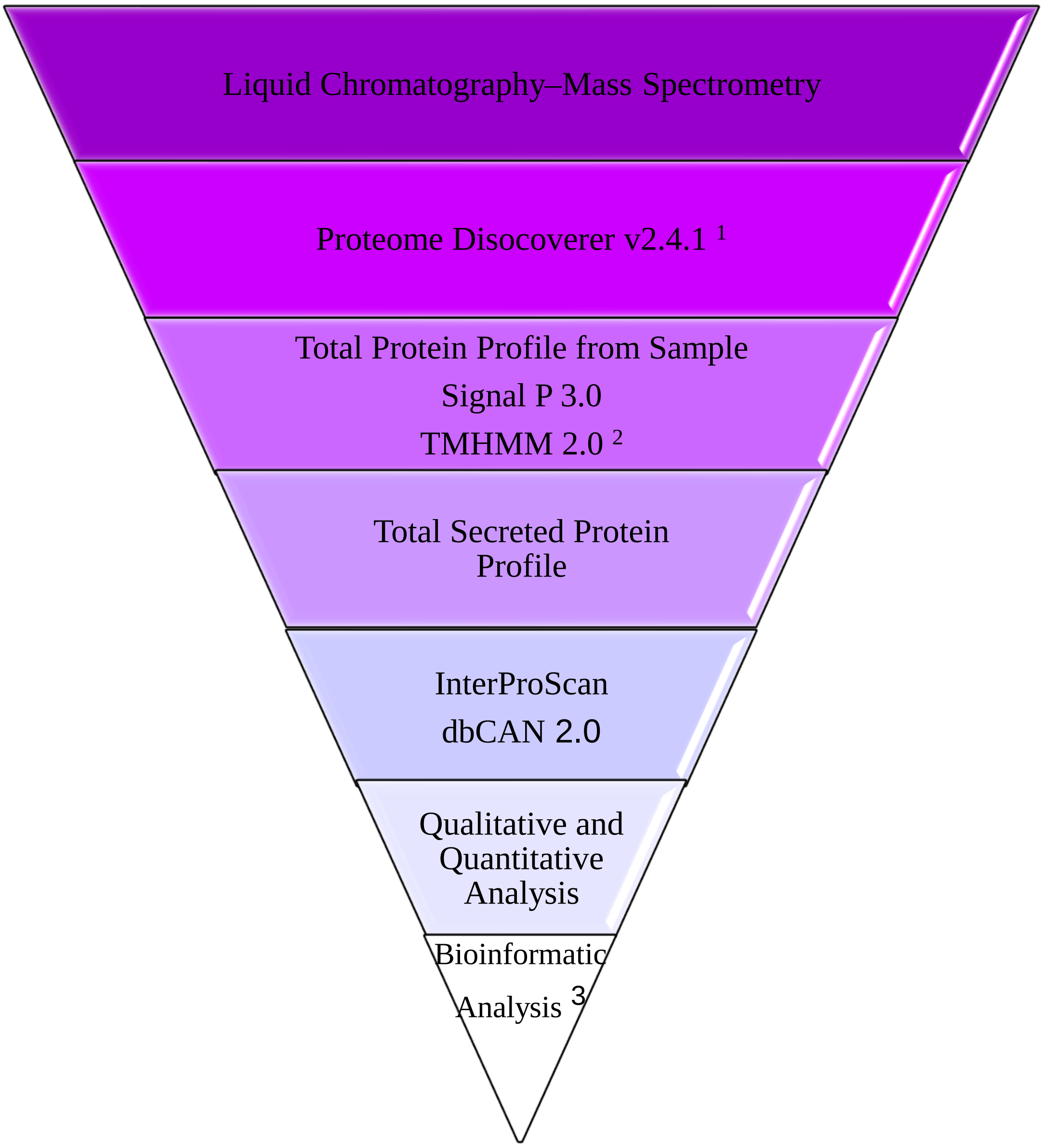

Figure A7. **Flowchart of protein analysis undertaken with each *Phytophthora agathidicida*, *Phytophthora cinnamomi* and *Phytophthora multivora* culture filtrate sample following liquid chromatography–mass spectrometry (LC–MS).** Raw peptides were generated through liquid chromatography – mass spectrometry according to Chapter 2, Section 2.3.5. Proteome Discoverer 2.4.1.15 was used to identify proteins in culture filtrate samples by searching raw spectra data with predicted proteomes of each species (*P. agathidicida*, *P. cinnamomi* and *P. multivora*). The searches generated a total protein output for each single species or multispecies sample. The total protein profile was searched on the SignalP v3.0 and TMHMM 2.0 webservers. Only proteins with a predicted signal peptide using SignalP v3.0 and no predicted transmembrane domain using TMHMM v2.0 continued through the following processes to identify candidate effector proteins. The secreted proteins were analysed for functional domains on both InterProScan and dbCAN 2.0 webservers. A qualitative (presence/ absence) and quantitative (abundance) analysis was carried out. Bioinformatic analysis was undertaken to determine the predicted function of candidate effector proteins (BLASTp, PyMol, AlphaFold2).

Table A1. **Fold change and -log10 values for each candidate effector protein from *Phytophthora agathidicida* that increased or decreased in abundance when co-cultured with another *Phytophthora* species, relative to growth alone.**

Accession	Description	Pfam number	P.a+P.c	P.a+P.m	P.a+P.c+P.m
KNV87_004047-T1	AA17		1.607	6.475	4.436
KNV87_004566-T1	Bacterial extracellular solute-binding protein	PF133143	1.666	3.207	4.604
KNV87_015800-T1	No prediction		2.948	7.454	3.245
KNV87_016404-T1	Cyclophilin type peptidyl-prolyl isomerase	PF00160	1.868	6.409	3.449
KNV87_017260-T1	Fibronectin type III-like domain	PF00933	3.137	9.335	2.920
KNV87_004012-T1	GH131	PF18271	2.863	5.318	1.890
KNV87_008864-T1	Lipoxygenase	PF00305	2.734	4.454	0.668
KNV87_009659-T1	Non-lysosomal ceramidase		3.773	9.124	2.248
KNV87_013190-T1	AA1		4.412	8.651	1.638
KNV87_011474-T1	Carboxylesterase family 24		2.571	5.957	1.801
KNV87_000692-T1	Transglutaminase elicitor	PF16683	0.402	3.488	-1.979
KNV87_001691-T1	GH17		3.379	6.099	3.073
KNV87_001705-T1	Lactonase 7 bladed beta propeller	PF10282	3.062	4.743	3.473
KNV87_002299-T1	No prediction		1.268	3.828	-1.926
KNV87_002401-T1	GH32	PF00251	1.075	5.719	1.350
KNV87_002474-T1	GH72		0	4.035	1.428
KNV87_002778-T1	GH5	PF00150	0.362	2.862	2.253
KNV87_003250-T1	AA17		2.474	4.611	-1.043
KNV87_003513-T1	No prediction		3.237	5.246	3.176
KNV87_003749-T1	GH53	PF07745	1.744	3.230	0.8915
KNV87_004038-T1	No prediction		3.420	3.614	-14.561
KNV87_007055-T1	Pectate lyase family 3	PF03211	3.428	5.295	4.765
KNV87_007219-T1	Thioredoxin	PF00085	1.925	4.318	0.077
KNV87_008614-T1	AA2	PF00141	1.068	3.507	0.185
KNV87_009532-T1	Partial alpha/beta hydrolase	PF04083	0.992	4.752	0.919
KNV87_009879-T1	No prediction		0.312	5.568	0.334
KNV87_010136-T1	GH30	PF17189	3.105	5.857	1.456
KNV87_010998-T1	No prediction		1.190	6.057	2.050
KNV87_011017-T1	GH30		1.620	5.225	0.792
KNV87_011222-T1	No prediction		2.182	4.520	-0.946
KNV87_011255-T1	AA17		1.061	3.571	1.850
KNV87_011407-T1	Cell wall protein	PF10287	0.599	4.848	-0.917
KNV87_011471-T1	Carboxylesterase family 26	PF00135	4.851	8.821	4.358
KNV87_011783-T1	AA17		2.155	2.951	0.706
KNV87_012622-T1	GH17	PF00332	1.651	1.719	0
KNV87_017473-T1	GH3	PF01915	2.172	-9.810	1.293
KNV87_013080-T1	Cell wall protein	PF10287	0.5488	2.977	-0.402

KNV87_011461-T1	Bacterial alpha-L-rhamnosidase	PF17389	2.992	5.452	2.829
KNV87_013802-T1	No prediction		-2.885	2.467	-0.636
KNV87_011473-T1	GH3	PF00933	1.835	-12.245	1.571
KNV87_014500-T1	GH30	PF14587	2.067	4.182	1.790
KNV87_011782-T1	AA17		1.964	0	0.815
KNV87_012250-T1	GH17	PF00332	2.212	6.500	-0.170
KNV87_012621-T1	GH17		0.646	1.385	-2.820
KNV87_015389-T1	Bacterial alpha-L-rhamnosidase	PF17390	2.534	-12.603	2.615
KNV87_017723-T1	Necrosis-inducing protein (NPP1)	PF05630	-16.263	1.782	1.215
KNV87_017848-T1	GH12	PF01670	0.555	-0.080	-1.001
KNV87_000012-T1	Calcineurin like phosphoesterase	PF00149	1.902	4.631	-2.215
KNV87_000586-T1	GH17	PF00332	2.220	3.307	-0.472
KNV87_000687-T1	Transglutaminase elicitor	PF16683	-0.102	2.726	-1.254
KNV87_000691-T1	Transglutaminase elicitor	PF16683	-0.185	3.625	-0.024
KNV87_001288-T1	Trypsin	PF00089	2.127	0.566	0
KNV87_005090-T1	PAN domain	PF14295	0.700	3.633	0.298
KNV87_005091-T1	PAN domain	PF14295	-0.2309	4.411	-0.085
KNV87_006670-T1	Cell wall protein	PF10290	0.1028	-1.326	-1.189
KNV87_006790-T1	Zinc carboxylpeptidase	PF00246	0.693	3.504	0
KNV87_001707-T1	Lactonase 7 bladed beta propeller	PF10282	0.104	3.885	0.752
KNV87_003613-T1	No prediction		1.640	3.304	-3.225
KNV87_003614-T1	No prediction		-1.152	4.602	1.812
KNV87_004010-T1	GH131	PF18271	1.594	4.456	1.693
KNV87_007315-T1	No prediction		1.782	4.405	-1.982
KNV87_007346-T1	GH105	PF07470	2.352	2.916	0.340
KNV87_008011-T1	Cysteine rich secretory protein family 43	PF00188	-0.286	2.383	-0.838
KNV87_008850-T1	AA7	PF08031	1.619	5.299	0.501
KNV87_009616-T1	Alpha/beta hydrolase	PF04083	0.760	6.315	0.909
KNV87_010137-T1	GH30	PF02055	1.965	5.233	0.602
KNV87_010140-T1	GH30	PF17189	2.320	4.770	-0.002
KNV87_011025-T1	Necrosis Inducing Protein (NPP1)	PF05630	-0.876	1.598	0.663
KNV87_011035-T1	GH10	PF00331	0.028	5.910	1.709

1. AA, Auxiliary Activity family; GH, Glycoside Hydrolase Family; P.a = *P. agathidicida*; P.c = *P. cinnamomi*; P.m = *P. multivora*.
2. Coloured by -$\log_{10}$ P-value (values not shown in table) = the higher -$\log_{10}$ value, the more statistically significantly the increased abundance of the protein is. Light purple = -$\log_{10}$ value between 1.3 and 2; dark purple = -$\log_{10}$ value between 2 and 3; dark pink = -$\log_{10}$ value >3. White = non-significant values.
3. Values in each column represents the $\log_2$ fold change value.
4. Species were cultured as single-species samples or multi-species samples in clarified V8 broth for seven days without shaking and the proteins secreted into the culture medium assessed for differences in abundance using LC–MS data generated from the Proteome Discoverer program after searching against respective proteome databases (Chapter 2: Section 2.2.2 and 2.3.5).

Table A2. **Fold change and -log$_{10}$ values for each candidate effector protein from *Phytophthora cinnamomi* that significantly increased or decreased in abundance when co-cultured with another *Phytophthora* species, relative to growth alone.**

Accession	Description	Pfam number	P.a + P.c	P.c + P.m	P.a + P.c+ P.m
Pci3750_009309-RA	Calcineurin like phosphoesterase	PF16683	-2.609	-2.113	-3.120
Pci3750_011995-RA	GH30	PF17189	-2.019	-2.537	-3.766
Pci3750_013531-RA	GH30	PF02055	-1.066	-1.689	-2.284
Pci3750_003423-RA	GH17		-0.592	-0.588	-2.581
Pci3750_007476-RA	Serine carboxypeptidase	PF00450	-2.400	-2.262	-2.633
Pci3750_013442-RA	GH31	PF01055	-1.063	-0.726	-1.419
Pci3750_013532-RA	NPP1	PF05630	-2.287	-1.845	-2.718
Pci3750_012168-RA	Partial alpha/beta hydrolase lipase	PF04083	-1.446	-1.912	-1.572
Pci3750_012520-RA	PAN domain	PF14295	-1.030	-1.146	-0.687
Pci3750_012942-RA	Palmitoyl thioesterase	PF02089	-3.004	-1.174	-4.241
Pci3750_011996-RA	GH30	PF02055	-3.013	0.097	-2.895
Pci3750_000241-RA	GH17	PF00332	-1.452	-0.876	-2.041
Pci3750_001393-RA	Non-lysosomal ceramidase	PF17048	-2.398	-0.082	-2.903
Pci3750_004996-RA	Bacterial extracellular solute-binding protein	PF13343	-1.602	-0.380	-2.460
Pci3750_005637-RA	Nuclease	PF02265	-1.543	-0.941	-3.364
Pci3750_008377-RA	No prediction		-2.507	-0.845	-2.943
Pci3750_010693-RA	No prediction		-1.694	-0.897	-3.954
Pci3750_002695-RA	Bacterial extracellular solute-binding protein	PF13343	-1.148	-1.150	
Pci3750_007002-RA	Aldose 1-epimerase		0	-1.478	
Pci3750_009836-RA	Pyridoxamine 5’ phosphatase oxidase		-1.549	-0.992	
Pci3750_013379-RA	Cysteine-rich secretory protein	PF00188	-1.296	-0.124	-2.558
Pci3750_014318-RA	Eukaryotic type carbonic anhydrase	PF00194	-1.448	-0.989	-2.791
Pci3750_014827-RA	Pectinacetylesterase	PF03283	-0.558	0.454	-1.271
Pci3750_001267-RA	AA3	PF00732	-3.016	-1.938	
Pci3750_008775-RA	GH17	PF00332	-2.429	-0.838	
Pci3750_004325-RA	Tyrosinase	PF00264	-3.195	-1.341	
Pci3750_004421-RA	Non-lysosomal ceramidase	PF17048	-1.599	-0.492	
Pci3750_004548-RA	Cell wall protein	PF10290	-3.307	-0.864	
Pci3750_006415-RA	GH53	PF07745	-2.915	-0.614	-1.910
Pci3750_006488-RA	GH131	PF18271	-3.487	-0.772	
Pci3750_007028-RA	Transglutaminase elicitor	PF16683	-1.129	-0.749	-1.335
Pci3750_007607-RA	No prediction		-1.703	-1.095	-1.411
Pci3750_008944-RA	Transglutaminase elicitor	PF16683	-2.692	0	

Pci3750_008956-RA	Partial alpha/beta hydrolase lipase	PF04083	-3.638	0	
Pci3750_008991-RA	Histidine phosphatase	PF00328	-1.560	-0.420	-2.124
Pci3750_009550-RA	GH1		-3.047	-3.552	
Pci3750_009828-RA	AA3	PF05199	-1.378	0.082	-0.887
Pci3750_010084-RA	Collagenase	PF12904	-1.433	0	
Pci3750_011737-RA	Peroxidase family 2	PF01328	-3.599	-0.272	
Pci3750_013170-RA	GH88	PF07470	-3.419	-1.003	
Pci3750_013492-RA	Cell wall protein	PF10287	-1.109	-0.581	-1.536
Pci3750_013785-RA	Elicitin	PF00964	-2.630	0	-1.252
Pci3750_014022-RA	Alkaline phosphatase	PF00245	-1.751	0	

1. AA, Auxiliary Activity family; GH, Glycoside Hydrolase Family; P.a = *P. agathidicida*; P.c = *P. cinnamomi*; P.m = *P. multivora*.
2. Coloured by -$\log_{10}$ P-value (values not shown in table) = the higher -$\log_{10}$ value, the more statistically significantly the increased abundance of the protein is. Light purple = -$\log_{10}$ value between 1.3 and 2; dark purple = -$\log_{10}$ value between 2 and 3; dark pink = -$\log_{10}$ value >3. White = non-significant values.
3. Values in each column represents the $\log_2$ fold change value.
4. Species were cultured as single-species samples or multi-species samples in clarified V8 broth for seven days without shaking and the proteins secreted into the culture medium assessed for differences in abundance using LC–MS data generated from the Proteome Discoverer program after searching against respective proteome databases (Chapter 2: Section 2.2.2 and 2.3.5).

Table A3. **Fold change and -$\log_{10}$ values for each candidate effector protein from *Phytophthora multivora* that significantly increased or decreased in abundance when co-cultured with another *Phytophthora* species, relative to growth alone.**

Protein ID/number	Description	Pfam number	P.c + P.m	P.a + P.m	P.a + P.c + P.m
Pmult_s010099g00017.1	GH17		-1.747	-0.817	-1.706
Pmult_s010146g00009.1	Nuclease	PF02265	-1.403	-1.459	-2.786
Pmult_s010235g00010.1	Ribonuclease T2 family	PF00445	-2.240	-1.971	-2.913
Pmult_s020194g00013.1	GH17		-1.427	-1.203	-3.468
Pmult_s010036g00021.1	No prediction		-1.50	-0.749	-2.626
Pmult_s010221g00007.1	Necrosis inducing protein (NPP1)	PF05630	-0.949	0.220	-1.289
Pmult_s010237g00006.1	Cell wall protein	PF10287	-1.022	-0.811	-2.803
Pmult_s010342g00011.1	Berberine	PF08031		-2.146	-3.575
Pmult_s010487g00001.1	GH5	PF00150	-0.421	-0.580	-3.156
Pmult_s011266g00002.1	Cyclophilin type peptidyl-propyl isomerase	PF00160	-1.337	-0.324	-1.567
Pmult_s011719g00001.1	No prediction		-0.803	-1.406	-2.904
Pmult_s010002g00057.1	AA17		-2.082		
Pmult_s010009g00038.1	GH17	PF00332	-0.687	-0.341	-2.383
Pmult_s010015g00047.1	Tyrosinase	PF00264	-0.702	-0.725	-1.192
Pmult_s010028g00023.1	GH1	PF00232	-0.811	-0.810	-3.459
Pmult_s010037g00028.1	No prediction		-1.379	0.200	-1.286
Pmult_s010044g00019.1	No prediction		0.323	0.181	-2.430
Pmult_s010047g00025.1	No prediction		-2.248		
Pmult_s010049g00004.1	Cysteine-rich secretory protein family 84	PF00188	-1.167	-0.198	
Pmult_s010059g00007.1	GH30	PF14587	-0.717	-0.958	-2.1408
Pmult_s010085g00013.1	Elicitin	PF00964	-3.961	-0.491	
Pmult_s010086g00006.1	Cysteine-rich secretory protein	PF00188	-1.438	0.402	-2.449
Pmult_s010086g00028.1	Cysteine-rich secretory protein	PF00188	-1.305	-1.491	
Pmult_s010116g00048.1	Partial alpha/beta hydrolase lipase	PF04083	-0.955	-0.618	-2.268
Pmult_s010179g00005.1	GH17	PF00332	-1.118	-0.109	-2.606
Pmult_s010203g00012.1	AA17		-1.435	-0.909	-3.563
Pmult_s010250g00002.1	Calcineurin-like phosphoesterase	PF00149	0.027	0.183	-2.292
Pmult_s010254g00007.1	Palmitoyl protein	PF02089	-1.127	-0.873	-2.416

Pmult_s010278g00014.1	GH12	PF01670	-0.693	-0.970	-2.996
Pmult_s010323g00007.1	AA17		-1.826		
Pmult_s010323g00010.1	Transglutaminase elicitor	PF16683	-1.174	-0.629	-3.044
Pmult_s010356g00005.1	GH6	PF01341		2.026	
Pmult_s010367g00002.1	No prediction		-0.717	-0.908	-1.911
Pmult_s010398g00005.1	Lactonase 7 bladed beta propeller	PF10282		-1.304	
Pmult_s010411g00004.1	Thioredoxin	PF00085	-0.696	-0.662	-1.660
Pmult_s010511g00002.1	Transglutaminase elicitor	PF16683	-1.024	-0.410	-2.724
Pmult_s010511g00003.1	Transglutaminase elicitor	PF16683	-0.964	0.834	-2.100
Pmult_s010534g00003.1	Lactonase	PF10282	-1.249	-0.326	-2.591
Pmult_s010548g00004.1	PAN domain	PF14295	-0.075	-1.432	-2.952
Pmult_s010615g00002.1	AA2	PF00141	-0.946	-0.838	-2.611
Pmult_s010626g00002.1	GH3	PF01915	-0.999	-0.384	-2.276
Pmult_s010632g00001.1	GH30	PF02055	-0.904	-0.275	-1.764
Pmult_s010639g00004.1	NPP1	PF05630	-0.005	0.495	-1.516
Pmult_s010696g00003.1	NPP1	PF05630	-2.419	-0.501	
Pmult_s010748g00001.1	Subtilase	PF00082	-0.598	0.184	-1.521
Pmult_s010854g00001.1	GH5	PF00150	-0.767	-0.035	-2.073
Pmult_s010946g00001.1	No prediction		-1.130	-0.401	-2.341
Pmult_s010970g00002.1	GH30	PF17189	-1.370	-0.676	-2.913
Pmult_s011313g00002.1	AA2	PF00141	-1.185	-0.942	-2.385
Pmult_s011347g00001.1	Cell wall protein	PF10290	-0.874	-0.409	-2.101

1. AA, Auxiliary Activity family; GH, Glycoside Hydrolase Family; P.a = *P. agathidicida*; P.c = *P. cinnamomi*; P.m = *P. multivora*.
2. Coloured by -$\log_{10}$ P-value (values not shown in table) = the higher -$\log_{10}$ value, the more statistically significantly the increased or decreased abundance of the protein is. Light purple = -$\log_{10}$ value between 1.3 and 2; dark purple = -$\log_{10}$ value between 2 and 3; dark pink = -$\log_{10}$ value >3. White = non-significant values.
3. Values in each column represents the $\log_2$ fold change value.
4. Species were cultured as single-species samples or multi-species samples in clarified V8 broth for seven days without shaking and the proteins secreted into the culture medium assessed for differences in abundance using LC–MS data generated from the Proteome Discoverer program after searching against respective proteome databases (Chapter 2: Section 2.2.2 and 2.3.5).

***Table A4:* Percentage of occurrences that lesion formation exceeded the size of the five mm agar plug on detached *Nicotiana benthamiana* leaves across the two experiments.** Experiment 1 involved wildtype *N. benthamiana* leaves of an unknown accession from Dr. K. Sohn (Massey University). Experiment 2 used *N. benthamiana* leaves of an unknown accession with and without a Δ*sobir1* knockout (Huang et al., 2021).

		6 hpi	1 dpi	2 dpi	3 dpi	4 dpi	5 dpi
Experiment 1[1]	P.a WT	0%	0%	33.30%	50%	66.60%	66.60%
	P.c WT	0%	0%	33.30%	50%	66.60%	66.60%
	P.m WT	0%	50%	100%	100%	100%	100%
Experiment 2[2]	P.a sWT	NA	0%	0%	0%	0%	0%
	P.c sWT	NA	0%	0%	0%	0%	0%
	P.m sWT	NA	37.50%	100%	100%	100%	NA
	P.a KO	NA	37.50%	75%	100%	100%	NA
	P.c KO	NA	0%	0%	0%	0%	12.50%
	P.m KO	NA	50%	87.50%	100%	100%	NA

1. Experiment 1 involved 3 biological replicates, each with two five mm agar plugs inoculated onto *N. benthamiana* wildtype detached leaves.
2. Experiment 2 involved 4 biological replicates, each with two five mm agar plugs inoculated onto *N. benthamiana* Δ*sobir1* knockout leaves and the corresponding wildtype background.
3. Values in each cell represent the total percentage of lesions across all biological replicates that are larger than the five mm agar plug at each given time point.
4. P.a = *P. agathidicida*, P.c = *P. cinnamomi*, P.m = *P. multivora*, WT = wildtype, sWT= Δ*sobir1* wildtype leaves, KO = Δ*sobir1* knockout, NA = Not available, hpi = hours post-inoculation, dpi = days post-inoculation

Table A5: **Raw ImageJ lesion area measurements for *Phytophthora agathidicida* and *Phytophthora multivora* on *Nicotiana benthamiana* Δ*sobir1* knockout plants and corresponding isogenic wildtype at two days post-inoculation.**

	Replicate Number	Lesion 1 Area	Lesion 2 Area	Total Area
P. agathidicida on Δ*sobir1* wildtype	1	0.062	0.068	0.13
	2	0.062	0.082	0.144
	3	0.041	0.069	0.11
	4	0.07	0.101	0.171
P. agathidicida on Δ*sobir1* knockout	1	2.699	3.039	5.738
	2	0.638	1.052	1.69
	3	2.787	0.574	3.361
	4	0.464	3.542	4.006
P. multivora on Δ*sobir1* wildtype	1	2.219	2.406	4.625
	2	2.81	1.667	4.477
	3	2.916	4.901	7.817
	4	6.072	3.742	9.814
P. multivora on Δ*sobir1* knockout	1	4.155	4.493	8.648
	2	3.048	0.209	3.257
	3	3.906	4.773	8.679
	4	4.821	4.736	9.557

Table A6: **Raw ImageJ lesion area measurements for *Phytophthora agathidicida* and *Phytophthora multivora* on *Nicotiana benthamiana* Δ*sobir1* knockout plants and corresponding isogenic wildtype at three days post-inoculation.**

	Replicate Number	Lesion 1 Area	Lesion 2 Area	Total Area
P. agathidicida on Δ*sobir1*wildtype	1	0.08	0.126	0.206
	2	0.17	0.191	0.361
	3	0.069	0.162	0.231
	4	0.135	0.1089	0.2439
P. agathidicida on Δ*sobir1* knockout	1	20.031	*	20.031
	2	7.25	9.329	16.579
	3	13.824	*	13.824
	4	17.555	*	17.555
P. multivora on Δ*sobir1* wildtype	1	7.278	5.436	12.714
	2	9.064	*	9.064
	3	5.994	4.359	10.353
	4	12.132	*	12.132
P. multivora on Δ*sobir1* knockout	1	17.46	*	17.46
	2	13.699	*	13.699
	3	10.626	7.906	18.532
	4	17.547	*	17.547

1. * = one area measurement was taken as there was no distinct separation between the two lesions.

1.4 Links to spreadsheets

Appendix 2: Raw data generated by Proteome Discoverer following liquid chromatography–mass spectrometry of *P. agathidicida*, *P. cinnamomi* and *P. multivora* grown in single-species and multi-species liquid cultures.

https://masseyuni-my.sharepoint.com/:x:/r/personal/cmesaric_massey_ac_nz/Documents/Taylah%20-%20MSc/Taylah%20-%20Thesis%20Supplementary%20Material/Raw%20Data%20-%20final%20thesis%20.xlsx?d=w5205a6ddc2bf4950a33c40f88434e234&csf=1&web=1&e=XmXYIV

Appendix 3: Spreadsheet for bioinformatic analysis and candidate effector identification. Raw data generated by Proteome Discoverer following liquid chromatography–mass spectrometry of *P. agathidicida*, *P. cinnamomi* and *P. multivora* grown in single-species and multi-species liquid cultures were merged using R Studio. The following sheets detail the various webservers used to identify potential candidate effectors.

https://masseyuni-my.sharepoint.com/:x:/g/personal/cmesaric_massey_ac_nz/EUgfObGamG5CmrW2wbNevZsBvwjXTTIz3pA63M6DpJkHig?e=FV3248

Appendix 4.1: Quantitative analysis comparing the protein abundance between the multi-species sample *P. agathidicida* + *P. cinnamomi* and the single species baseline sample of *P. agathidicida* only.

https://masseyuni-my.sharepoint.com/:x:/g/personal/cmesaric_massey_ac_nz/ESJGwquqqA5PuSaNBn57yvEBjr9mgjhGLdZiF5x8o54BBQ?e=wDzDT1

Appendix 4.2: Quantitative analysis comparing the protein abundance between the multi-species sample *P. agathidicida* + *P. cinnamomi* + *P. multivora* and the single species baseline sample of *P. agathidicida* only.

https://masseyuni-my.sharepoint.com/:x:/g/personal/cmesaric_massey_ac_nz/EYe1Cj62b1dDsN6aWuDkgbwB230Q8iNkrQ_1jlLFT0zTHg?e=fbWqGE

Appendix 4.3: Quantitative analysis comparing the protein abundance between the multi-species sample *P. agathidicida* + *P. cinnamomi* + *P. multivora* and the single species baseline sample of *P. agathidicida* only.

https://masseyuni-my.sharepoint.com/:x:/g/personal/cmesaric_massey_ac_nz/EVx9PF_3An1PgLoW31rPHUsBC2UHby_pUHRrj2pDPKdCOg?e=myohi9

Appendix 4.4: Quantitative analysis comparing the protein abundance between the multi-species sample *P. agathidicida* + *P. cinnamomi* and the single species baseline sample of *P. cinnamomi* only.

https://masseyuni-my.sharepoint.com/:x:/g/personal/cmesaric_massey_ac_nz/EbkbYJNmGJlFsDns15ov_-wBxPnN5S_q9QrPIGP2Dak6RQ?e=pVlS4J

Appendix 4.5: Quantitative analysis comparing the protein abundance between the multi-species sample *P. cinnamomi* + *P. multivora* and the single species baseline sample of *P. cinnamomi* only.

https://masseyuni-my.sharepoint.com/:x:/g/personal/cmesaric_massey_ac_nz/Eepgm1d9DIFKiLkQqA0tB_kBHIoN-KRLjdkg_69kBacq3w?e=NJUoGV

Appendix 4.6: Quantitative analysis comparing the protein abundance between the multi-species sample *P. agathidicida* + *P. cinnamomi* + *P. multivora* and the single species baseline sample of *P. cinnamomi* only.

https://masseyuni-my.sharepoint.com/:x:/g/personal/cmesaric_massey_ac_nz/EeQTNFSgNVpDgIMHol8DUm0BgUvlPpBdPiVX5Ao4UYnVXA?e=G1LhPN

Appendix 4.7: Quantitative analysis comparing the protein abundance between the multi-species sample *P. agathidicida* + *P. multivora* and the single species baseline sample of *P. multivora* only.

https://masseyuni-my.sharepoint.com/:x:/g/personal/cmesaric_massey_ac_nz/EbLpvnqYsRFJjUGZlN56E9IB5Uu08Bkh1CuXb2xulawDag?e=MVffj9

Appendix 4.8: Quantitative analysis comparing the protein abundance between the multi-species sample *P. cinnamomi* + *P. multivora* and the single species baseline sample of *P. multivora* only.

https://masseyuni-my.sharepoint.com/:x:/g/personal/cmesaric_massey_ac_nz/EVj8S0u6TERKtx1DYe6W40cB8X1YmsN-FE8f6pKhycYx-A?e=SISGFp

Appendix 4.9: Quantitative analysis comparing the protein abundance between the multi-species sample *P. agathidicida* + *P. cinnamomi* + *P. multivora* and the single species baseline sample of *P. multivora* only.

https://masseyuni-my.sharepoint.com/:x:/g/personal/cmesaric_massey_ac_nz/EQqE_dOcxEdOllWIJ7OwqtcBsJFL5B2iskuw5k-U1x8weQ?e=dwfuyT

References

Adejumo, T. O., Ikotun, T., & Florini, D. A. (1999). Biological control of *Protomycopsis phaseoli*, the causal agent of leaf smut of cowpea. *Journal of Phytopathology*, *147*(6), 371-375.

Agler, M. T., Ruhe, J., Kroll, S., Morhenn, C., Kim, S.-T., Weigel, D., & Kemen, E. M. (2016). Microbial hub taxa link host and abiotic factors to plant microbiome variation. *PLoS Biology*, *14*(1), e1002352.

Albert, I., Böhm, H., Albert, M., Feiler, C. E., Imkampe, J., Wallmeroth, N., Brancato, C., Raaymakers, T. M., Oome, S., Zhang, H., Krol, E., Grefen, C., Gust, A. A., Chai, J., Hedrich, R., Van den Ackerveken, G., & Nürnberger, T. (2015). An RLP23-SOBIR1-BAK1 complex mediates NLP-triggered immunity. *Nature Plants*, *1*, 15140.

Aley, J. P., Espiner, S., & MacDonald, E. (2023). Behaviour change interventions to facilitate forest trail users' biosecurity compliance. *Journal of Sustainable Tourism*, 1-22.

Altschul, S. F., Madden, T. L., Schäffer, A. A., Zhang, J., Zhang, Z., Miller, W., & Lipman, D. J. (1997). Gapped BLAST and PSI-BLAST: A new generation of protein database search programs. *Nucleic Acids Research*, *25*(17), 3389-3402.

Anagnostakis, S. L. (1987). Chestnut blight: The classical problem of an introduced pathogen. *Mycologia*, *79*(1), 23-37.

Anasontzis, G. E., Lebrun, M.-H., Haon, M., Champion, C., Kohler, A., Lenfant, N., Martin, F., O'Connell, R. J., Riley, R., Grigoriev, I. V., Henrissat, B., Berrin, J.-G., & Rosso, M.-N. (2019). Broad-specificity GH131 β-glucanases are a hallmark of fungi and oomycetes that colonize plants. *Environmental Microbiology*, *21*(8), 2724-2739.

Anderson, P. K., Cunningham, A. A., Patel, N. G., Morales, F. J., Epstein, P. R., & Daszak, P. (2004). Emerging infectious diseases of plants: pathogen pollution, climate change and agrotechnology drivers. *Trends in Ecology & Evolution*, *19*(10), 535-544.

Andersson, J. O. (2006). Convergent evolution: Gene sharing by eukaryotic plant pathogens. *Current Biology*, *16*(18), R804-R806.

Andronis, C. E., Jacques, S., Lipscombe, R., & Tan, K.-C. (2022). Comparative sub-cellular proteome analyses reveals metabolic differentiation and production of effector-like molecules in the dieback phytopathogen *Phytophthora cinnamomi*. *Journal of Proteomics*, *269*, 104725.

Baldauf, S. L., Roger, A. J., Wenk-Siefert, I., & Doolittle, W. F. (2000). A kingdom-level phylogeny of eukaryotes based on combined protein data. *Science*, *290*(5493), 972-977.

Bärenstrauch, M., Mann, S., Jacquemin, C., Bibi, S., Sylla, O.-K., Baudouin, E., Buisson, D., Prado, S., & Kunz, C. (2020). Molecular crosstalk between the endophyte *Paraconiothyrium variabile* and the phytopathogen *Fusarium oxysporum*–modulation of lipoxygenase activity and beauvericin production during the interaction. *Fungal Genetics and Biology*, *139*, 103383.

Bashyal, B. M., Rawat, K., Sharma, S., Kulshreshtha, D., Gopala Krishnan, S., Singh, A. K., Dubey, H., Solanke, A. U., Sharma, T. R., & Aggarwal, R. (2017). Whole genome sequencing of *Fusarium fujikuroi* provides insight into the Role of secretory proteins and cell wall degrading enzymes in causing bakanae disease of rice. *Frontiers in Plant Science*, *8*.

Beever, R. E., Waipara, N. W., Ramsfield, T. D., Dick, M. A., & Horner, I. J. (2009). Kauri (*Agathis australis*) under threat from *Phytophthora*. *Phytophthoras in Forests and Natural Ecosystems*, *74*, 74-85.

Belisle, R. J., McKee, B., Hao, W., Crowley, M., Arpaia, M. L., Miles, T. D., Adaskaveg, J. E., & Manosalva, P. (2019). Phenotypic characterization of genetically distinct *Phytophthora cinnamomi* isolates from avocado. *Phytopathology*, *109*(3), 384-394.

Bellgard, S., & Probst, C. (2018). 18883: Oospore deactivation of *Phytophthora agathidicida*: Desktop review: Alkaline-based solutions. *Biosecurity New Zealand Technical Paper* (2018/02), 16.

Bendtsen, J. D., Nielsen, H., von Heijne, G., & Brunak, S. (2004). Improved prediction of signal peptides: SignalP 3.0. *Journal of Molecular Biology*, *340*(4), 783-795.

Berka, M., Greplová, M., Saiz-Fernández, I., Novák, J., Luklová, M., Zelená, P., Tomšovský, M., Brzobohatý, B., & Černý, M. (2020). Peptide-based identification of *Phytophthora* isolates and *Phytophthora* detection *in planta*. *International Journal of Molecular Sciences*, *21*(24), 9463.

Black, A., Waipara, N., & Gerth, M. (2018). Calling time on New Zealand's oldest tree species. *Nature*, *561*(7722), 177-178.

Boller, T., & Felix, G. (2009). A renaissance of elicitors: perception of microbe-associated molecular patterns and danger signals by pattern-recognition receptors. *Annual Review of Plant Biology*, *60*(1), 379-406.

Bourret, T. B., Choudhury, R. A., Mehl, H. K., Blomquist, C. L., McRoberts, N., & Rizzo, D. M. (2018). Multiple origins of downy mildews and mito-nuclear discordance within the paraphyletic genus *Phytophthora*. *PLoS One*, *13*(3), e0192502.

Bradley, E. L. (2022). Identification and functional characterisation of glycoside hydrolases from the kauri dieback pathogen, *Phytophthora agathidicida.* Massey University.

Bradshaw, R., Bellgard, S., Black, A., Burns, B., Gerth, M., McDougal, R., Scott, P., Waipara, N., Weir, B., & Williams, N. (2020). *Phytophthora agathidicida*: Research progress, cultural perspectives and knowledge gaps in the control and management of kauri dieback in New Zealand. *Plant Pathology*, *69*(1), 3-16.

Brasier, C., Scanu, B., Cooke, D., & Jung, T. (2022). *Phytophthora*: An ancient, historic, biologically and structurally cohesive and evolutionarily successful generic concept in need of preservation. *IMA Fungus*, *13*(1), 12.

Bronkhorst, J., Kasteel, M., van Veen, S., Clough, J. M., Kots, K., Buijs, J., van der Gucht, J., Ketelaar, T., Govers, F., & Sprakel, J. (2021). A slicing mechanism facilitates host entry by plant-pathogenic *Phytophthora*. *Nature Microbiology*, *6*(8), 1000-1006.

Cahill, D. M., Rookes, J. E., Wilson, B. A., Gibson, L., & McDougall, K. L. (2008). *Phytophthora cinnamomi* and Australia’s biodiversity : Impacts, predictions and progress towards control. *Australian Journal of Botany*, *56*, 279-310.

Cantarel, B. L., Coutinho, P. M., Rancurel, C., Bernard, T., Lombard, V., & Henrissat, B. (2008). The carbohydrate-active enzymes database (CAZy): An expert resource for glycogenomics. *Nucleic Acids Research*, *37*, D233-D238.

Caten, C. E. (1972). Vegetative incompatibility and cytoplasmic infection in fungi. *Microbiology*, *72*(2), 221-229.

Cooke, D., Drenth, A., Duncan, J., Wagels, G., & Brasier, C. (2000). A molecular phylogeny of *Phytophthora* and related oomycetes. *Fungal Genetics and Biology*, *30*(1), 17-32.

Cox, M. P., Guo, Y., Winter, D. J., Sen, D., Cauldron, N. C., Shiller, J., Bradley, E. L., Ganley, A. R., Gerth, M. L., Lacey, R. F., McDougal, R. L., Panda, P., Williams, N. M., Grunwald, N. J., Mesarich, C. H., & Bradshaw, R. E. (2022). Chromosome-level assembly of the *Phytophthora agathidicida* genome reveals adaptation in effector gene families [Original Research]. *Frontiers in Microbiology*, *13*.

de Sampaio e Paiva Camilo-Alves, C., da Clara, M. I. E., & de Almeida Ribeiro, N. M. C. (2013). Decline of Mediterranean oak trees and its association with *Phytophthora cinnamomi*: A review. *European Journal of Forest Research*, *132*, 411-432.

Dell, B., & Malajczuk, N. (1989). Jarrah dieback — A disease caused by *Phytophthora cinnamomi*. In B. Dell, J. J. Havel, & N. Malajczuk (Eds.), *The Jarrah forest: A complex mediterranean ecosystem* (pp. 67-87). Springer Netherlands.

Dick, M. A., Williams, N. M., Bader, M. K.-F., Gardner, J. F., & Bulman, L. S. (2014). Pathogenicity of *Phytophthora pluvialis* to *Pinus radiata* and its relation with red needle cast disease in New Zealand. *New Zealand Journal of Forestry Science*, *44*(1), 6.

Dick, M. W. (2001). The Peronosporomycetes. In D. J. McLaughlin, E. G. McLaughlin, & P. A. Lemke (Eds.), *Systematics and Evolution: Part A* (pp. 39-72). Springer Berlin Heidelberg.

Dickinson, C., & Boardman, F. (1970). Physiological studies of some fungi isolated from peat. *Transactions of the British Mycological Society*, *55*, 293-305.

Dobbie, K., Scott, P., Taylor, P., Panda, P., Sen, D., Dick, M., & McDougal, R. (2022). *Phytophthora podocarpi* sp. nov. from diseased needles and shoots of *Podocarpus* in New Zealand. *Forests*, *13*(2), 214.

Dobson, A., & Foufopoulos, J. (2001). Emerging infectious pathogens of wildlife. *Philosophical Transactions of the Royal Society of London. Series B: Biological Sciences*, *356*(1411), 1001-1012.

Doehlemann, G., Ökmen, B., Zhu, W., & Sharon, A. (2017). Plant pathogenic fungi. *Microbiology Spectrum*, *5*(1), 5.1. 14.

Ebstrup, T., Saalbach, G., & Egsgaard, H. (2005). A proteomics study of *in vitro* cyst germination and appressoria formation in *Phytophthora infestans*. *Proteomics*, *5*(11), 2839-2848.

Eggert, C., LaFayette, P. R., Temp, U., Eriksson, K.-E. L., & Dean, J. F. D. (1998). Molecular analysis of a laccase gene from the white rot fungus *Pycnoporus cinnabarinus*. *Applied and Environmental Microbiology*, *64*(5), 1766-1772.

Eitzen, K., Sengupta, P., Kroll, S., Kemen, E., & Doehlemann, G. (2021). A fungal member of the *Arabidopsis thaliana* phyllosphere antagonizes *Albugo laibachii* via a GH25 lysozyme. *eLife*, *10*, e65306.

Esser, K., & Meinhardt, F. (1984). Barrage formation in fungi. In H. F. Linskens & J. Heslop-Harrison (Eds.), *Cellular Interactions* (pp. 350-361). Springer Berlin Heidelberg.

Fabro, G. (2022). Oomycete intracellular effectors: specialised weapons targeting strategic plant processes. *New Phytologist*, *233*(3), 1074-1082.

Fang, Y., Coelho, M. A., Shu, H., Schotanus, K., Thimmappa, B. C., Yadav, V., Chen, H., Malc, E. P., Wang, J., Mieczkowski, P. A., Kronmiller, B., Tyler, B. M., Sanyal, K., Dong, S., Nowrousian, M., & Heitman, J. (2020). Long transposon-rich centromeres in an oomycete reveal divergence of centromere features in Stramenopila-Alveolata-Rhizaria lineages. *PLoS Genetics*, *16*(3), e1008646.

Fawke, S., Doumane, M., & Schornack, S. (2015). Oomycete interactions with plants: Infection strategies and resistance principles. *Microbiology and Molecular Biology Reviews*, *79*(3), 263-280.

Ferrari, R., Lacaze, I., Le Faouder, P., Bertrand-Michel, J., Oger, C., Galano, J.-M., Durand, T., Moularat, S., Chan Ho Tong, L., Boucher, C., Kilani, J., Petit, Y., Vanparis, O., Trannoy, C., Brun, S., Lalucque, H., Malagnac, F., & Silar, P. (2018). Cyclooxygenases and lipoxygenases are used by the fungus *Podospora anserina* to repel nematodes. *Biochimica et Biophysica Acta (BBA) - General Subjects*, *1862*(10), 2174-2182.

Franceschetti, M., Maqbool, A., Jiménez-Dalmaroni, M. J., Pennington, H. G., Kamoun, S., & Banfield, M. J. (2017). Effectors of filamentous plant pathogens: Commonalities amid diversity. *Microbiology and Molecular Biology Reviews*, *81*(2).

Freire, D. M., Gutierrez, C., Garza-Garcia, A., Grabowska, A. D., Sala, A. J., Ariyachaokun, K., Panikova, T., Beckham, K. S. H., Colom, A., Pogenberg, V., Cianci, M., Tuukkanen, A., Boudehen, Y.-M., Peixoto, A., Botella, L., Svergun, D. I., Schnappinger, D., Schneider, T. R., Genevaux, P., de Carvalho, L. P. S., Wilmanns, M., Parret, A. H. A., & Neyrolles, O. (2019). An NAD+ phosphorylase toxin triggers *Mycobacterium tuberculosis* cell death. *Molecular Cell*, *73*(6), 1282-1291.e1288.

Froud, K., Chew, C. Y., Kean, J., Meiforth, J., Killick, S., Ashby, E., Taua-Gordon, R., Jamieson, A., & Tolich, L. (2022). 2021 Waitākere Ranges kauri population health monitoring survey.

Gadgil, P. D. (1974). *Phytophthora heveae*, a pathogen of kauri. *New Zealand Journal of Forestry science*, *4*, 59-63.

Gómez-Pérez, D., Schmid, M., Chaudhry, V., Hu, Y., Velic, A., Maček, B., Ruhe, J., Kemen, A., & Kemen, E. (2023). Proteins released into the plant apoplast by the obligate parasitic protist *Albugo* selectively repress phyllosphere-associated bacteria. *New Phytologist*.

Goodin, M. M., Zaitlin, D., Naidu, R. A., & Lommel, S. A. (2008). *Nicotiana benthamiana*: Its history and future as a model for plant-pathogen interactions. *Molecular Plant-Microbe Interactions*, *21*(8), 1015-1026.

Grenville-Briggs, L. J., Avrova, A. O., Bruce, C. R., Williams, A., Whisson, S. C., Birch, P. R., & van West, P. (2005). Elevated amino acid biosynthesis in *Phytophthora infestans* during appressorium formation and potato infection. *Fungal Genetics and Biology*, *42*(3), 244-256.

Guest, D., & Grant, B. (1990). The complex action of phosphonates as antifungal agents. *Biological Reviews*, *66*, 159-187.

Gunderson, J. H., Elwood, H., Ingold, A., Kindle, K., & Sogin, M. L. (1987). Phylogenetic relationships between chlorophytes, chrysophytes, and oomycetes. *Proceedings of the National Academy of Sciences*, *84*(16), 5823-5827.

Guo, Y., Dupont, P. Y., Mesarich, C. H., Yang, B., McDougal, R. L., Panda, P., Dijkwel, P., Studholme, D. J., Sambles, C., & Win, J. (2020). Functional analysis of RXLR effectors from the New Zealand kauri dieback pathogen *Phytophthora agathidicida*. *Molecular Plant Pathology*, *21*(9), 1131-1148.

Haddad Momeni, M., Fredslund, F., Bissaro, B., Raji, O., Vuong, T. V., Meier, S., Nielsen, T. S., Lombard, V., Guigliarelli, B., Biaso, F., Haon, M., Grisel, S., Henrissat, B., Welner, D. H., Master, E. R., Berrin, J.-G., & Abou Hachem, M. (2021). Discovery of fungal oligosaccharide-oxidising flavo-enzymes with previously unknown substrates, redox-activity profiles and interplay with LPMOs. *Nature Communications*, *12*(1), 2132.

Halkett, J. (1983). A basis for the management of New Zealand kauri (*Agathis Australis*(D. Don) Lindl.) forest. *New Zealand Journal of Forestry*, *28*(1), 15-23.

Hardham, A. R. (2005). *Phytophthora cinnamomi*. *Molecular Plant Pathology*, *6*(6), 589-604.

Hardham, A. R. (2006). Cell biology of plant–oomycete interactions. *Cellular Microbiology*, *9*(1), 31-39.

Hardham, A. R., & Blackman, L. M. (2018). *Phytophthora cinnamomi*. *Molecular Plant Pathology*, *19*(2), 260-285.

Hardy, G. S. J., Barrett, S., & Shearer, B. (2001). The future of phosphite as a fungicide to control the soilborne plant pathogen *Phytophthora cinnamomi* in natural ecosystems. *Australasian Plant Pathology*, *30*, 133-139.

Heitman, J. (2011). Microbial pathogens in the fungal kingdom. *Fungal Biology Reviews*, *25*(1), 48-60.

Hill, L., Waipara, N., Stanley, R., & Hammon, C. (2017). Kauri dieback Report 2017: An investigation into the distribution of kauri dieback, and implications for its future management, within the Waitakere Ranges Regional Park

Ho, H. H. (1978). Hyphal branching systems in *Phytophthora* and other phycomycetes. *Mycopathologia*, *64*(2), 83-86.

Ho, W., Thangavel, R., Alexander, B., Ashcroft, T., Anderson, P., & Waipara, N. (2010). *Phytophthora species associated with kawakawa tree decline in New Zealand* Presentation at the 5th IUFRO Working Party SO7, New Zealand

Holm, L., Laiho, A., Törönen, P., & Salgado, M. (2023). DALI shines a light on remote homologs: One hundred discoveries. *Protein Science*, *32*(1), e4519.

Horner, I. J., & Hough, E. G. (2011). *Phosphorous acid for controlling Phytophthora taxon agathis in kauri*.

Horner, I. J., & Hough, E. G. (2014). Pathogenicity of four *Phytophthora* species on kauri *in vitro* and glasshouse trials. *New Zealand Plant Protection*, *67*(0), 54-59.

Horner, I. J., Hough, E. G., & Horner, M. B. (2015). Forest efficacy trials on phosphite for control of kauri dieback. *New Zealand Plant Protection*, *68*(0), 7-12.

Huang, W. R. H., Schol, C., Villanueva, S. L., Heidstra, R., & Joosten, M. H. A. J. (2020). Knocking out SOBIR1 in *Nicotiana benthamiana* abolishes functionality of transgenic receptor-like protein Cf-4. *Plant Physiology*, *185*(2), 290-294.

Ihssen, J., Schubert, M., Thöny-Meyer, L., & Richter, M. (2014). Laccase catalyzed synthesis of iodinated phenolic compounds with antifungal activity. *PLOS ONE*, *9*(3), e89924.

The introduction of Phytophthora agathidicida to Aotearoa. (2021). New Zealand's Biological Hertitage. https://bioheritage.nz/the-introduction-of-phytophthora-agathidicida-to-aotearoa/

Ivanov, A. A., Ukladov, E. O., & Golubeva, T. S. (2021). *Phytophthora infestans*: An overview of methods and attempts to combat late blight. *Journal of Fungi*, *7*(12), 1071.

Jones, J. D. G., & Dangl, J. L. (2006). The plant immune system. *Nature*, *444*(7117), 323-329.

Judelson, H. S. (2017). Metabolic diversity and novelties in the oomycetes. *Annual Review of Microbiology*, *71*(1), 21-39.

Judelson, H. S., & Blanco, F. A. (2005). The spores of *Phytophthora*: Weapons of the plant destroyer. *Nature Reviews Microbiology*, *3*(1), 47-58.

Jumper, J., Evans, R., Pritzel, A., Green, T., Figurnov, M., Ronneberger, O., Tunyasuvunakool, K., Bates, R., Žídek, A., Potapenko, A., Bridgland, A., Meyer, C., Kohl, S. A. A., Ballard, A. J., Cowie, A., Romera-Paredes, B., Nikolov, S., Jain, R., Adler, J., Back, T., Petersen, S., Reiman, D., Clancy, E., Zielinski, M., Steinegger, M., Pacholska, M., Berghammer, T., Bodenstein, S., Silver, D., Vinyals, O., Senior, A. W., Kavukcuoglu, K., Kohli, P., & Hassabis, D. (2021). Highly accurate protein structure prediction with AlphaFold. *Nature*, *596*(7873), 583-589.

Kaliszan, R., Kaliszan, A., & Wainer, I. W. (1993). Prediction of drug binding to melanin using a melanin-based high-performance liquid chromatographic stationary phase and chemometric analysis of the chromatographic data. *Journal of Chromatography 615*(2), 281-288.

Kamoun, S., Furzer, O., Jones, J. D., Judelson, H. S., Ali, G. S., Dalio, R. J., Roy, S. G., Schena, L., Zambounis, A., & Panabières, F. (2015). The top 10 oomycete pathogens in molecular plant pathology. *Molecular Plant Pathology*, *16*(4), 413-434.

Kaur, K., Sharma, A., Capalash, N., & Sharma, P. (2019). Multicopper oxidases: Biocatalysts in microbial pathogenesis and stress management. *Microbiological Research*, *222*, 1-13.

Keller, N. P. (2019). Fungal secondary metabolism: Regulation, function and drug discovery. *Nature Reviews Microbiology*, *17*(3), 167-180.

Kettles, G. J., Bayon, C., Sparks, C. A., Canning, G., Kanyuka, K., & Rudd, J. J. (2018). Characterization of an antimicrobial and phytotoxic ribonuclease secreted by the fungal wheat pathogen *Zymoseptoria tritici*. *New Phytologist*, *217*(1), 320-331.

Kong, P., Hong, C. X., & Richardson, P. A. (2003). Rapid detection of *Phytophthora cinnamomi* using PCR with primers derived from the Lpv putative storage protein genes. *Plant Pathology*, *52*(6), 681-693.

Kostov, K., Verstappen, E. C. P., Bergervoet, J. H. W., de Weerdt, M., Schoen, C. D., Slavov, S., & Bonants, P. J. M. (2016). Multiplex detection and identification of *Phytophthora* spp. using target-specific primer extension and Luminex xTAG technology. *Plant Pathology*, *65*(6), 1008-1021.

Krogh, A., Larsson, B., von Heijne, G., & Sonnhammer, E. L. L. (2001). Predicting transmembrane protein topology with a hidden markov model: Application to complete genomes *Journal of Molecular Biology*, *305*(3), 567-580.

Lacey, R. F., Fairhurst, M. J., Daley, K. J., Ngata-Aerengamate, T. A., Patterson, H. R., Patrick, W. M., & Gerth, M. L. (2021). Assessing the effectiveness of oxathiapiprolin toward *Phytophthora agathidicida*, the causal agent of kauri dieback disease. *FEMS Microbes*, *2*, xtab016.

Latijnhouwers, M., de Wit, P. J., & Govers, F. (2003). Oomycetes and fungi: Similar weaponry to attack plants. *Trends in Microbiology*, *11*(10), 462-469.

Lawrence, S. A., Burgess, E. J., Pairama, C., Black, A., Patrick, W. M., Mitchell, I., Perry, N. B., & Gerth, M. L. (2019). Mātauranga-guided screening of New Zealand native plants reveals flavonoids from kānuka (*Kunzea robusta*) with anti-*Phytophthora* activity. *Journal of the Royal Society of New Zealand*, *49*(sup1), 137-154.

Leeder, A. C., Palma-Guerrero, J., & Glass, N. L. (2011). The social network: Deciphering fungal language. *Nature Reviews Microbiology*, *9*(6), 440-451.

Levasseur, A., Drula, E., Lombard, V., Coutinho, P. M., & Henrissat, B. (2013). Expansion of the enzymatic repertoire of the CAZy database to integrate auxiliary redox enzymes. *Biotechnology for Biofuels*, *6*(1), 41.

Li, J., & Tax, F. E. (2013). Receptor-like kinases: Key regulators of plant development and defense. *Journal of Integrative Plant Biology*, *55*(12), 1184-1187.

Liebrand, T. W., van den Berg, G. C., Zhang, Z., Smit, P., Cordewener, J. H., America, A. H., Sklenar, J., Jones, A. M., Tameling, W. I., Robatzek, S., Thomma, B. P., & Joosten, M. H. (2013). Receptor-like kinase SOBIR1/EVR interacts with receptor-like proteins in plant immunity against fungal infection. *Proceedings of the National Academy of Sciences of the United States of America 110*(24), 10010-10015.

Liebrand, T. W., van den Burg, H. A., & Joosten, M. H. (2014). Two for all: Receptor-associated kinases SOBIR1 and BAK1. *Trends in Plant Science*, *19*(2), 123-132.

Lucas, J. A., Greer, G., Oudemans, P. V., & Coffey, M. D. (1990). Fungicide sensitivity in somatic hybrids of *Phytophthora capsici* obtained by protoplast fusion. *Physiological and Molecular Plant Pathology*, *36*(2), 175-187.

Ma, Z., Song, T., Zhu, L., Ye, W., Wang, Y., Shao, Y., Dong, S., Zhang, Z., Dou, D., Zheng, X., Tyler, B. M., & Wang, Y. (2015). A *Phytophthora sojae* glycoside hydrolase 12 protein is a major virulence factor during soybean infection and is recognized as a PAMP. *Plant Cell*, *27*(7), 2057-2072.

Meijer, H. J. G., Mancuso, F. M., Espadas, G., Seidl, M. F., Chiva, C., Govers, F., & Sabidó, E. (2014). Profiling the secretome and extracellular proteome of the potato late blight pathogen *Phytophthora infestans*. *Molecular & Cellular Proteomics*, *13*(8), 2101-2113.

Mewis, K., Lenfant, N., Lombard, V., & Henrissat, B. (2016). Dividing the large glycoside hydrolase family 43 into subfamilies: a motivation for detailed enzyme characterization. *Applied and Environmental Microbiology*, *82*(6), 1686-1692.

Miao, J., Dong, X., Lin, D., Wang, Q., Liu, P., Chen, F., Du, Y., & Liu, X. (2016). Activity of the novel fungicide oxathiapiprolin against plant-pathogenic oomycetes. *Pest Management Science*, *72*(8), 1572-1577.

Michalski, A., Damoc, E., Hauschild, J.-P., Lange, O., Wieghaus, A., Makarov, A., Nagaraj, N., Cox, J., Mann, M., & Horning, S. (2011). Mass spectrometry-based proteomics using Q Exactive, a high-performance benchtop quadrupole orbitrap mass spectrometer. *Molecular & Cellular Proteomics*, *10*(9).

Mirdita, M., Schütze, K., Moriwaki, Y., Heo, L., Ovchinnikov, S., & Steinegger, M. (2022). ColabFold: making protein folding accessible to all. *Nature Methods*, *19*(6), 679-682.

Money, N. P. (2021). Hyphal and mycelial consciousness: The concept of the fungal mind. *Fungal Biology*, *125*(4), 257-259.

Neilson, E. H., Goodger, J. Q., Woodrow, I. E., & Møller, B. L. (2013). Plant chemical defense: At what cost? *Trends in Plant Science*, *18*(5), 250-258.

Nekiunaite, L., Arntzen, M. Ø., Svensson, B., Vaaje-Kolstad, G., & Abou Hachem, M. (2016). Lytic polysaccharide monooxygenases and other oxidative enzymes are abundantly secreted by *Aspergillus nidulans* grown on different starches. *Biotechnology for Biofuels*, *9*(1), 187.

Nelson, N. (1994). Energizing porters by proton-motive force. *Journal of Experimental Biology*, *196*(1), 7-13.

Newman, M. A., Sundelin, T., Nielsen, J. T., & Erbs, G. (2013). MAMP (microbe-associated molecular pattern) triggered immunity in plants. *Frontiers in Plant Science*, *4*, 139.

Nickel, W., & Rabouille, C. (2009). Mechanisms of regulated unconventional protein secretion. *Nature Reviews Molecular Cell Biology*, *10*(2), 148-155.

Nowicki, M., Foolad, M. R., Nowakowska, M., & Kozik, E. U. (2012). Potato and tomato late blight caused by *Phytophthora infestans*: An overview of pathology and resistance breeding. *Plant Disease*, *96*(1), 4-17.

Page, R., & Peti, W. (2016). Toxin-antitoxin systems in bacterial growth arrest and persistence. *Nature Chemical Biology*, *12*(4), 208-214.

Panstruga, R., & Dodds, P. N. (2009). Terrific protein traffic: The mystery of effector protein delivery by filamentous plant pathogens. *Science*, *324*(5928), 748-750.

Paysan-Lafosse, T., Blum, M., Chuguransky, S., Grego, T., Pinto, B. L., Salazar, G. A., Bileschi, M. L., Bork, P., Bridge, A., Colwell, L., Gough, J., Haft, D. H., Letunić, I., Marchler-Bauer, A., Mi, H., Natale, D. A., Orengo, C. A., Pandurangan, A. P., Rivoire, C., Sigrist, C. J. A., Sillitoe, I., Thanki, N., Thomas, P. D., Tosatto, S. C. E., Wu, C. H., & Bateman, A. (2023). InterPro in 2022. *Nucleic Acids Research*, *51*(D1), D418-d427.

Pela, F. (2004). Biological activities of fungal metabolites. In *Handbook of Industrial Mycology* (pp. 68-111). CRC Press.

Porter, C. L. (1924). Concerning the characters of certain fungi as exhibited by their growth in the presence of other fungi. *American Journal of Botany*, 168-188.

Powderly, W. G. (2019). How infection shaped history: lessons from the Irish famine. *Transactions of the American Clinical and Climatological Association*, *130*, 127.

Pruitt, R. N., Gust, A. A., & Nürnberger, T. (2021). Plant immunity unified. *Nature Plants*, *7*(4), 382-383.

Quinlan, R. J., Sweeney, M. D., Lo Leggio, L., Otten, H., Poulsen, J.-C. N., Johansen, K. S., Krogh, K. B. R. M., Jørgensen, C. I., Tovborg, M., Anthonsen, A., Tryfona, T., Walter, C. P., Dupree, P., Xu, F., Davies, G. J., & Walton, P. H. (2011). Insights into the oxidative degradation of cellulose by a copper metalloenzyme that exploits biomass components. *Proceedings of the National Academy of Sciences*, *108*(37), 15079-15084.

Rajput, N. A., Zhang, M., Ru, Y., Liu, T., Xu, J., Liu, L., Mafurah, J. J., & Dou, D. (2014). *Phytophthora sojae* effector PsCRN70 suppresses plant defenses in *Nicotiana benthamiana*. *PLoS One*, *9*(5), e98114.

Rands, R. (1922). Stripe canker of cinnamon caused by *Phytophthora cinnamomi* n. sp. *Mededelingen van het Instituut voor Plantenziekten*, *54*.

Reeser, P., Sutton, W., & Hansen, E. (2013). *Phytophthora pluvialis* , a new species from mixed tanoak-Douglas-fir forests of western Oregon, U.S.A [Oomycetes; canopy drip; rainwater; streams; soil; environmental Phytophthora]. *North American Fungi*, *8*, 8.

Rigling, D., & Prospero, S. (2018). *Cryphonectria parasitica*, the causal agent of chestnut blight: invasion history, population biology and disease control. *Molecular Plant Pathology*, *19*(1), 7-20.

Rizzo, D. M., Garbelotto, M., Davidson, J. M., Slaughter, G. W., & Koike, S. T. (2002). *Phytophthora ramorum* as the cause of extensive mortality of *Quercus* spp. and *Lithocarpus densiflorus* in California. *Plant Disease*, *86*(3), 205-214.

Rocafort, M., Fudal, I., & Mesarich, C. H. (2020). Apoplastic effector proteins of plant-associated fungi and oomycetes. *Current Opinion in Plant Biology*, *56*, 9-19.

Romero, P., Obradovic, Z., Li, X., Garner, E. C., Brown, C. J., & Dunker, A. K. (2001). Sequence complexity of disordered protein. *Proteins: Structure, Function, and Bioinformatics*, *42*(1), 38-48.

Rovenich, H., Boshoven, J. C., & Thomma, B. P. H. J. (2014). Filamentous pathogen effector functions: of pathogens, hosts and microbiomes. *Current Opinion in Plant Biology*, *20*, 96-103.

Royse, D., & Ries, S. (1978). The influence of fungi isolated from peach twigs on the pathogenicity of C*ytospora cincta*. *Phytopathology*, *68*(4), 603-607.

Ryder, J. (2016). *What is the host range of Phytophthora agathidicida (causal agent of kauri dieback disease) in New Zealand?* ResearchSpace@ Auckland.

Sabbadin, F., Urresti, S., Henrissat, B., Avrova, A. O., Welsh, L. R. J., Lindley, P. J., Csukai, M., Squires, J. N., Walton, P. H., Davies, G. J., Bruce, N. C., Whisson, S. C., & McQueen-Mason, S. J. (2021). Secreted pectin monooxygenases drive plant infection by pathogenic oomycetes. *Science*, *373*(6556), 774-779.

Sandrock, R. W., DellaPenna, D., & VanEtten, H. D. (1995). Purification and characterization of beta 2-tomatinase, an enzyme involved in the degradation of alpha-tomatine and isolation of the gene encoding beta 2-tomatinase from *Septoria lycopersici*. *Molecular Plant-Microbe Interactions*, *8*(6), 960-970.

Schneider, C. A., Rasband, W. S., & Eliceiri, K. W. (2012). NIH image to ImageJ: 25 years of image analysis. *Nature Methods*, *9*(7), 671-675.

Schrodinger, L. & DeLano, W (2020). PyMOL.

Scott, P. M., Burgess, T., Barber, P., Shearer, B., Stukely, M., Hardy, G. S. J., & Jung, T. (2009). *Phytophthora multivora* sp. nov., a new species recovered from declining *Eucalypt*us, *Banksia*, *Agonis* and other plant species in Western Australia. *Persoonia-Molecular Phylogeny and Evolution of Fungi*, *22*(1), 1-13.

Sena, K., Crocker, E., Vincelli, P., & Barton, C. (2018). *Phytophthora cinnamomi* as a driver of forest change: Implications for conservation and management. *Forest Ecology and Management*, *409*, 799-807.

Shepherd, S. J., Van West, P., & Gow, N. A. (2003). Proteomic analysis of asexual development of *Phytophthora palmivora*. *Mycological Research*, *107*(4), 395-400.

Silvester, W., & Orchard, T. (1999). The biology of kauri (*Agathis australis*) in New Zealand. Production, biomass, carbon storage, and litter fall in four forest remnants. *New Zealand Journal of Botany, 37*(3), 553-571.

Skidmore, A., & Dickinson, C. (1976). Colony interactions and hyphal interference between *Septoria nodorum* and phylloplane fungi. *Transactions of the British Mycological Society*, *66*(1), 57-64.

Snelders, N. C., Rovenich, H., Petti, G. C., Rocafort, M., van den Berg, G. C. M., Vorholt, J. A., Mesters, J. R., Seidl, M. F., Nijland, R., & Thomma, B. P. H. J. (2020). Microbiome manipulation by a soil-borne fungal plant pathogen using effector proteins. *Nature Plants*, *6*(11), 1365-1374.

Soanes, D. M., Richards, T. A., & Talbot, N. J. (2007). Insights from sequencing fungal and oomycete genomes: What can we learn about plant disease and the evolution of pathogenicity? *The Plant Cell*, *19*(11), 3318-3326.

Sogin, M. L., & Silberman, J. D. (1998). Evolution of the protists and protistan parasites from the perspective of molecular systematics. *International Journal for Parasitology, 28*(1), 11-20.

Sonnhammer, E. L. L., Heijne, G. v., & Krogh, A. (1998). A hidden markov model for predicting transmembrane helices in protein sequences. Proceedings of the 6th International Conference on Intelligent Systems for Molecular Biology.

Speckbacher, V., Ruzsanyi, V., Martinez-Medina, A., Hinterdobler, W., Doppler, M., Schreiner, U., Böhmdorfer, S., Beccaccioli, M., Schuhmacher, R., Reverberi, M., Schmoll, M., & Zeilinger, S. (2020). The lipoxygenase lox1 is involved in light- and injury-response, conidiation, and volatile organic compound biosynthesis in the mycoparasitic fungus *Trichoderma atroviride*. *Frontiers in Microbiology, 11*.

Sperschneider, J., & Dodds, P. N. (2022). EffectorP 3.0: Prediction of apoplastic and cytoplasmic effectors in fungi and oomycetes. *Molecular Plant-Microbe Interactions*, *35*(2), 146-156.

Sperschneider, J., Williams, A. H., Hane, J. K., Singh, K. B., & Taylor, J. M. (2015). Evaluation of secretion prediction highlights differing approaches needed for oomycete and fungal effectors. *Frontiers in Plant Science*, *6*.

Steward, G. A., & Beveridge, A. E. (2010). A review of New Zealand kauri (*Agathis australis* (D. Don) Lindl.): Its ecology, history, growth and potential for management for timber. *New Zealand Journal of Forestry Science*, *40*.

Strange, R. N., & Scott, P. R. (2005). Plant disease: A threat to global food security. *Annual Review of Phytopathology*, *43*, 83-116.

Studholme, D. J., McDougal, R. L., Sambles, C., Hansen, E., Hardy, G., Grant, M., Ganley, R. J., & Williams, N. M. (2016). Genome sequences of six *Phytophthora* species associated with forests in New Zealand. *Genomics Data*, *7*, 54-56.

Than, D. J., Hughes, K. J. D., Boonhan, N., Tomlinson, J. A., Woodhall, J. W., & Bellgard, S. E. (2013). A TaqMan real-time PCR assay for the detection of *Phytophthora* 'taxon *Agathis*' in soil, pathogen of kauri in New Zealand. *Forest Pathology, 43*(4), 324-330.

Tsuda, K., & Katagiri, F. (2010). Comparing signaling mechanisms engaged in pattern-triggered and effector-triggered immunity. *Current Opinion in Plant Biology*, *13*(4), 459-465.

Tsykun, T., Prospero, S., Schoebel, C. N., Rea, A., & Burgess, T. I. (2022). Global invasion history of the emerging plant pathogen *Phytophthora multivora*. *BMC Genomics*, *23*(1), 153.

Turrà, D., Nordzieke, D., Vitale, S., El Ghalid, M., & Di Pietro, A. (2016). Hyphal chemotropism in fungal pathogenicity. *Seminars in Cell & Developmental Biology, 57,* 69-75.

Tyler, B. M. (2002). Molecular basis of recognition between *Phytophthora* pathogens and their hosts. *Annual Review of Phytopathology, 40,* 137-167.

Uwamori, T., Inoue, K., Kida, C., Morita, Y., Park, P., Nakayashiki, H., Kanematsu, S., & Ikeda, K. (2015). Self- and nonself recognition during hyphal interactions in *Rosellinia necatrix*. *Journal of General Plant Pathology*, *81*(6), 420-428.

van der Burgh, A. M., & Joosten, M. H. A. J. (2019). Plant immunity: Thinking outside and inside the box. *Trends in Plant Science*, *24*(7), 587-601.

van Kempen, M., Kim, S., Tumescheit, C., Mirdita, M., Lee, J., Gilchrist, C., Söding, J., & Steinegger, M. (2023). Fast and accurate protein structure search with foldseek. *Nature Biotechnology,* 1-4.

Velázquez-Cedeño, M., Farnet, A. M., Billette, C., Mata, G., & Savoie, J.-M. (2007). Interspecific interactions with *Trichoderma longibrachiatum* induce *Pleurotus ostreatus* defence reactions based on the production of laccase isozymes. *Biotechnology Letters*, *29*(10), 1583-1590.

Verkaik, E., Jongkind, A. G., & Berendse, F. (2006). Short-term and long-term effects of tannins on nitrogen mineralisation and litter decomposition in kauri (*Agathis australis* (D. Don) Lindl.) forests. *Plant and Soil*, *287,* 337-345.

Vey, A., Hoagland, R. E., & Butt, T. M. (2001). 12 toxic metabolites of fungal biocontrol agents. In *Fungi as biocontrol agents* (pp. 311).

Waipara, N., Hill, S., Hill, L., Carroll, E., & Horner, I. (2013). Surveillance methods to determine tree health, distribution of kauri dieback disease and associated pathogens. *New Zealand Plant Protection*, *66*, 235-241.

Wang, J., Shen, D., Ge, C., Du, Y., Lin, L., Liu, J., Bai, T., Jing, M., Qian, G., & Dou, D. (2020). Filamentous *Phytophthora* pathogens deploy effectors to interfere with bacterial growth and motility. *Frontiers in Microbiology*, *11*.

Wang, Y., Xu, Y., Sun, Y., Wang, H., Qi, J., Wan, B., Ye, W., Lin, Y., Shao, Y., Dong, S., Tyler, B. M., & Wang, Y. (2018). Leucine-rich repeat receptor-like gene screen reveals that *Nicotiana* RXEG1 regulates glycoside hydrolase 12 MAMP detection. *Nature Communications*, *9*(1), 594.

Weir, B. S., Paderes, E. P., Anand, N., Uchida, J. Y., Pennycook, S. R., Bellgard, S. E., & Beever, R. E. (2015). A taxonomic revision of *Phytophthora* clade 5 including two new species, *Phytophthora agathidicida* and *P. cocois*. *Phytotaxa*, *205*(1), 21–38-21–38.

Whisson, S. C., Boevink, P. C., Wang, S., & Birch, P. R. (2016). The cell biology of late blight disease. *Current Opinion in Microbiology*, *34*, 127-135.

Wilcox, W. F. (1992). *Phytophthora* root and crown rot. https://ecommons.cornell.edu/handle/1813/43116

Winkworth, R. C., Bellgard, S. E., McLenachan, P. A., & Lockhart, P. J. (2021). The mitogenome of *Phytophthora agathidicida*: Evidence for a not so recent arrival of the "kauri killing" *Phytophthora* in New Zealand. *PLoS One*, *16*(5), e0250422.

Wyse, S. V., & Burns, B. R. (2011). Do host bark traits influence trunk epiphyte communities? *New Zealand Journal of Ecology*, *35*(3), 296-301.

Wyse, S. V., Burns, B. R., & Wright, S. D. (2013). Distinctive vegetation communities are associated with the long-lived conifer *Agathis australis* (New Zealand kauri, Araucariaceae) in New Zealand rainforests. *Austral Ecology*, *39*(4), 388-400.

Xu, Y., Zhang, Y., Zhu, J., Sun, Y., Guo, B., Liu, F., Huang, J., Wang, H., Dong, S., Wang, Y., & Wang, Y. (2021). *Phytophthora sojae* apoplastic effector AEP1 mediates sugar uptake by mutarotation of extracellular aldose and is recognized as a MAMP. *Plant Physiology*, *187*(1), 321-335.

Yamaguchi, Y., Park, J.-H., & Inouye, M. (2011). Toxin-antitoxin systems in bacteria and archaea. *Annual Review of Genetics*, *45*(1), 61-79.

Yin, Y., Mao, X., Yang, J., Chen, X., Mao, F., & Xu, Y. (2012). dbCAN: a web resource for automated carbohydrate-active enzyme annotation. *Nucleic Acids Research*, *40*(W1), W445-W451.

Zahid, M. A., Sandroni, M., Vetukuri, R. R., & Andreasson, E. (2021). A fast, nondestructive method for the detection of disease-related lesions and wounded leaves. *Biotechniques*, *71*(2), 425-430.

Zhang, H., Yohe, T., Huang, L., Entwistle, S., Wu, P., Yang, Z., Busk, P. K., Xu, Y., & Yin, Y. (2018). dbCAN2: a meta server for automated carbohydrate-active enzyme annotation. *Nucleic Acids Research*, *46*(W1), W95-w101.

Zhang, Y., Fletcher, K., Han, R., Michelmore, R., & Yang, R. (2020). Genome-wide analysis of cyclophilin proteins in 21 oomycetes. *Pathogens*, *9*(1), 24.

Zhao, Z., Liu, H., Wang, C., & Xu, J. R. (2013). Comparative analysis of fungal genomes reveals different plant cell wall degrading capacity in fungi. *BMC Genomics*, *14*, 274.

Zhi, H., & Wang, D. (2022). Inheritance and prevention of soybean root rot. In H.-M. Lam & M.-W. Li (Eds.), *Advances in Botanical Research* (Vol. 102, pp. 105-119). Academic Press.

Zhong, Z., Li, N., Liu, L., He, B., Igarashi, Y., & Luo, F. (2018). Label-free differentially proteomic analysis of interspecific interaction between white-rot fungi highlights oxidative stress response and high metabolic activity. *Fungal Biology*, *122*(8), 774-784.

Zipfel, C. (2014). Plant pattern-recognition receptors. *Trends in Immunology*, *35*(7), 345-351.